UNIVERSITA' DEGLI STUDI DI PARMA

Dottorato di ricerca in medicina molecolare

Ciclo XXIX

Role of the cryptic fragment 53-74 of pre-pro TRH as a growth factor for rat anterior pituitary cells

Coordinatore:

Chiar.mo Prof. Luciano Polonelli

Tutor:

Chiar.mo Prof. Roberto Toni

Dottorando: Fulvio Barbaro

INTRODUCTION

Biosynthesis, processing, and distribution of putative secretory products of preproTRH in the rat, hypothalamic tuberoinfundibular system

In rat hypothalamic tuberoinfundibular neurons (1), prepro-TRH is a 29-kDa polypeptide composed of 255 amino acids. It contains an N-terminal 25-amino acid signal (or leader) sequence, a long N-terminal flanking peptide, five copies of the TRH progenitor sequence Gln-His-Pro-Gly flanked by paired basic amino acids (Lys-Arg or Arg-Arg), seven non-TRH peptides lying between the TRH progenitor sequences, and a long C-terminal flanking peptide (2, 3, 4).

Biosynthesis

The biosynthesis of TRH and pro-TRH-derived peptides begins with mRNA-directed ribosomal translation. Hormone precursors are synthesized on membrane-bound ribosomes, by which they are translocated into the lumen of the RER via a signal recognition peptide. During vectorial transport through the Gc and beyond, the newly synthesized proteins are subjected to posttranslational processing.

6

Post-translational processing

Mature TRH (pyro-Glu-His-Pro-NH2) and non-TRH peptides corresponding to the cryptic sequences, all originates from the post-translational processing of proTRH based on the activity of the pro-hormone convertase enzymes PC1, -2, and -3. These enzymes act at basic amino acid pair sites, followed by removal of the basic residue(s) by carboxypeptidase enzymes (2, 5, 6, 7). Such a model of pro-TRH post-translational processing has originally been developed in experiments with transfected AtT_{20} cells expressing rat prepro-TRH (8).

a.   Signal sequence

The signal peptide is separated from the N-terminal flanking peptide (prepro-TRH$_{25-50}$-R-R-prepro-TRH$_{53-74}$) of proTRH by endoproteolytic cleavage, giving rise to a 26-kDa precursor (5, 6, 7).

b.   proTRH peptide

Pulse-chase studies indicated that the 26-kDa precursor, proTRH is cleaved at two mutually exclusive dibasic sites to generate the first intermediate forms (Fig. 1). One possible cleavage generates a 15-kDa N-terminal peptide (prepro-TRH$_{25-151 \text{ or } 157}$) and a 10-kDa C-terminal peptide (prepro-TRH$_{154 \text{ or } 160-255}$). This processing yields the first molecule of TRH progenitor sequence (Gln-His-Pro-Gly). An alternate cleavage at residues

107-108 may generate a 9.5-kDa N-terminal peptide (prepro-TRH$_{25–106 \text{ or } 112}$),

and a 16.5-kDa C-terminal peptide (prepro-TRH$_{109 \text{ or } 115–255}$) (7, 8, 9).

c. N-terminal fragment

In subsequent steps, the 15-kDa N-terminal intermediate moiety of pro-TRH

is processed to a 6-kDa peptide, corresponding to prepro-TRH$_{25–74}$, and a

3.8- kDa peptide corresponding to prepro-TRH$_{77–106}$ (likely associated to

another less characterized peptide fragment, pAV37 or preproTRH$_{115-151}$).

This cleavage is able to release a second molecule of TRH progenitor

sequence. Further processing of prepro-TRH$_{77–106}$ gives rise to the novel

peptide, prepro-TRH$_{83–106}$ and a third molecule of TRH progenitor sequence.

Prepro-TRH$_{25–74}$, in turn, gives rise to the N-terminal peptides

prepro-TRH$_{25–50}$ or pYE27 and prepro-TRH$_{53–74}$ or pFT22. Similar, the

alternate processing of the 9.5-kDa N-terminal fragment is postulated to result

in the production of the N-terminal peptides prepro-TRH$_{25–50}$, prepro-TRH$_{53–74}$,

and prepro-TRH$_{83–106}$ or pEH$_{24}$. Collectively, initial breakdown of the proTRH

molecule and its N-terminal fragment results in 3 TRH progenitor molecules

and 3 cryptic peptides, all having the molecular features to be released

extracellularly as hormonally-active factors (Fig. 1) (9).

d. C-terminal fragment

It is proposed that processing at residues Lys^{152}-Arg^{153} of the 10-kDa C-terminal fragment produces the two C-terminal flanking peptides, 5.6-KDa prepro-TRH$_{160-199}$ and 5.4-kDa prepro-TRH$_{208-255}$ (8, 10). After cleavage of basic residues at positions 199–200 or 207–208, a fourth TRH progenitor sequence is made free, and the 5.6-kDa peptide is further processed to generate prepro-TRH$_{160-169}$ or pST$_{10}$, and prepro-TRH$_{178-199}$ or pFE$_{22}$. The latter proteolysis yields a fifth TRH progenitor sequence. Finally, prepro-TRH$_{178-199}$ is further cleaved to both the 1.6 kDa peptide, prepro-TRH$_{178-184}$ (pFQ7) and the 0.84 kDa peptide, prepro-TRH$_{186-199}$ (pSE$_{14}$) (10). In the case of alternate processing, the 16.5-kDa fragment would yield only the 5.4-kDa peptide, prepro-TRH$_{208-255}$ although availability of the classical TRH progenitor sequences follows a cleavage pattern identical to that previously described. Thus, processing of the C-terminal fragment results in 2 TRH progenitor molecules and 4 cryptic peptides, all having the molecular features to be released extracellularly as hormonally-active factors (Fig. 1) (9).

Secretion

Partially processed and unprocessed proTRH reach the last compartment of the Golgi complex, the *trans*-Golgi Network where they are sorted to a regulated secretory pathway, and initially stored in immature secretory

granules (11, 12, 13, 14). Maturation is based on modifications including glycosylation, phosphorylation, amidation, acetylation, and proteolytic conversion (15, 16, 17, 18) which confers bioactivity to many peptides (19). As a result, electron-dense secretory granules containing all sorted products (5 mature TRH or pGln-His-Pro-NH$_2$ molecules, and 7 non-TRH peptides) can fuse with the plasma membrane in response to an extracellular stimulation, and in a calcium-dependent manner thereby releasing their content into the hypothalamic-pituitary portal system (Fig. 1) (9, 20).
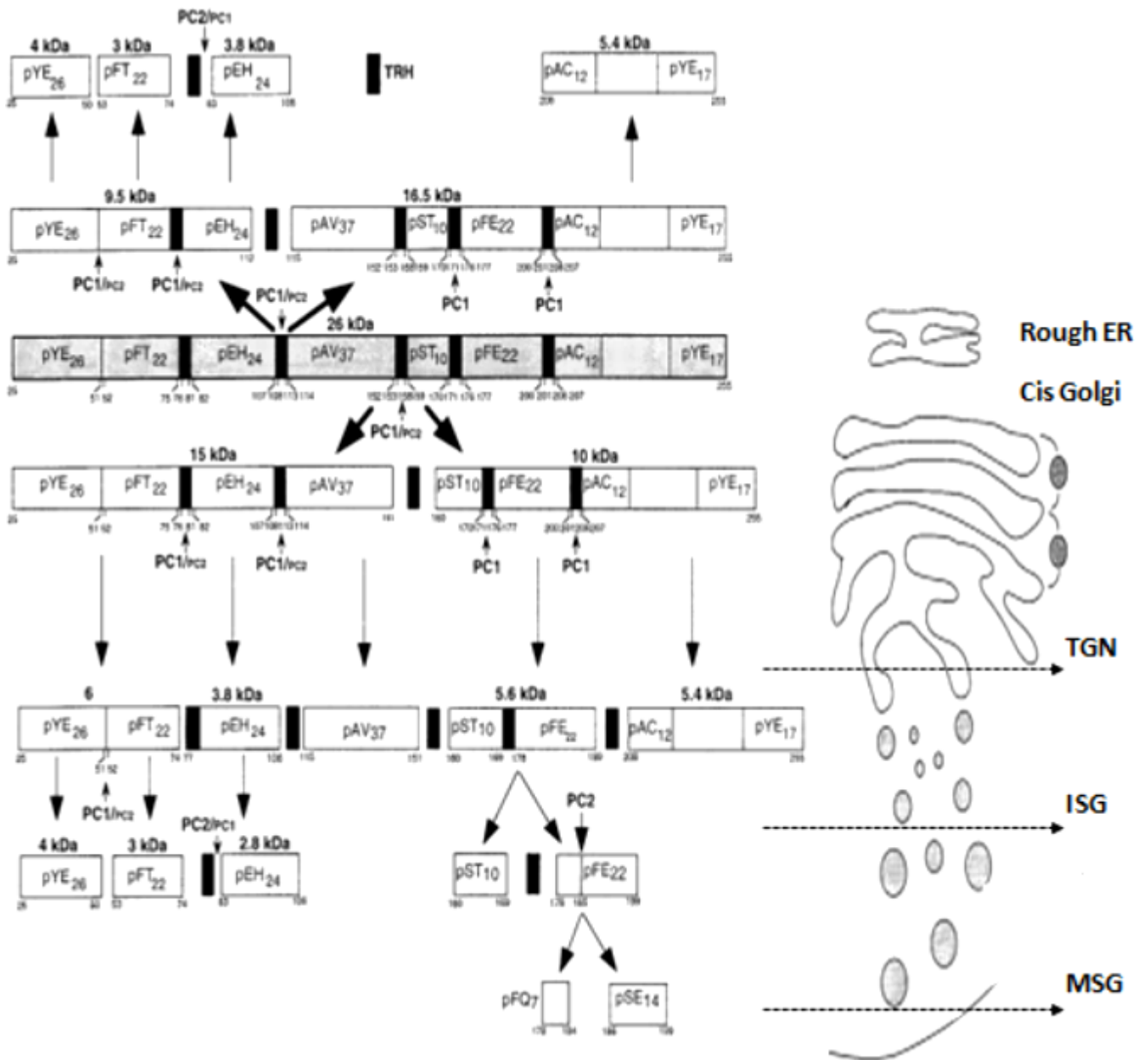
FIG. 1: Diagrammatic representation of the proposed processing model of rat pro-TRH to non-TRH peptides and TRH, and the postulated involvement of PC1 and PC2 as determined from our studies. The small arrows indicate PC1 and PC2 activity. Cleavage sites and direction of the processing cascade are indicated with longer arrows. Thicker arrows indicate that most of the initial cleavage of the intact precursor was produced at this site. The positions of paired basic residues are indicated by numbers. Non-TRH peptides are indicated in the shaded pro-TRH molecule, and TRH is indicated by a black rectangle. On the right, a cartoon showing the distribution of organelles within the regulated secretory pathway. TGN, trans-Golgi-network; MSG, mature secretory granules; ISG, immature secretory granules. (9)

Anatomical localization of proTRH and proTRH-derived cryptic peptides in the rat tuberoinfundibular system

Extended forms of the TRH progenitor sequence located in both the 5.6 kDa and 5.4 kDa fragments of the C-terminal portion of the TRH prohormone, and the cryptic peptides prepro-TRH$_{25-50}$ and prepro- TRH$_{53-74}$ derived from the N-terminal fragment of proTRH have been found by immunocytochemistry and in situ hybridization histochemistry in neurons and fibers of the rat tuberoinfundibular system. Specifically, these neuropeptides were identified in the medial and periventricular parvocellular subdivisions of the hypothalamic paraventricular nucleus, and external layer of the median eminence (9, 21). Due to their distribution, it is expected that they could physiologically be available in the portal blood to reach the anterior pituitary cells. Consistently, *in vitro* studies using dissected median eminence from thyroidectomized, hypothyroid rats have shown that both mature TRH and N-terminal fragments of proTRH (pYE27 and pFT22) are released under depolarization conditions (Fig.2) suggesting a role for these cryptic peptides in the regulation of the anterior pituitary cells (9, 22), primarily in conditions of reduced levels of circulating thyroid hormone
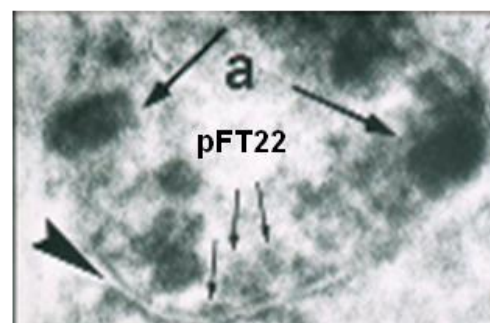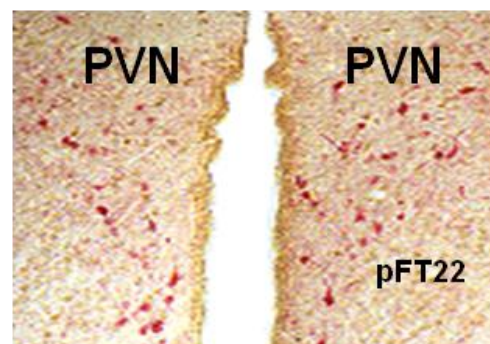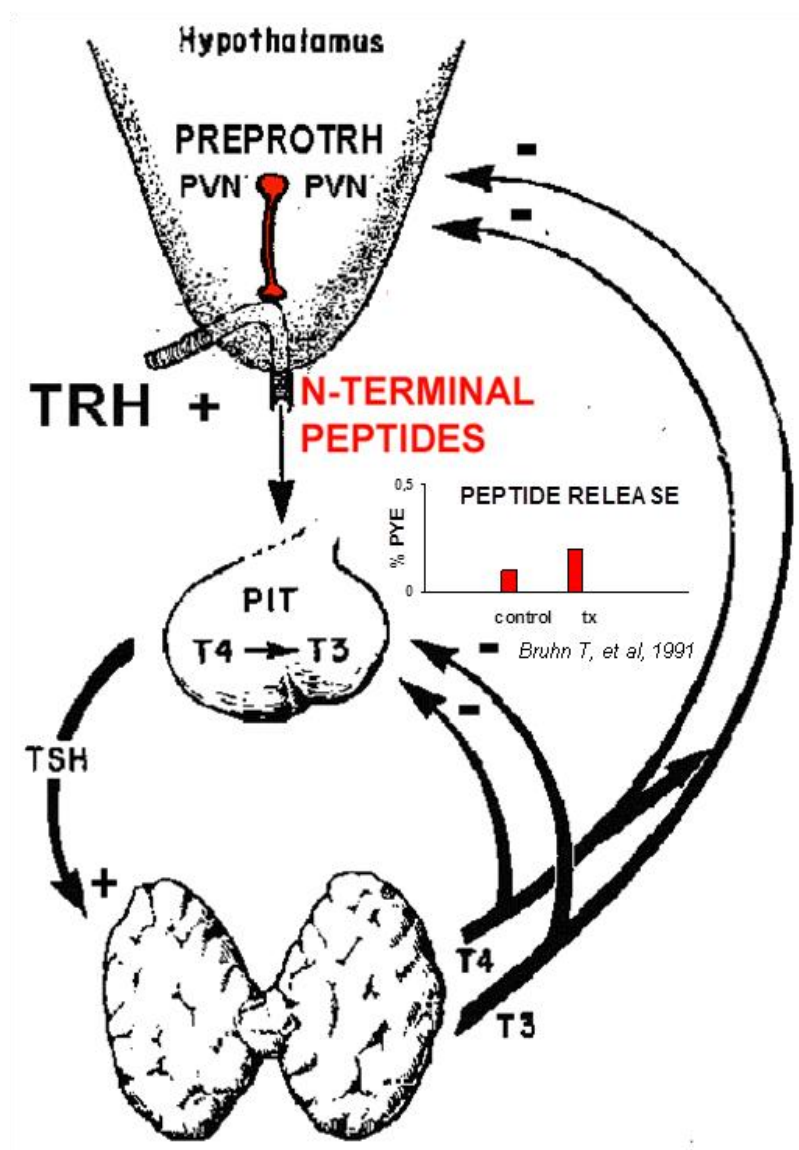
FIG. 2.

Presence of TRH, proTRH, and cryptic nonTRH fragments in the rat anterior pituitary cells

In intact adult, male rat pituitaries TRH immunoreactivity (IR) was localized in secretory granules of thyrotrophs, gonadotrophs and corticotrophs (23). Consistently, IR-TRH was found in a population of adult rat pituitary cells in primary monolayer culture, remaining detectable up to 3 weeks (23). Possible cellular sources have been shown to be both gonadotrophs (23, 24) and corticotrophs (23, 24, 25).

Similar, proTRH mRNA and the nonTRH cryptic peptide preproTRH$_{25-50}$ (pYE27) were identified in long-term (18 days) primary monolayer cultures of 15-days-old male rats. In particular, levels of proTRH mRNA resulted comparable to those in the whole hypothalamus. In addition, a substantial increase in cellular GH content (around 46% above control values at initial culture times) occurred at the end of the culture period, suggesting that the site for anterior pituitary proTRH biosynthesis could be the somatotrophs. Indeed, combined in situ hybridization for proTRH mRNA and immunocytochemistry (IC) for GH revealed their colocalization in a subpopulation of somatotrophs. In contrast, no other anterior pituitary cell type proved to be co-localized with proTRH. Consistently, pYE27 was observed in secretory granules of a subpopulation of anterior pituitary cells (Fig. 3), likely corresponding to somatotrophs (26).
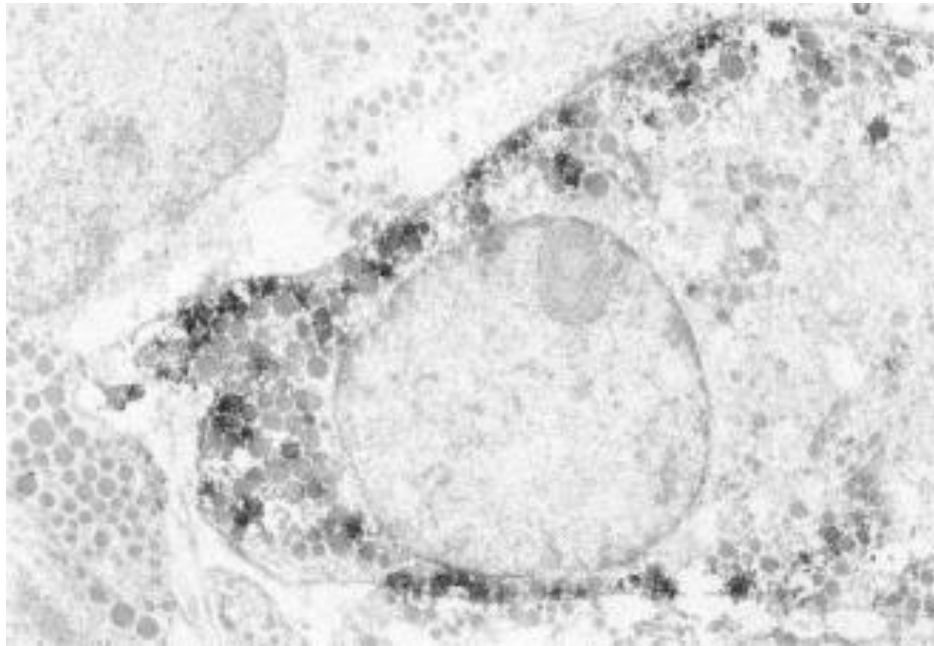
FIG. 3: EM analysis of a pro-TRH-positive anterior pituitary cell. ICC for prepro-TRH-(25-50). Note that a subpopulation of secretory granules contains prepro-TRH-(25-50). Scope magnification, X3257; print magnification, x9160 (26).

The possibility that proTRH processing and secretion of both TRH and nonTRH cryptic peptides occur inside anterior pituitary cells as a physiological event has been indirectly studied by comparing the capacity of dissociated versus re-aggregated anterior pituitary cultures to *in vitro* synthesize proTRH and release TRH in the culture medium (24, 27). Results showed that proTRH biosynthesis in gonadotrophs and, likely somatotrophs in culture occurred as a mechanism of "derepression" from a normal repressed state present in the intact pituitary, as opposed to a *de novo* induction.

This phenomenon raises the possibility that "derepression" might also takes place *in vivo,* as a compensatory mechanism in conditions requiring effects of TRH beyond the classical regulation of thyroid hormone secretion. In particular, since proTRH mRNA expression occurs in human, anterior pituitary adenomas (28, 29) it is tempting to speculate that TRH itself and/or its associated nonTRH cryptic peptides might play an autocrine / paracrine regulatory role for growth and proliferation of adenomatous pituitary cells. Indeed, growth of adenomatous cells is associated with profound structural re-arrangement of the affected pituitary tissue and of the tissue surrounding the tumor, thus representing an ideal condition for a compensatory mechanism of transcription based on "derepression". This would also be consistent with the evidence that proTRH and pYE27 are expressed in growing somatotrophs of young animals, where they might contribute to an autocrine / paracrine regulation of anterior pituitary cell growth towards an adult size (26, 27). Finally, a regulatory role of this "derepression" seems confirmed by the evidence that it can occur in the presence of a classical hormone-receptor interaction, like that occurring when GnRH was administered and equally mimicked by depolarizing agents (K^+, calcium ionophores). Indeed, all these condition are able to induce a regulated release of TRH and pYE27 from anterior pituitary cells in culture (27, 24), as expected in the case of their involvement as autocrine / paracrine regulators of pituitary cell growth.

Further momentum to this hypothesis comes from the evidence that both glucocorticoids and thyroid hormones resulted paradoxically able to stimulate the biosynthesis of proTRH and release of TRH and pYE27 in culture media of primary pituitary cultures responding with increased expression of the protoncogene c-fos and c-jun, in association with increased cellular expression and content of GH. This has suggested that such a tissue-specific response was evidence for increased activation of somatotrophs (30-32) and share similarities with the effect of TRH in adenomatous, somatomammotroph cell lines (33-35).

Known functional role of cryptic fragments derived from preproTRH

Very few data are available on the biological activities of the pro-TRH-derived peptides, and clues to the roles of these peptides may be suggested, at least partially, by an examination of their regional distribution and evidence of regulation under specific physiological and pathological conditions.

prepro-TRH$_{160-199}$ (pST10)

Prepro-TRH$_{160-199}$ (also known as Ps4 and TRH-potentiating peptide) is the best characterized of the non-TRH cryptic peptides. It is released from rat hypothalamic slices and median eminence under depolarizing agents,

thus making it a potential candidate for an hypophysiotropic role (36). In particular, it enhances TRH-stimulated TSH release from the anterior pituitary (12) and stimulates TSHβ gene promoter activity (37, 38). Ps4 receptors in the rat anterior pituitary are localized primarily on the folliculo-stellate cells. It is conceivable that Ps4 can regulate the secretion of a paracrine factor by these cells to be released in the pituitary interstitium, which in turn would be responsible for enhancing the response of TSH cells to TRH (39, 40). Alternatively, folliculo-stellate cells may mediate the effect of Ps4 on TSH release by means of outputs passing through gap junctions (41).

prepro-TRH$_{178-199}$, prepro-TRH$_{178-185}$, prepro-TRH$_{186-199}$

Prepro-TRH$_{178-199}$ has been reported to be a corticotroph-inhibiting factor, able to reduce POMC mRNA and inhibit ACTH release (42, 43). Specifically, prepro-TRH$_{178-199}$ inhibits stress-induced ACTH and corticosterone release (43), and may also act as a PRL secretagogue in primary rat pituitary cultures (9, 10).

Similar to prepro-TRH$_{178-199}$, the intermediate products prepro-TRH$_{178-185}$ and prepro-TRH$_{186-199}$ stimulate the release of PRL from primary rat pituitary cultures, suggesting that an amino acid sequence necessary for PRL regulation is contained within this peptide sequence (9, 10).

prepro-TRH$_{83-106}$ and prepro-TRH$_{208-255}$

Prepro-TRH mRNA is increased in the periaqueductal gray (PAG) during opiate withdrawal (44, 45). In similar conditions, peptide analysis shows also an accumulation of the N-terminal peptide prepro-TRH$_{83-106}$, and a reduction of the C-terminal peptide prepro-TRH$_{208-255}$, with respect to control animals (46). Opiate withdrawal also increases prepro-TRH$_{83-106}$ in the lateral hypothalamus (9).

prepro-TRH$_{53-74}$ (pFT22)

Prepro-TRH$_{53-74}$ (pFT22) is a 3-kDa peptide derived from the N-terminal flanking peptide (prepro-TRH25–50-R-R-prepro-TRH53–74), further cleaved at the C-terminal side of the arginine pair site, and released from the median eminence (ME) and isolated anterior pituitary cells in response to depolarizing concentrations of K$^+$ (22).

a.   pain modulator

Prepro- TRH$_{53-74}$ displays a unique localization in the rostral two-thirds of the ventrolateral PAG (47, 48). Electrical stimulation or injection of excitatory amino acids into this region produce analgesia (49, 50), and this region is very sensitive to the development of morphine-induced antinociception (51). Although the lateral PAG is more commonly associated with non-opioid-mediated antinociception (52), there is limited evidence that non-opioid

antinociception is also mediated within the ventrolateral PAG (53). Thus, prepro- TRH$_{53-74}$ might either be a candidate molecule to mediate non-opiate pain perception in this region or to play a modulatory role in opiate-mediated pain mechanisms (48, 54). Confirmation of this possibility is offered by the evidence that   prepro-TRH mRNA in highly expressed in the reticular nucleus of the thalamus, PAG, raphe nuclei, and to a limited extent dorsal horns of the spinal cord, all structure involved in pain regulation (55).

b.   growth factor

Very preliminary studies from our group have suggested that pFT22 might act as a regulatory factor for growth of rat anterior pituitary cells (56, 57), raising the possibility that it could also be involved in inducing proliferation of adult anterior pituitary stem cells.

c.   unknown functions

Outside of the central nervous system (SCN), prepro- TRH$_{53-74}$ has been detected into developing, rat β-cells of the pancreas and thyroid parafollicular cells (58, 59, 60). However, no data are available for its role in these sites.

GH4C1 rat adenoma cells as model of somatomammotroph secretion and proliferation

GH4C1 are a rat adenoma pituitary cells line (Rattus norvegicus) derived from clonal expansion of another pituitary cell line, GH3 cells (61, 62). GH4C1 are hypertriploid cells with the modal number of 65, including a range from 60 to 68 chromosomes. In standard culture conditions, this cell line grows loosely adherent with floating clusters, and secretes GH and PRL. In particular, both hormones are released at comparable rates although PRL secretion (0,006 - 0,012 μg/mg protein/day) results more variable than that of GH (0,06 μg/mg protein/day). Both hormones can be induced by steroids and numerous peptides added to the culture medium (63).

a.   Regulation of secretion

In GH4C1 cells, TRH 10^{-7} M administration can induce both PRL and GH secretion in a biphasic manner. Specifically, it stimulates PRL and GH release within 5 s without a detectable lag period, reaching the highest peak (250-700% of basal secretion) in the following 8 minutes (first phase), to decline sharply at about 150% of basal secretion thereafter (second phase). Both phases are, at least partially, dependent on extracellular Ca^{2+} (33, 34). In fact, preincubation of the cells in Ca^{2+}-free medium significantly depresses the secretion of both hormones. Over a 2-days period, a single TRH dose (as

above) still maintains an increase in PRL synthesis but it is no more able to sustain that of GH, that is inhibited (34).

Within an interval of 6 days, TRH administration depicts an effect similar to that of EGF administration. In particular, both peptides can increase the synthesis and release of PRL, while inhibiting that GH. TRH 10^{-7} M alone causes a 15% decrease in GH production, whereas EGF10^{-8} M causes a 40% decrease. The effects of TRH and EGF on PRL stimulation and GH inhibition are additive (Fig. 4). Furthermore, similar effects on GH and PRL secretion have been observed with fibroblast growth factor 10^{-8} M (FGF) treatment, meanwhile neither insulin 10^{-7} M nor multiplication stimulating activity (MSA) 1,5 x 10^{-8} M alter PRL synthesis (Fig. 5) (35).
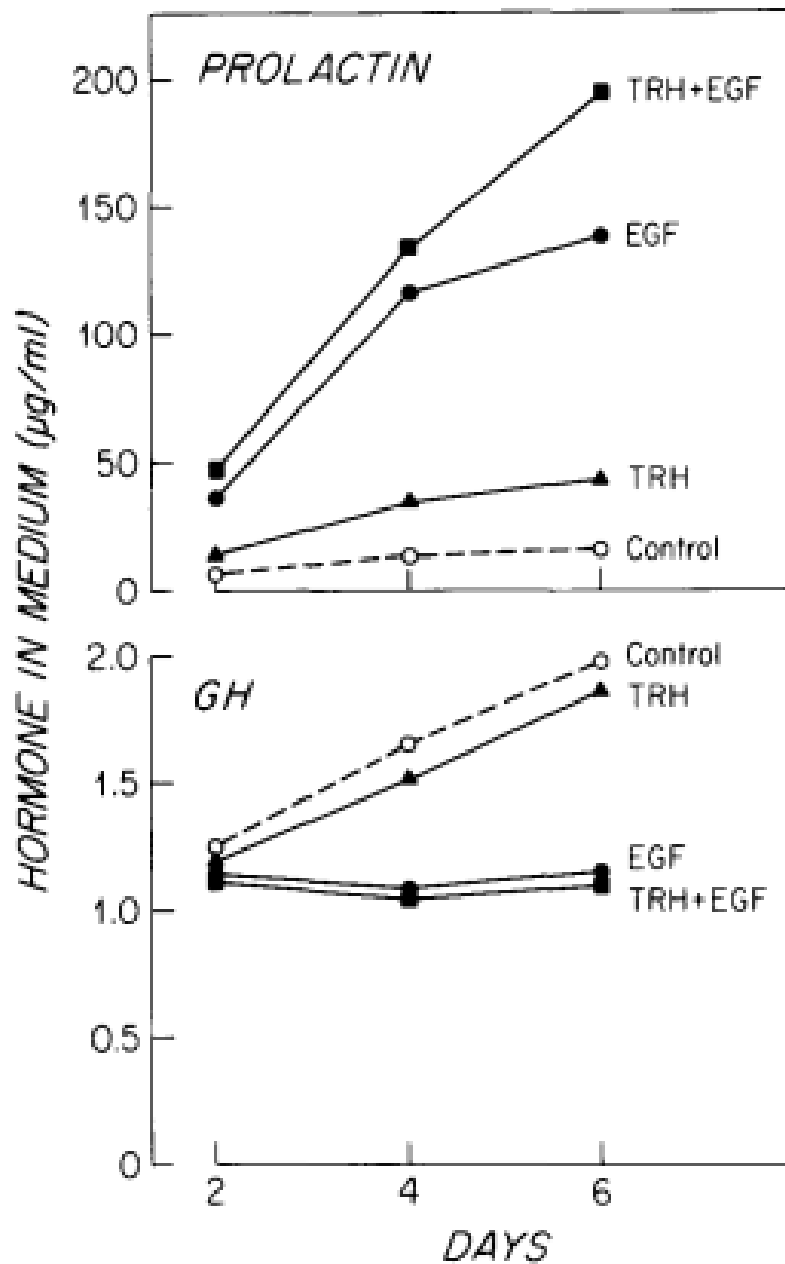
FIG. 4: Effect of EGF alone, TRH alone, and EGF plus TRH on hormone production. GH4 C 1 cells were plated at a density of 10' cells/35-mm dish . 3 d after plating, cultures were fed with fresh media without any additions (0) or containing TRH 10^{-7} M (▲),EGF10^{-8} M (●), or both peptides (■). Medium from replicate dishes was harvested every 48 h, and fresh medium with or without the peptides was added to the remaining dishes. The content of prolactin (top panel) and growth hormone (bottom panel) was determined for each 48-h collection as described in Materials and Methods. Each point gives the mean value of duplicate dishes. The range did not exceed ±l0% of the mean value (35).

23
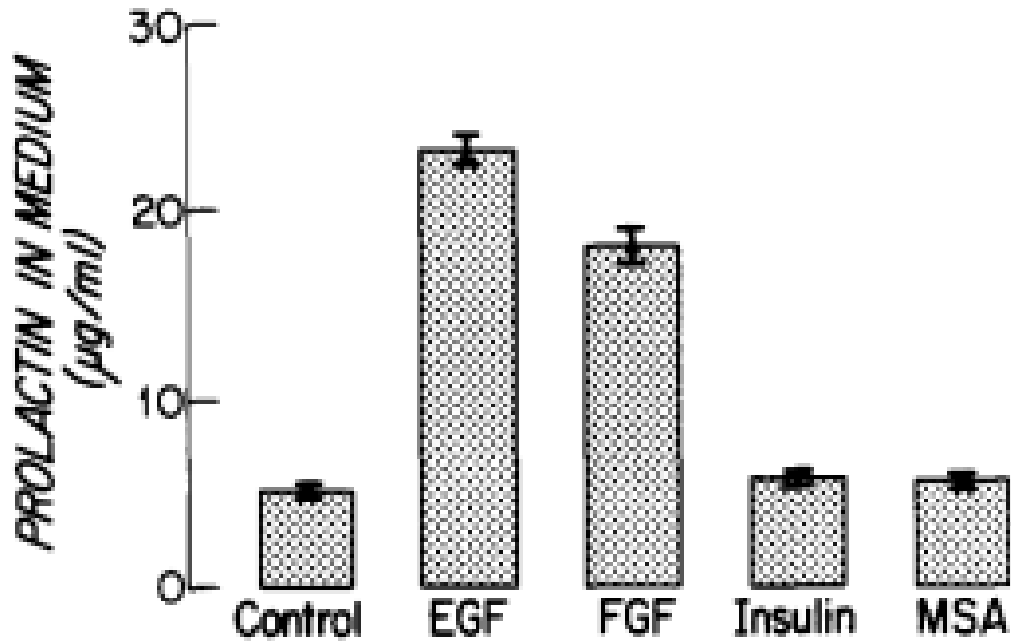
FIG. 5: Effects of different growth factors on prolactin production by GH4 C1, cells. GH4 C1, cells were plated at a density of 1 .4 x 10' cells/35-mm dish. 3 days after plating, cultures were fed with fresh medium containing either no additions or EGF10^{-8} M, FGF 10^{-8} M, insulin 10^{-7} M, or MSA (1,5 x 10^{-8} M). After 3 d, media were collected and prolactin was determined as described in Materials and Methods. Each bar gives the mean value of triplicate dishes and the brackets show the standard deviation (35).

Secretion of PRL can also be induced by a combination of insulin (180nM) and estradiol (1nM), although no effect is detectable with each single hormone. The combination yields a 190% increase in intracellular PRL, and a 50% increase in extracellular PRL above control. These responses are concentration-dependent (64).

Finally, a significant increase of PRL secretion has been observed using 1 nM T3 (118% increase above the control values) (65 - 68).

b. Regulation of cell growth

Treatment of GH4C1 cells for 6 days with EGF10^{-8} M decreases by 30-40% both the rate of cell proliferation and the plateau density reached by cultures. Inhibition of cell proliferation was accompanied by a change in cellular morphology, from a spherical appearance to an elongated flattened shape and by a 40-60% increase in cell volume. These actions of EGF are qualitatively similar to those of TRH 10^{-7} M which decreases the rate of cell proliferation by 10-20%, and causes a 15% increase in cell volume. The presence of supramaximal concentrations of both EGF10^{-8} M and TRH 10^{-7} M results in greater effects on cell volume and cell multiplication than either peptide alone (Fig. 6).
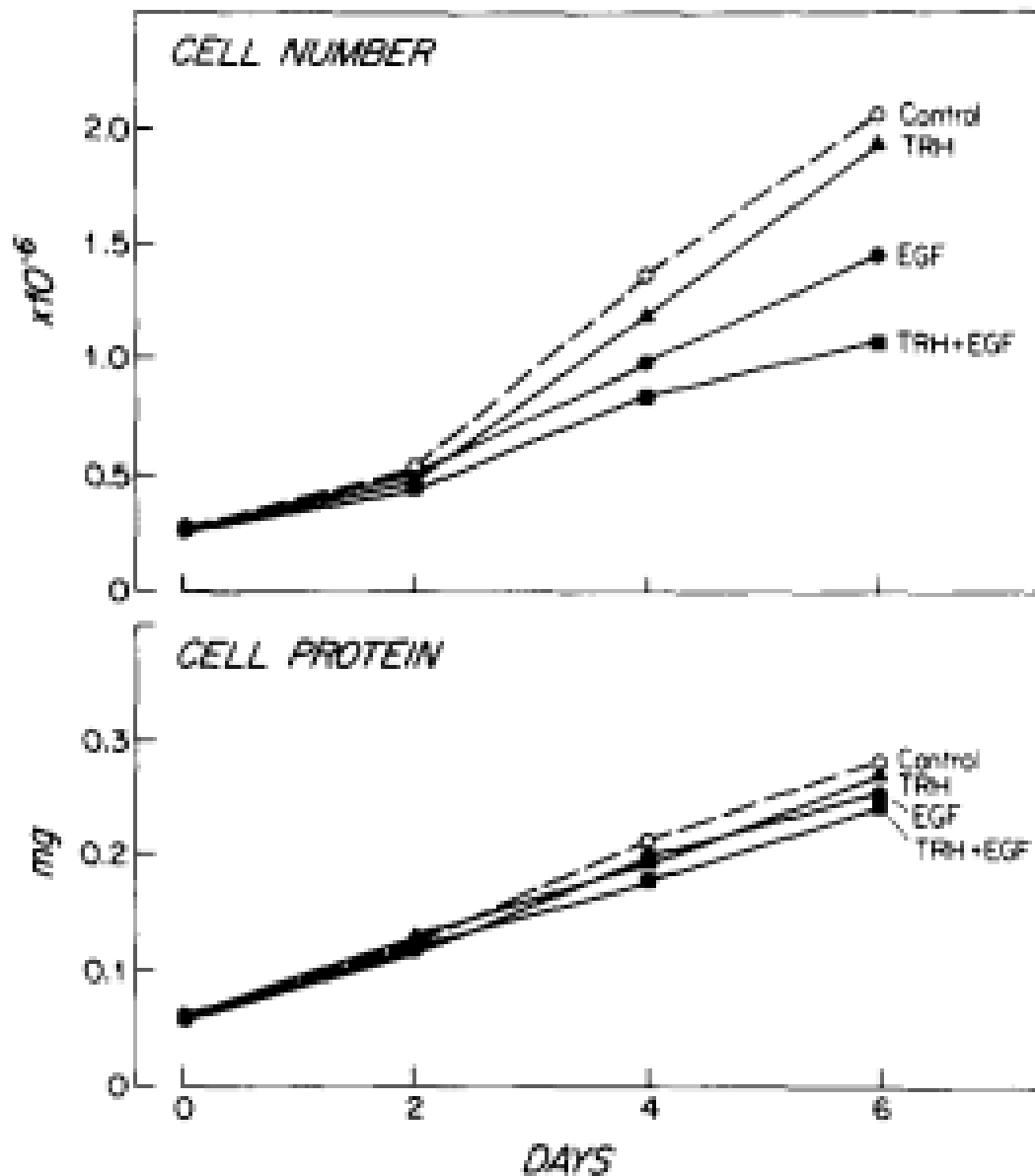
FIG. 6: Effect of EGF and TRH on cell proliferation and cell protein. GH4C1 cells were plated at a density of 10^5 cells/35-mm dish . 3 d after plating, cultures were fed with fresh media lacking any additions (O) or containing TRH 10^{-7} M (▲),EGF10^{-8} M (●), or both peptides (■). Replicate dishes were harvested every 2 d, and fresh medium with or without the peptides was added to the remaining dishes. Cell number (top panel) and total cell protein (bottom panel) per dish were determined as described in Materials and Methods. Each point gives the mean value of triplicate dishes. The standard deviation did not exceed $\pm$ 5% of the mean for cell number determinations and $\pm$ 10% of the mean for protein measurement (35).

FGF, too, increases cell volume and decreases cell proliferation, and the magnitude of these changes results smaller than that caused by EGF. Insulin and MSA have no effect on cell growth or cell volume (35). Similar, both insulin and estradiol decrease cell number 10 - 20 % with respect to the control, raising it up to 25 -30 % when used in combination (Fig. 7). The reduced cell number after hormone treatment results from both a decreased rate of proliferation, and a reduction in final density that the cells reach at plateau (64). Similar, insulin and estradiol modify the pattern of growth: in fact, treated cells never reach subconfluence but grow in small clumps piled on top of each other (69). All these effects are concentration-dependent (64).
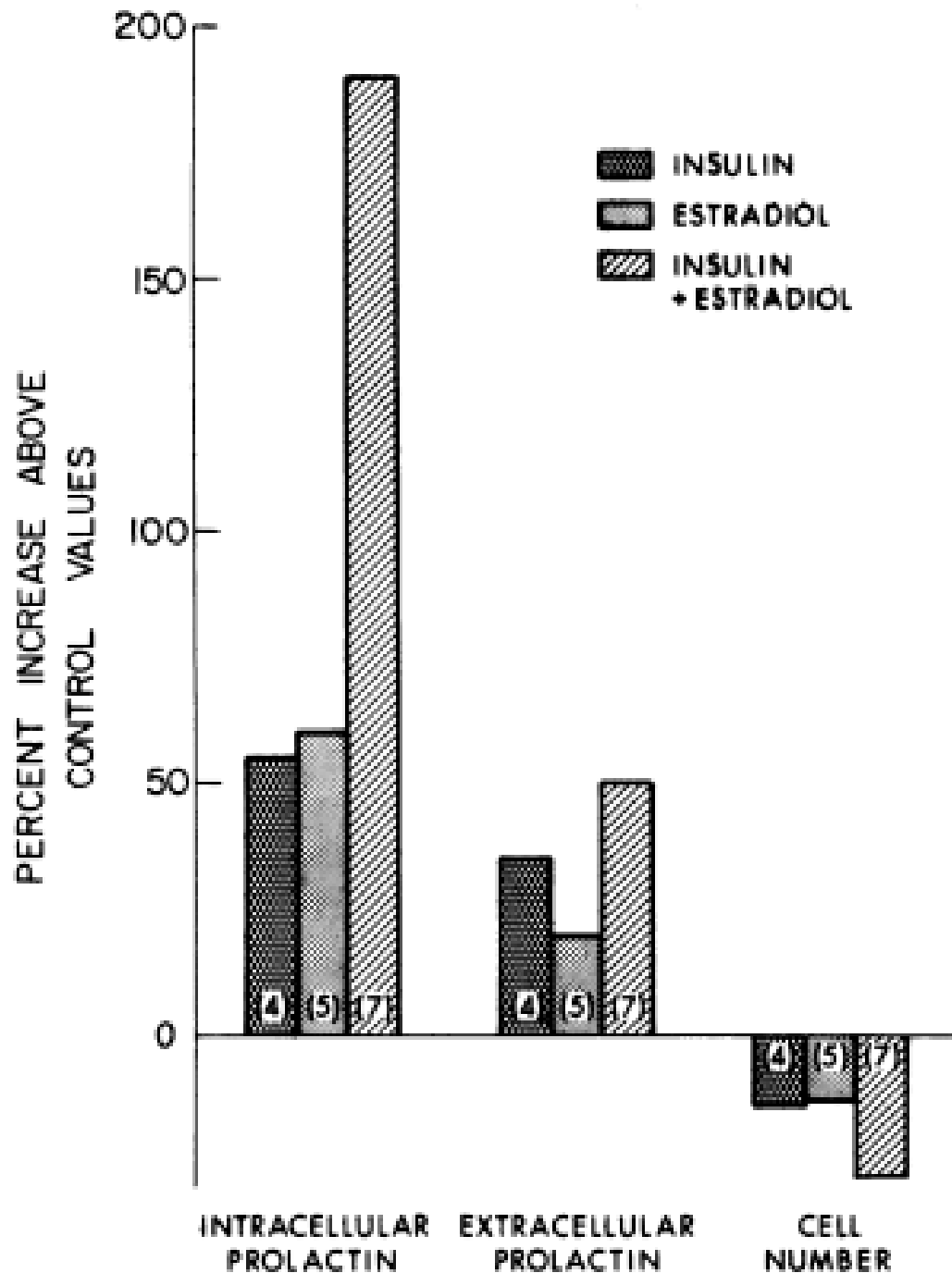
FIG. 7: Effects of insulin, estradiol, and insulin plus estradiol on prolactin and cell number. GH4C1 cells were plated at 10^6 cells/35 mm tissue-culture well and treated for six days with 180 nM insulin, 1 nM estradiol, or insulin and estradiol together. Each bar represents the mean of several independent experiments, the number of which are indicated within each bar. Measurements of intracellular and extracellular prolactin were normalized to cell number before the ratio of hormone- treated to controls was calculated. Control values averaged 0.86 μg/10^6 cells for intracellular prolactin, 15.7 μg/(10^6 cells 48 hours) for extracellular prolactin, and 2.75 x 10^6 cells/well (64).

In experiments performed in a medium completely depleted of thyroid hormones and supplemented with T3 at different concentrations (up to 0.025 nM) a significant increase in the rate of cell division was detected. Higher T3 concentrations had opposite effects, by reducing cell growth to control levels (65).

Using a serum-free medium (designated TRM-1) supplemented with 10 pg/ml bovine insulin, 10 µg/ml human transferrin (Tf), 10 ng/ml selenous acid, 10 nM T3, 50 µM ethanolamine (Etn), and 500 µg/ml bovine serum albumin, a variety of other substances have been tested for their effects on growth of GH4C1 cells. At up to 50 ng/ml, platelet-derived growth factor (PDGF), parathyroid hormone (PTH), and TRH had no positive or negative effects. GH itself (130 µM) showed only a slight stimulation (*i.e.* 15%) of cell number. EGF (10 ng/ml) confirmed its increasingly inhibitory effect on cell growth, similar to bFGF alone (5 ng/ml). The combination of both factors resulted in 80% inhibition of GH4C1 cell number over a period of 9 days of culture. In the same way, 10 ng/ml of acidic fibroblast growth factor (aFGF) was a very much less effective inhibitor than a similar concentration of bFGF (Fig. 8). These observations agree with those showing that bFGF was 30 to 50 times more biologically active than aFGF, as determined by receptor binding and cell growth assays (70, 71).
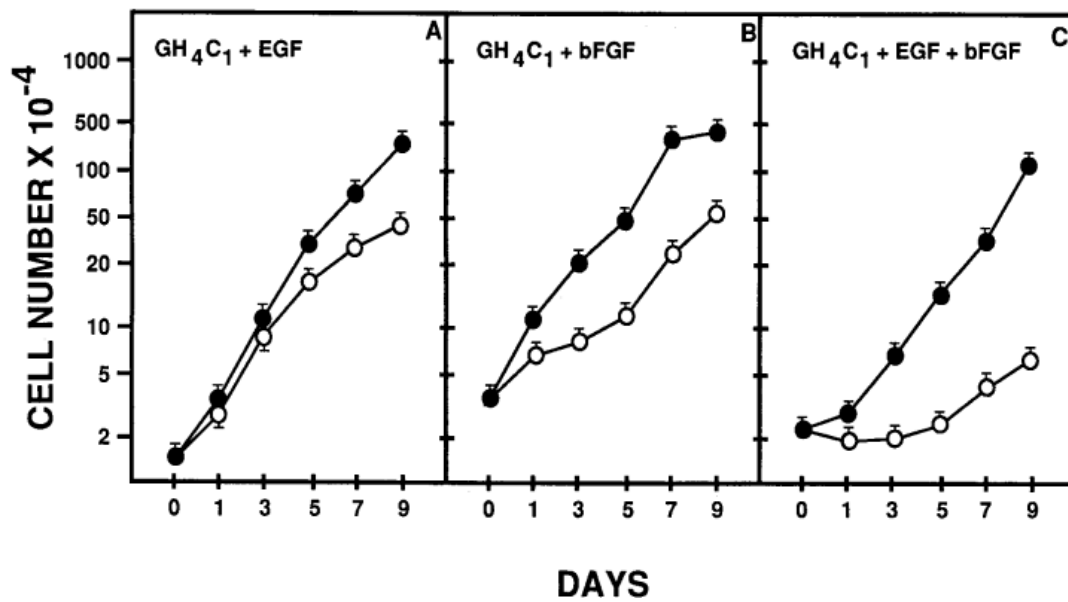
FIG. 8: Effects of EGF, bFGF, and the combination of the two factors on growth of the GH4C1 cells in TRM-1. In all three panels, cells were seeded at 0.5-3.0 X 104/35-mm diameter dish in 3.0 ml of TRM-1. A, EGF (10 ng/ml) added within 1 h of seeding. Additional concentrations of EGF (1.7 ng/ml) were added on Days 3 and 6. B, a similar experiment with addition of bFGF (5 ng/ml) at the start of the experiment and 1.7 ng/ml on Days 3 and 6 C, the experiment in which both EGF and FGF were added simultaneously as described in A and B. Al values are the means (±.SD, bars) of triplicate plates (70).

The effects of estradiol and T3 on growth of GH4C1 cells could be mediated by production of autocrine growth factors (67, 68). In particular, it has been shown that at a low population density (10.500 cells/cm^2) estradiol stimulates production of IGF-I by 4.2-fold. At this density, the antiestrogen tamoxifen (TAM) has no significant effect, whereas T3 stimulates IGF-I production by 3.3-folds, like in the parental GH3 cell line (72). Interestingly, at a low population density estradiol and T3 stimulate also the production of insulin like binding protein (IGFBP-3) by 6- and 11-folds, respectively. All these effects are neutralized by increasing the cell population (42.000 cells/cm^2 or higher) (Fig. 9) (68).
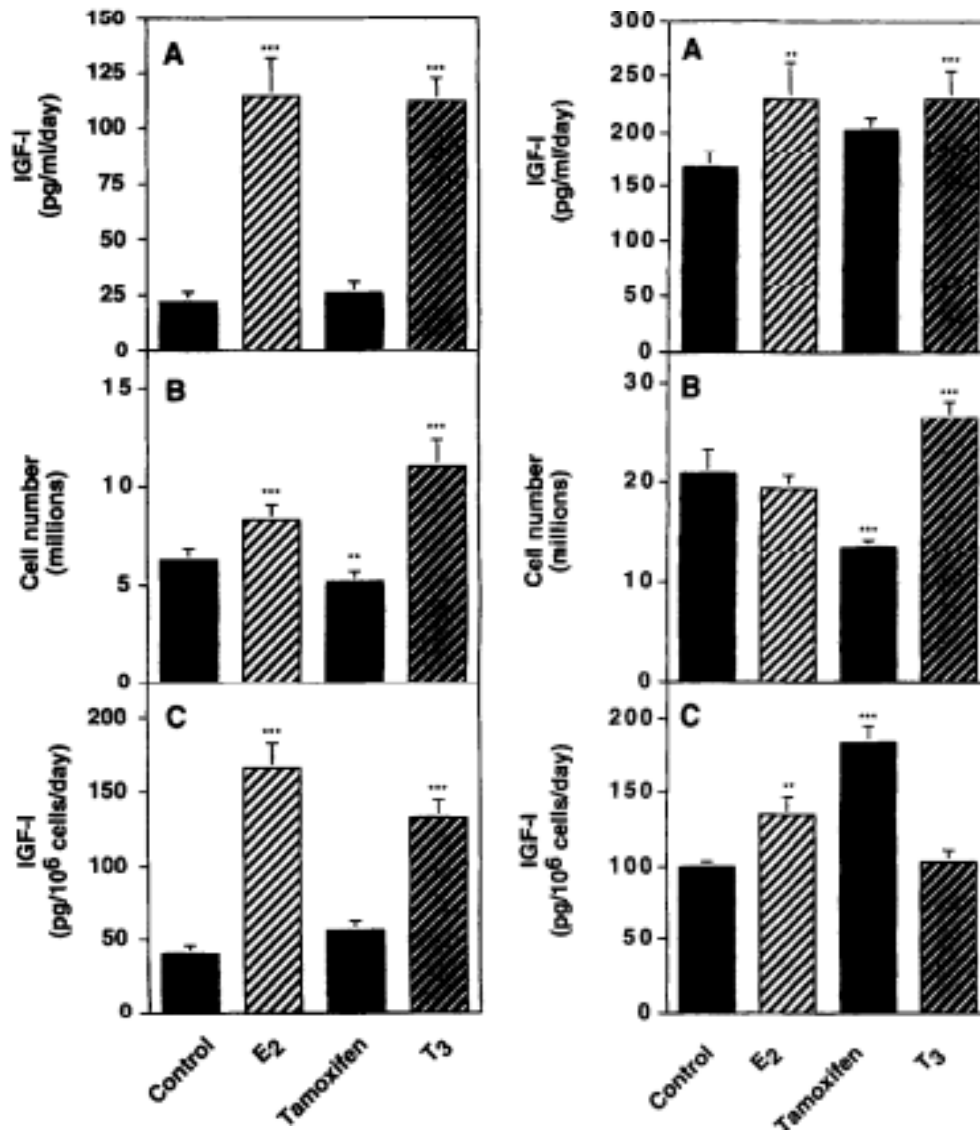
FIG. 9 (left): Effects of E2, TAM, and T3 on IGF-I production by GH4C1, cells cultured at the low population density. GH4C1 cells were plated at the low population density (10.500 cells/cm2) in phenol red-free DMEM/Fl2 medium supplemented with charcoal-stripped sera. Two days later, the culture medium was changed and treatments with 1 nM E2, 1 µM TAM, 10 nM T3, or vehicle were begun. Treatments were continued for 3 days, with the culture medium being changed daily. The cells were then incubated twice for 30 min at 37°C in serum-free medium supplemented with the appropriate hormones, and subsequently incubated in serum-free medium, again containing appropriate hormones, for 48 h. The latter conditioned media were collected, detached cells were removed by centrifugation, and the media were retained and stored at -20°C pending assay of IGF-I and IGFBPs. Adherent cells from each culture were harvested, combined with the detached cells, and total cell number per culture was determined using a Coulter counter. Conditioned media were acid extracted to remove IGFBPs and IGF-I was measured by RIA, all as described in Materials and methods. Data are expressed as: (A) pg IGF-I produced per ml culture medium per day; (B) total cells harvested upon termination of the experiment; and (C) pg IGF-I produced per 10^6 cells. Each data bar represents the mean ± S.E.M. from two independent experiments, each of which contained four to six samples

per experimental group. Statistical significance was determined using the general linear model and the Dunnett's t-test; **P < 0.01; ***p < 0.001.

FIG. 9 (right): Effects of E2, TAM and T, on IGF-I production by GH4C1 cells cultured at the high population density. Methods were as described in the legend to Fig. 9 left, except the GH4C1 cells were plated at the high population density (42.000 cells/cm2), and serum-free conditioned media were collected following 24 h. Data are expressed as: (A) pg IGF-I produced per ml culture medium per day, (B) total cells harvested upon termination of the experiment; and (C) pg IGF-I produced per 10^6 cells. Each data bar represents the mean f S.E.M. from three independent experiments, each of which contained three to six samples per experimental group. Statistical significance was determined using the general linear model and the Dunnett's f-test: **P < 0.01; ***P < 0.001 (68).

We conclude that the GH4C1 cell line may be considered a suitable neuroendocrine system to investigate *in vitro* the effect of unknown peptide factors on the growth rate and pattern of anterior pituitary cells of the somatomammotroph lineage, and to analyze how these factors may influence the proliferation rate in a model of pituitary adenoma secreting GH and PRL.

Aim of the study

The aim of the present study has been to investigate: 1) the existence of similarities (*i.e.* degree of identity) and homologies (*i.e.* common phylogenetic origin) in the amino-acid (AA) sequence of the N-terminal fragment of the rat TRH prohormone, prepro- TRH_{53-74} (pFT22) within proteins of Invertebrates and Vertebrates, man included. This, to understand to which degree pFT22 is maintained in different animal species, and whether it is evolutionarily conserved either in proTRH or other prohormones / proteins; 2) the putative three-dimensional (3D) molecular structure of pFT22 in aqueous medium, to mimic its conformational state in basic physiological conditions; 3) the *in vitro* cell growth effect of pFT22 on the adult male rat, anterior pituitary cells of the somatomammotroph lineage using as experimental model the GH4C1 adenoma cell line. This effect is studied in comparison with that of insulin growth factor I (IGF-1) chosen as a well established growth factor for anterior pituitary cells, primarily for rat somatotrophs; 4) the *in vitro* cell growth effect of pFT22 on adult male rat, primary monolayer cultures of anterior pituitary cells; 5) the development of different protocols for synchronization of GH4C1 cells, based on either serum deprivation or the administration of hydroxyurea at different concentrations. This, with the intent to obtain the largest pool possible of cells in quiescent state (G0-G1 phases of the cell cycle) as an ideal condition for further investigations on the pFT22 growth effect.

The results of this study are expected to clarify whether the nonTRH cryptic sequence of rat proTRH, prepro- TRH$_{53-74}$ may exert a regulatory action on growth and proliferation of rat anterior pituitary cells, in particular on the somatomammotroph lineage and whether this effect is observable in pituitary adenoma cells like the GH4C1 cell line. Applications of these results to the understanding of autocrine / paracrine regulatory mechanisms operating in growth hormone-secreting pituitary adenomas, to the regenerative medicine of anterior pituitary, and to the *ex situ* bioengineering of a bioartificial pituitary gland are discussed.

MATERIALS AND METHODS

Bioinformatics studies

The search for AA similarities, *i.e.* the degree of identity between AA in different protein sequences, and that of homologies, *i.e.* protein sequences that share a common evolutionary ancestor, was carried out for the rat pFT22 within the Invertebrate and Vertebrate lineages, man included (73). This study was performed in collaboration with Prof. Riccardo Percudani, Dept. of Biosciences, University of Parma, Parma, Italy using a well established bioinformatic procedure.

In a first step, to obtain the FASTA format (*i.e.* each AA in a single-letter code) of pFT22, the entire 29 kDa rat preproTRH sequence was requested in FASTA codex using the UniProtKB database, that yielded the accession number P01150. In a second step, following retrieval of the pFT22 FASTA format from the complete preproTRH sequence, multiple alignments of Invertebrate and Vertebrate proteins were performed using the algorithm BLASTP (Protein Protein Basic Local Alignment Search Tool), that allows for comparison between different AA sequences. Specifically, pFT22 FASTA sequence was used as a query input, setting the following scoring parameters: a) non-redundant protein sequences (nr); b) a maximal threshold of 10 e^{-3} for an expected value (E-value), and c) a matrix BLOSUM 62. FASTA sequences of proteins with a significant E-value were included in a .txt file, that was opened in the CLUSTALX 1.81 software for their alignment

in comparison to the query sequence, *i.e.* to pFT22. To visualize the identities of the alignments, an .aln file was obtained from CLUSTALX, and further imported in GeneDoc software.

In addition, the evolutionary relationships between the AA sequences having identities with pFT22 were determined based on the same .txt file of the aligned FASTA sequences (see above), used to generate a Neighbor Joining phylogenetic tree.

Finally, to get information on the chemical-physical properties of pFT22, the ProtParam software was used.

Circular Dichroism

The putative, 3D secondary structure of pFT22 in aqueous medium was investigated using the circular dichroism spectrometry. All experiments were carried out in collaboration with Prof. Lorella Franzoni, Section of Biochemistry - Dept. of Biomedical, Biotechnological, and Translational Sciences, University of Parma, Parma, Italy.

Samples of 10 μM and 30 μM, synthetic pFT22 (American Peptide Company n. 58-0-92) were dissolved in a crystal cuvette with an optical pathway of 2 mm, using distilled water as a solvent. PFT22 solutions were analyzed using a Jasco J-715 spectropolarimeter, equipped with a Peltier system (PTC-348 WVI) for temperature control. Spectra were collected at a constant temperature of 298 K; parameters were set as follows: band width 2

nm, speed 50 nm/min, response 4 sec and data pitch 0.5 nm. The far-UV (190-250 nm) absorption band was used as the response to the polarized light stimulus. The pure water signal was used as a baseline, and subtracted by the sample signal to get the final spectrum of the peptide. All data were collected as the mean of three separate recordings.

Cell cultures

a.   rat, mouse, and human cell lines

GH4C1 rat pituitary, adenoma cells (courtesy of Stephanie Lee MD, PhD., Section of Endocrinology, Nutrition and Diabetes, Boston University School of Medicine, Boston, USA) were grown in Ham's F10 w/o glutamine medium (Aurogene, AU-L0145) supplemented with horse serum (HS) 15% (AU-S0900) and fetal bovine serum (FBS) 2.5% (AU-S1810).

Swiss 3T3, mouse fibroblasts (courtesy of Prof. Lucio Cocco, Cell Signalling Laboratory, Dept. of Biomedical and Neuromotor Sciences, University of Bologna School of Medicine, Bologna, Italy) were grown in Dulbecco's Modified Eagle's Medium high glucose (D5671 Sigma) supplemented with FBS to a final concentration of 10%.

Hep G2, human hepatocellular carcinoma cells (courtesy of Prof. Prisco Mirandola and Marco Vitale, Section of Human Anatomy, Dept. of Biomedical, Biotechnological, and Translational Sciences, University of Parma, Parma,

Italy) were grown in Eagle's Minimum Essential Medium with Earle's Salts (ECB2071L) supplemented with FBS to a final concentration of 10%.

All cell cultures were seeded in monolayer at a density of 40.000 cells/cm^2 and grown to subconfluence in their respective media at 37°C in humidified atmosphere and 5% CO2, before the beginning of each experiment. All growth media were supplemented with1% L-glutamine (AU-X0550), 1% nonessential amino acids (AU-XO557), 1% gentamicin (Sigma G-1397), 1% penicillin/streptomycin (AU-L0022) previously filtered with a 0,2 µm filter to ensure adequate sterility.

Swiss 3T3 and Hep G2 cell lines were used to set up fluorescence-activated cell sorting (FACS) studies in standard conditions, and in response to trophic stimuli.

b.   primary male rat, anterior pituitary cells

Sprague Dawley (SD) male rats (50-75 and 220-250 gr) were used as anterior pituitary donors. Animals were purchased from Harlan Ldt free of disease, and housed in the animal facilities of the Department of Experimental medicine - Section of Biochemistry of the University of Parma, Parma, Italy. Quarantine was made in plexiglas cages (38x20x18 cm) with wood shaving bedding under standard diet, at 22±2°C in a 12-hours light-dark cycle (light between 7.00 AM and 7.00 PM). All experimental procedures on the animals were conducted in accordance with the European Communities

Council Directive of 24 November 1986 (86/EEC), and the protocols approved by the Ethical Committee of the University of Parma.

Pituitary glands were removed aseptically from the sella turcica, and the anterior lobe separated from the intermediate and posterior lobes, maintaining intact the transitional zone, where adult anterior pituitary stem cells are localized (74). Tissues were then gathered in sterile Hank's Buffered Salt Solution (HBSS). Trunkal blood was collected from animal carcasses in 25 ml flasks, blood cells let to deposit overnight at 4°C, gently centrifuged (2000 rpm x 10-15 min), the overhead serum fraction removed, and stored at -20°C for cell culture media. After mechanical chopping of the anterior pituitary to obtain small size pieces, cells were incubated for 1 hour at 37°C in waterbath (under shaking) with 2mg/ml of collagenase type I (SIGMA). Tissues were then centrifuged at 1300 rpm for 3 min, the supernatant discarded, and cells submitted to a second digestion step using a solution of 0,25% trypsin-ETDA (SIGMA) / 0,1 mg/ml DNase I (SIGMA) for 30 min at 37°C in waterbath (under shaking). Cells were rinsed with HBSS and triturated with siliconized (Sigmacote SL-2, Sigma) fire-polished pipette and filtered through a 70μm mesh (BD Falcon) into a sterile conical centrifuge tube. The cells were centrifuged again at 1300 rpm for 3 min, and the supernatant discarded. The cellular pellet was resuspended in Dulbecco's Modified Eagle Medium (D-MEM; EuroClone S.p.A., Milano, Italy) low glucose, supplemented with 2,5% fetal calf serum, 3% horse serum,

10% rat serum (from sacrificed rats), 1% gentamycin, and 1% Nystastin. Media, sera, supplements and enzymes were previously filtered with a 0,2 µm filter to ensure adequate sterility. Cells were finally seeded in 25 ml Falcon flasks for 3 day at 37 °C in humidified atmosphere and 5% CO_2, then detached by trypsinization (0,25% trypsin-ETDA), and counted in a Neubauer chamber using Trypan blue as supravital dye, to be eventually seeded for experimental procedures (see below).

Analysis of cell proliferation based on DNA quantitation

Initially, the analysis of GH4C1 cells proliferation was carried out using the CyQUANT® Cell Proliferation Assay Kit (Invitrogen, C7026), based on the fluorimetric analysis of the DNA content in the cell population under study. Since the amount of DNA is proportional to the number of cells in the sample, an increase in the sample fluorescence measured as its optical density (OD) is believed to be proportional to the amount of cells, thus providing an indirect measurement of cell proliferation.

GH4C1 cells were seeded in Ham's F10 medium without serum, at a density of 40.000/cm^2 for 72h before treatment. Following serum starvation, a culture medium change was made, cells were incubated in medium Ham's F10 serum free, and treated with either 10 or 100 nM prepro- TRH_{53-74} (pFT22;). In separate experiments, cells were treated with either 10 or 100 nM IGF-1 (recombinant human IGF-1, PeproTech 100-11).

Negative controls were treated with buffer, added in amount equal to that of medium used to administer the peptides. Medium containing either pFT22 or IGF-1 was changed every 48 hs, up to 144 hs (*i.e.* up to 7 days). DNA content were measured every 24hs. At least three replicates for each condition were made.

DNA content of treated and control cells was analyzed as follows: 1) for each experimental point, multiwells were inverted, blotted onto paper towels to remove excess medium, washed carefully with 0.1 M phosphate buffered saline pH 7.4 (PBS), and stored at -70°C prior to lyse the cells; 2) after sitting at RT for 30 minutes, 200 µL of the CyQUANT® GR dye/cell-lysis buffer were added to each sample well, and incubated 5 minutes at RT, in the dark; 3) measurement of fluorescence for each sample was carried out using the fluorescence microplate reader, Victor 3V 1420 instrument (Perkin Elmer) with filters appropriate for an excitation λ of 485 nm, and an emission λ of 535 nm (fluorescein protocol). The results were expressed as the mean percentage of the OD of treated samples vs untreated controls.

Flow cytometric analysis of the cell cycle

The cell cycle of:

a) asynchronously growing GH4C1 cells, and following attempts of their synchronization with either serum deprivation (controls) or administration of hydroxyurea (Sigma, H 8627) at different concentrations;

b) asynchronously growing GH4C1, Swiss 3T3, HepG2 cell lines, and primary anterior pituitary cells from 225-250g animals (see above) following administration of either pFT22 or IGF-1;

all were investigated using Fluorescence Activated Cell Sorting (FACS), also known as flow cytometry. A Beckman Coulter Epics XL-MCL flow cytometer was used, equipped with an argon ion laser having emission λ of 488nm and an absorption λ of 605-635 nm, an FL3 sensor, and a CXP Analysis data analysis software. This software allows for detection of PI fluorescence intensity going beyond the linear scale of the FL3 channel of the cytometer, *i.e.* corresponding to a DNA content on the abscissa higher than 9n, using a logarithmic scale transformation.

In initial studies, cell ploidy was investigated using the supravital dye, propidium iodide (PI) (Sigma-Aldrich, λ absorption of 480nm, λ emission of 620nm), which binds to DNA obtaining the percentages of cells in the G0-G1 and G2-M phases of the cell cycle, up to 120 hs. In other studies, the entire cell cycle kinetic of cells treated with growth factors every 48hs was analyzed up to 96hs, using a bivariate bromodeoxyuridine (BrdU) / DNA analysis in flow that combines the detection of newly synthesized DNA (S phase, detected by the thymidine analogue BrDU) with that of total DNA (G0-G1 and G2-M phases, detected by PI). To increase the interphase incorporation of BrDU (Sigma B5002) in the nucleus, measurements were done following

inhibition of the enzyme thymidylate synthase with fluorodeoxyuridine (FldU, Sigma F0503). BrdU was visualized using a FITC-conjugated, monoclonal mouse anti-BrdU antibody (BD Pharmigen Set n., 556028, λ absorption at 495nm, λ emission at 521nm).

Specifically, cells were initially incubated with 15 µM BrdU/ 1,5 µM FldU into the culture medium either 24 hs for GH4C1 or 12 hs for primary cultures before the FACS analysis, respectively to allow for nuclear incorporation of BrdU. In a second step, cells were collected, fixed in ethanol 70% for 1h, and washed in PBS. In a third step, cells were treated in the dark with 4 N HCl containing 0.5% (vol/vol) Triton X-100 for 30 min at RT, to permeabilize the cells and open the DNA double helix. After washing in PBS and pelletting by centrifugation at 500g for 10 minutes, the samples were neutralized with 0.1 M sodium tetraborate (pH 8.5) for 5 minutes at RT, washed again in PBS, centrifuged, the resulting pellets resuspended in 10% normal goat for 30 minutes at RT, and washed again in PBS containing 0.5% (vol/vol) Tween 20. After a new pelletting, cells were resuspended in either 20µl of FITC mouse IgG1 κ isotype (51-3540X-2) as a control, or in 20µl of FITC mouse anti-Brdu (51-33284X), for 30 minutes at +4°C in the dark. Finally, total DNA was stained using PI as follows: samples were washed in PBS, resuspended in 500 µl of PBS containing 20 µg/ml of PI and 100 µg/ml of RNase for 15 minutes, at +4°C, in the dark (75, 76).

Analysis of cell proliferation based on immunocytochemistry of BrdU

To test the capacity of anterior pituitary cells to maintain a basal replication rate for a time interval compatible with that planned to be used to study the putative growing effect of pFT22 (up to 7 days), viable adenohypophysial cells from 50-75 g male rats were used. After 72 hs in Falcon flasks, cells were seeded in 48 well plates at density $40.000/cm^2$ and asynchronously grown using serum-free medium M199 (Sigma Aldrich M4530) or standard medium plus serum (see section on primary pituitary cultures). Media were changed every 72 hs up to 168 hs, and 100 μM BrdU / 10 μM FldU was added in the last 12 hs for light microscopic analysis. At the end of treatment, cells were detached with trypsin, centrifuged in Eppendorf vials at 1300 rpm for 3 min, and counted. $2x10^5$ cells were aliquoted for each vial, and resuspended in 200 ml of PBS. Cells were cytospinned onto glass slides at 1300 rpm for 4 min, fixed with 4% paraformaldehyde for 1 h, washed in PBS 3 times for 10 min, then treated with 4N HCl for 30 min at RT for DNA denaturation. Following 4 consecutive washes of 5 min with PBS, cytospinned cells were incubated with 3% H_2O_2 x30 min, to quench endogenous peroxidase. Samples, then, were conditioned with 10% Normal Goat Serum in PBS for 30 min, and washed again with PBS, 3 times for 15 min. Finally, slides were incubated with a primary anti-BrdU antibody diluted 1:25 (Becton Dickinson, Anti-BrdU-Cat. No. 7580; mouse mAb) in PBS/2% BSA overnight at +4°C in moist chamber. The following day, slides were

washed in PBS 3 times for 15 min and incubated with universal biotinylated anti-mouse / rabbit IgG (1:50) (VECTASTAIN® Elite® ABC System) in PBS with NHS, in moist chamber for 30 min at RT. Samples, then, were incubated with the avidin-biotin complex (VECTASTAIN® Elite® ABC System) for 30 min at RT, and washed for 5 min with PBS. BrdU immunoreactivity was visualized using 3,3'-Diaminobenzidine (DAB) as a chromogen and 0,03% H_2O_2, up to 15 min. After development, slides were rinsed in PBS, cleared, and mounted in Pertex.

In another series of experiments, viable cells from 225-250 g male rats were used to test the growing effect of pFT22. After 72 hs in Falcon flasks, cells were seeded on MgCl-$CaCl_2$-coated glass coverslips, and asynchronously grown in 6 well plates at density of 40,000/cm^2. 100 nM pFT22 or an equal volume of medium without peptide (controls) were added to the culture, and cells incubated up to 36 hs without any medium change. In the last 12 hs, 100 μM BrdU / 10 μM FldU was added for light microscopic analysis. At the end of the treatment, cells were processed for immunocytochemistry as described above. BrdU-immunopositive cells in control and treated cultures were analyzed at the light microscopic level (Zeiss Axiophot) using unbiased counting methods.

Analysis of BrdU staining patterns using immunofluorescence

To gain information on the capacity of the BrdU labeling to display cells in primary culture to grow through the S phase of the cell cycle (early-, middle-, and late-S phases), viable cells from 225-250 g male rats were used. After 72 hs in Falcon flasks, cells were seeded on polylisine-coated glass coverslips, asynchronously grown in 6 well plates at density of 40.000/cm^2, and incubated with 100 μM BrdU / 10 μM FldU in the last 12 hs for light microscopic analysis. At the end of treatment, glass coverslips were rinsed with PBS four times for 5 min at RT, and permeabilized using 1% BSA 0,2% Triton X-100 (Sigma) in PBS four times for 5 min. Samples were blocked with 5% Normal Goat Serum in PBS for 1 h, and incubated with the anti BrdU antibody (see above) diluted 1:25 in PBS / 1% goat serum overnight at +4°C in moist chamber. The following day, samples were washed in PBS three times for 5 min, incubated with a secondary goat anti-mouse, FITC - IgGs (Sigma F-0257) in PBS (1:50) for 1 h in moist chamber. Then, coverslips were rinsed with PBS three times for 5 min, and were mounted with buffered glycerol.

Synchronization studies

Attempts were made to synchronize GH4C1 cells grown in their standard culture medium, to obtain the highest number possible of cells in the G0 / G1 phase. This, with the intent to set an experimental system to eventually gain

an analysis of the effect of pFT22 on the cell cycle of this adenomatous line even more detailed of that derived using asynchronously growing cells. The synchronization strategy was based on either serum deprivation of the culture medium or use of hydroxyurea (HU) (Sigma, H 8627) administered for different time intervals (12-72h) and concentrations (2-10 mM) to serum-deprived cultures.

Statistical analysis

Differences in the number (or proportion) of replicating cells between controls and either pFT22, IGF-1, serum-starved, or hydroxyurea treated cells were evaluated using one-way ANOVA, Student-Newman-Keuls test for multiple means, and non-parametric chi-squared test. Differences were considered statistically significant if $p < 0.05$.

RESULTS

Bioinformatics studies

Figure 10 shows that a statistically significant AA identity (E-value $\leq 10\ e^{-3}$) between the rat pFT22 and other Invertebrate and Vertebrate proteins can be found only inside the proTRH molecule of the rodents group (GeneDoc software). Within this group, rat pFT22 shares a similarity between 83% and 95% of AA.
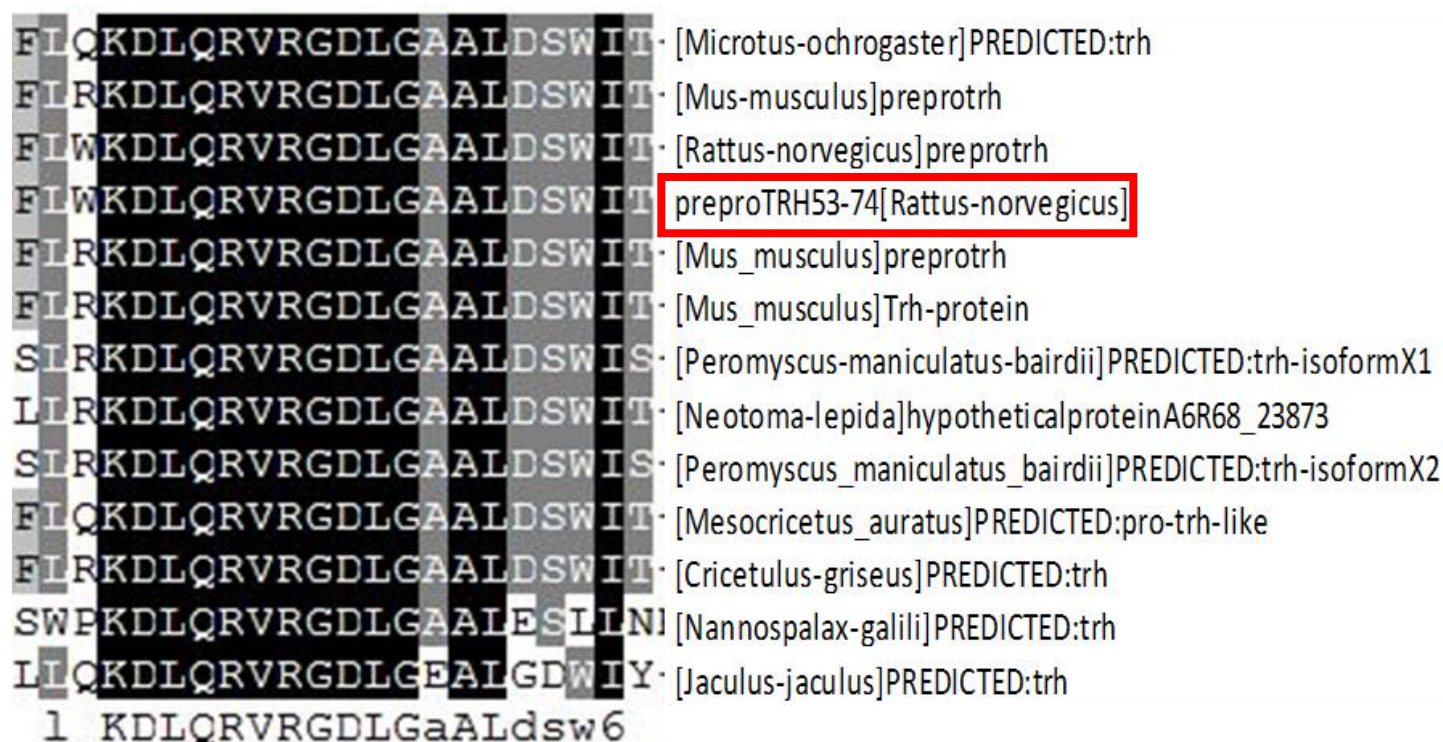

FIG. 10: Alignment amino acid sequence of rat prepro- TRH$_{53-74}$ compared with the counterpart from other rodents using CLUSTALX 1.81 and visualized with GeneDoc software. Black color corresponds to identical residues and gray color to conserved residues.

Figure 11 shows that this result is consistent with an evolutionary origin of pFT22 common to all members of the rodent group, that exhibits only irrelevant AA mutations (< 1 AA) for the peptide in each of its members.
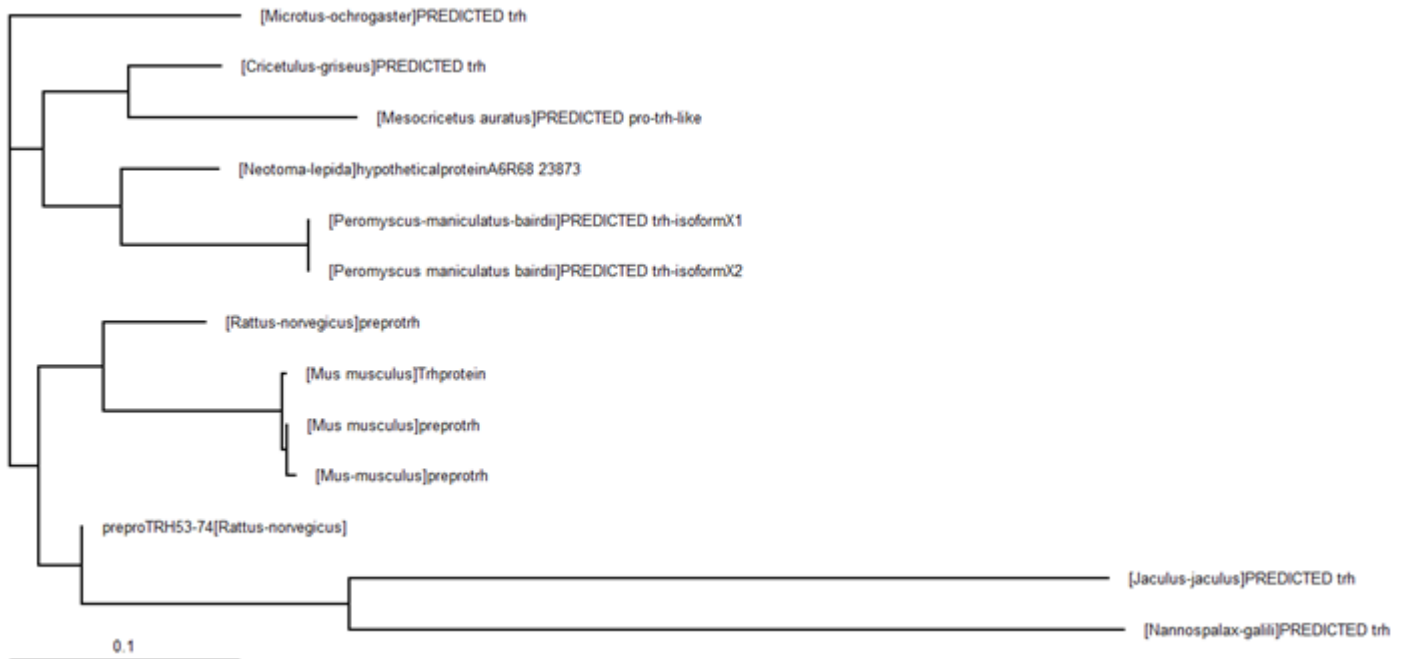

FIG. 11: Neighbor Joining tree of rat prepro- TRH_{53-74} sequence obtained with Clustalx 1.81 and visualized with TreeView software. Phylogenetic tree branch lengths scale of "0.1", meaning 0.1 amino-acidic substitutions per site.

However, Figure 12 A shows that a comparison between the rat pFT22 sequence (AA 53-74), beyond which the first rat TRH progenitor sequence occurs and the equivalent sequence in humans, corresponding to the N-terminal AA 53-83 beyond which the first human TRH progenitor sequence is cleaved, share a 32% of AA identity (equally expressed by fig. 13B, as the 50% of the 14 AA recognized by the BLASTP software yielding the best match sequence between rat and human in the peptide interval analyzed).
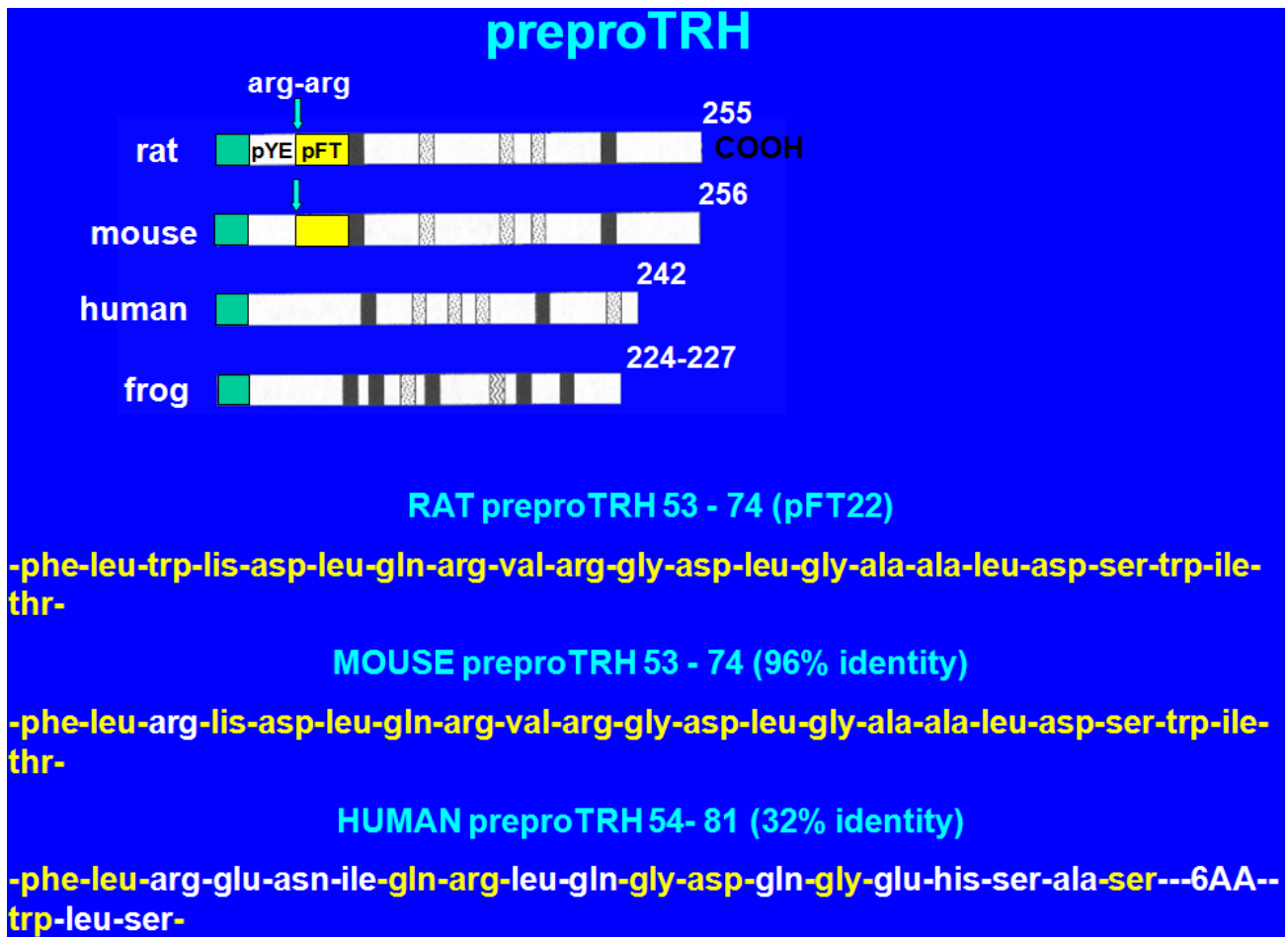
FIG. 12: A) schematics of the AA (yellow) shared by pFT22 in mouse and humans; B) BLASTP output of pFT22 in confronting the rat and human peptide, where the best matched sequence is made of only 14 AA whose 50% is common to both species.

Finally, Figure 13A, and 13B show the list of chemical-physical properties of pFT22, obtained using the ProtParam software. These include the molecular weight, theoretical isoelectric point (pI), AA composition, atomic composition, extinction coefficient, estimated half-life, instability index, aliphatic index, and grand average of hydropathicity

```
Molecular weight: 2560.94

Theoretical pI: 6.04

Amino acid composition:
Ala (A)     2          9.1%
Arg (R)     2          9.1%
Asn (N)     0          0.0%
Asp (D)     3         13.6%
Cys (C)     0          0.0%
Gln (Q)     1          4.5%
Glu (E)     0          0.0%
Gly (G)     2          9.1%
His (H)     0          0.0%
Ile (I)     1          4.5%
Leu (L)     4         18.2%
Lys (K)     1          4.5%
Met (M)     0          0.0%
Phe (F)     1          4.5%
Pro (P)     0          0.0%
Ser (S)     1          4.5%
Thr (T)     1          4.5%
Trp (W)     2          9.1%
Tyr (Y)     0          0.0%
Val (V)     1          4.5%
Pyl (O)     0          0.0%
Sec (U)     0          0.0%

  (B)       0          0.0%
  (Z)       0          0.0%
  (X)       0          0.0%


Total number of negatively charged residues (Asp + Glu): 3
Total number of positively charged residues (Arg + Lys): 3
```

A)

Atomic composition:

```
Carbon      C        118
Hydrogen    H        182
Nitrogen    N         32
Oxygen      O         32
Sulfur      S          0
```

Formula: $C_{118}H_{182}N_{32}O_{32}$
Total number of atoms: 364

Extinction coefficients:

Extinction coefficients are in units of $M^{-1} cm^{-1}$, at 280 nm measured in water.

```
Ext. coefficient     11000
Abs 0.1% (=1 g/l)    4.295
```

Estimated half-life:

The N-terminal of the sequence considered is F (Phe).

The estimated half-life is: 1.1 hours (mammalian reticulocytes, in vitro).
                            3 min (yeast, in vivo).
                            2 min (Escherichia coli, in vivo).

Instability index:

The instability index (II) is computed to be 36.16
This classifies the protein as stable.

Aliphatic index: 110.91

Grand average of hydropathicity (GRAVY): -0.032

B)

FIG 13.

Circular Dichroism

Figure 14 shows the spectrum of absorbance in the far-UV of synthetic pFT22 dissolved in distilled water. In the experimental conditions chosen, the curve profile indicates that the peptide does not possesses any stable ordered secondary structure, but it is in a random coil conformation. This means that it is like a tangle flexible enough to assume all needed 3D ordered conformations in the presence of adequate molecular interactions in the solvent. The spectrum was not affected by changes in peptide concentration within the 10 – 30 µM range.
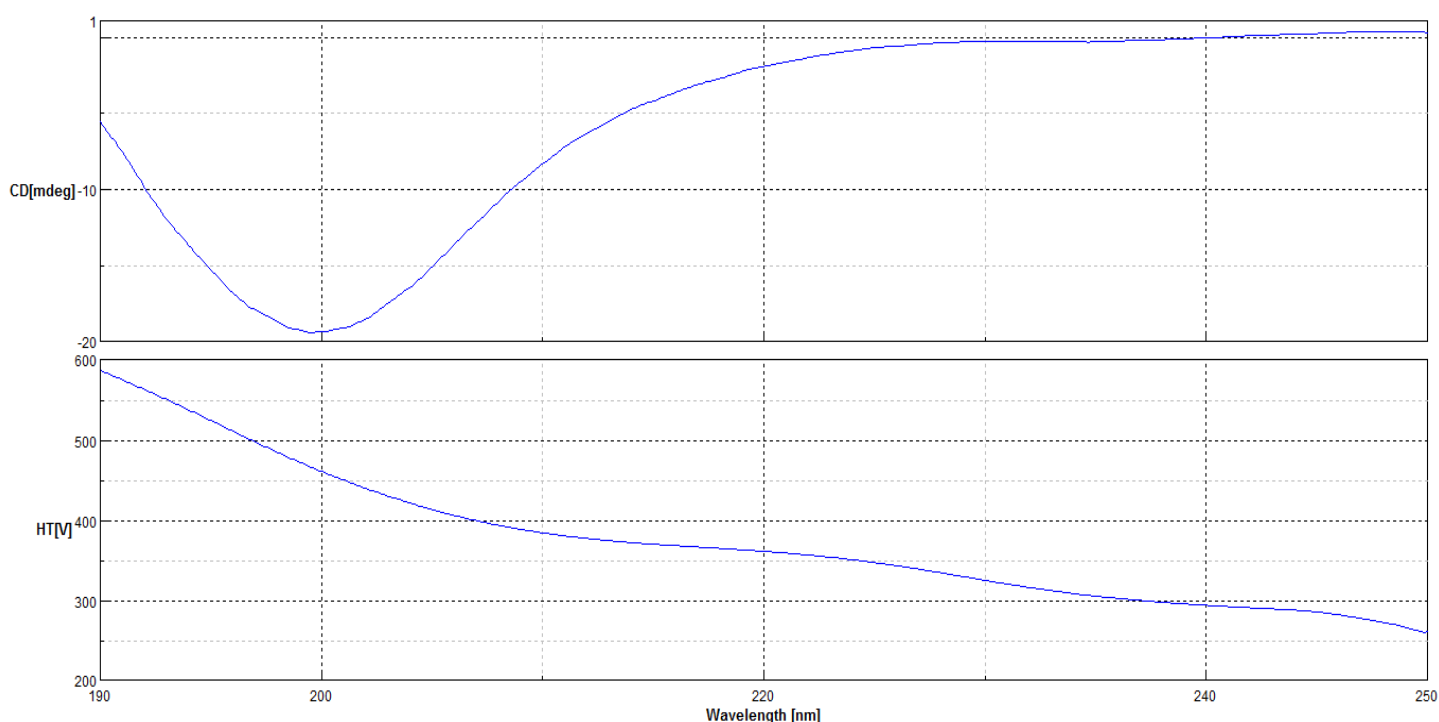

FIG.14: far-UV CD spectrum of prepro TRH$_{53-74}$, 30 µM in water.

Analysis of cell proliferation based on DNA quantitation

Figures 15 and 16 summarize the results of the DNA quantitation of GH4C1 cells treated with repeated doses of either 10nM or 100nM IGF-1, and either 10nM or 100nM pFT22, every 48hs for 7 days in serum free medium. In the attempt to gain a synchronization, cells were subjected to a serum-free starvation period of 72 hs before initiation of any experiment. DNA content was measured every 24 hs, and the results expressed as the mean percentage of the DNA fluorescence (or O.D) of treated samples above the DNA fluorescence of controls taken as the baseline, *i.e.* considered equal to 0%.

Figure 15 shows that both 10nM and 100nM IGF-1 exert a statistically significance growth effect in a time range of 96 hs. In particular, 10nM IGF1 leads to 40% increase in DNA content above controls at 24 hs, and 30% increase at 72 hs. Similar, 100nM IGF1 induces a 55% increase in DNA content above control at 24 hs, and 70% increase at 72hs. In contrast, a reduction in the DNA content below control levels (and thus an inhibition of cell growth) occurs in the remaining 48 hs of the experimental protocol, with both peptide concentrations
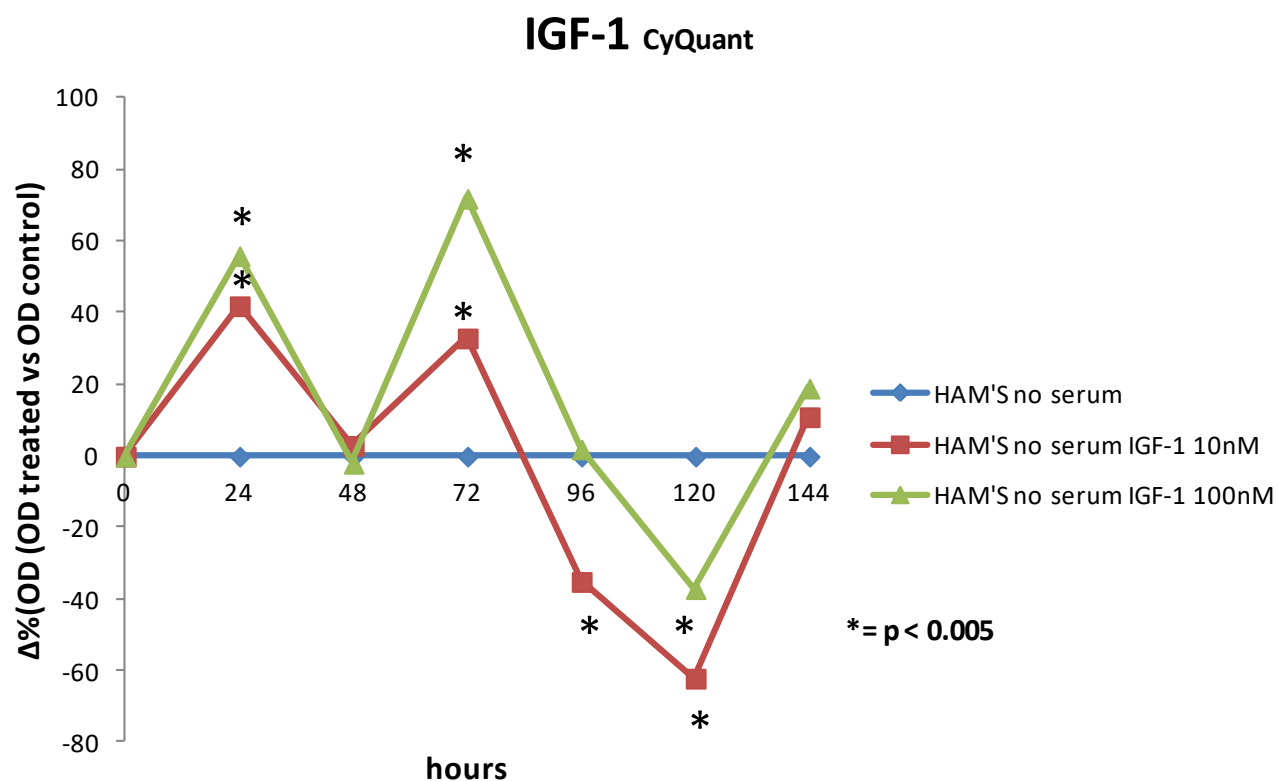
IGF-1 CyQuant

FIG. 15: GH4C1 IGF-1 10nM and 100nM treatment up to 144hs. The results are express as the mean percentage of the OD of treated samples vs untreated control (triplicate)

Figure 16 shows that both 10nM and 100nM, pFT22 exerts a statistically significance growth effect in a time range of 96 hs, to an extent even higher than that of IGF-1. In particular, 10nM pFT22 leads to 70% increase in DNA content above controls at 24 hs, and 50% increase at 72 hs. Similar, 100nM pFT22 induces a 50% increase in DNA content above control at 24 hs, and 100% increase at 72hs. In contrast, a reduction in the DNA content below control levels (and thus an inhibition of cell growth) occurs in the remaining 48 hs of the experimental protocol, with both peptide concentrations.
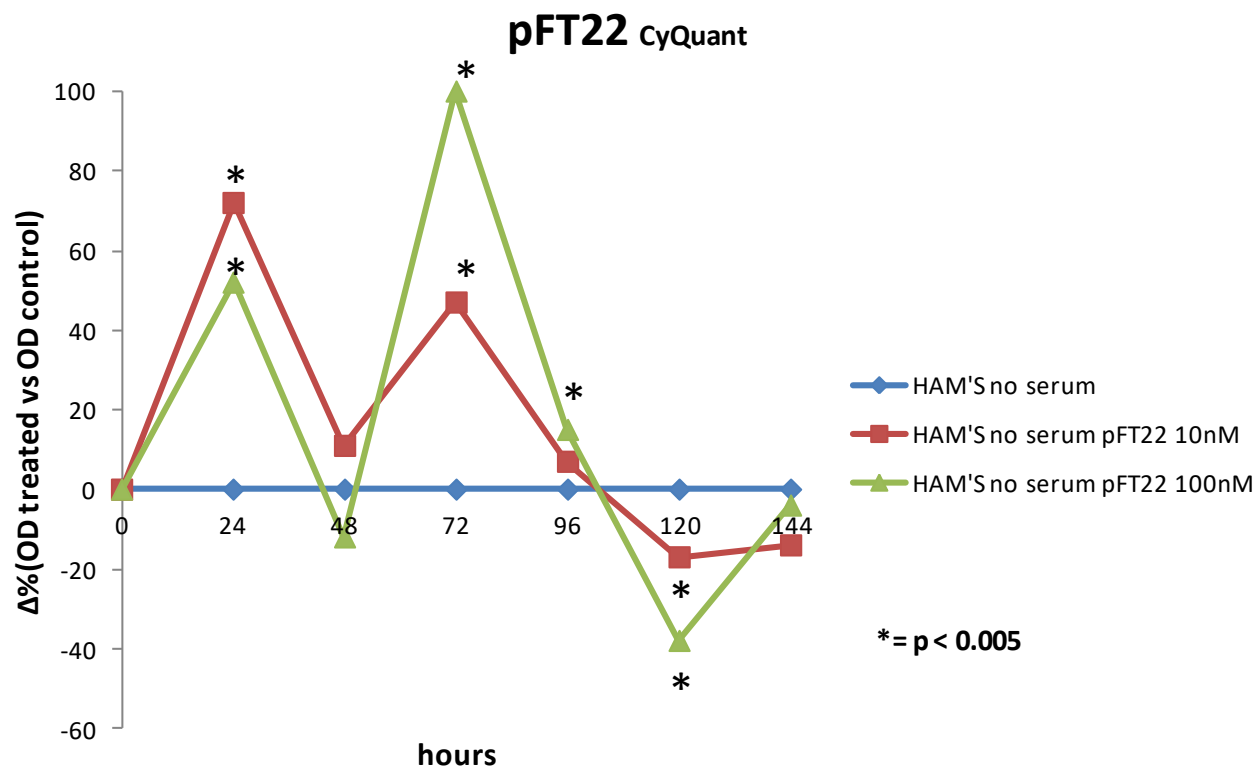
FIG. 16: GH4C1 pFT22 10nM and 100nM treatment up to 144hs. The results are express as the mean percentage of the OD of treated samples vs untreated control (triplicate)

GH4C1 cell cycle in standard conditions

Fig. 17A and B shows the flow cytometric profiles of the basal cell cycle of GH4C1 cells in a time interval of 84 hs.. About 60-67% of cells were found to be in the G0/G1 phase, 6-10% of cells in the S phase, and 27% of cells in the G2/M.

A)

GH4C1 cell cycle in standard condition
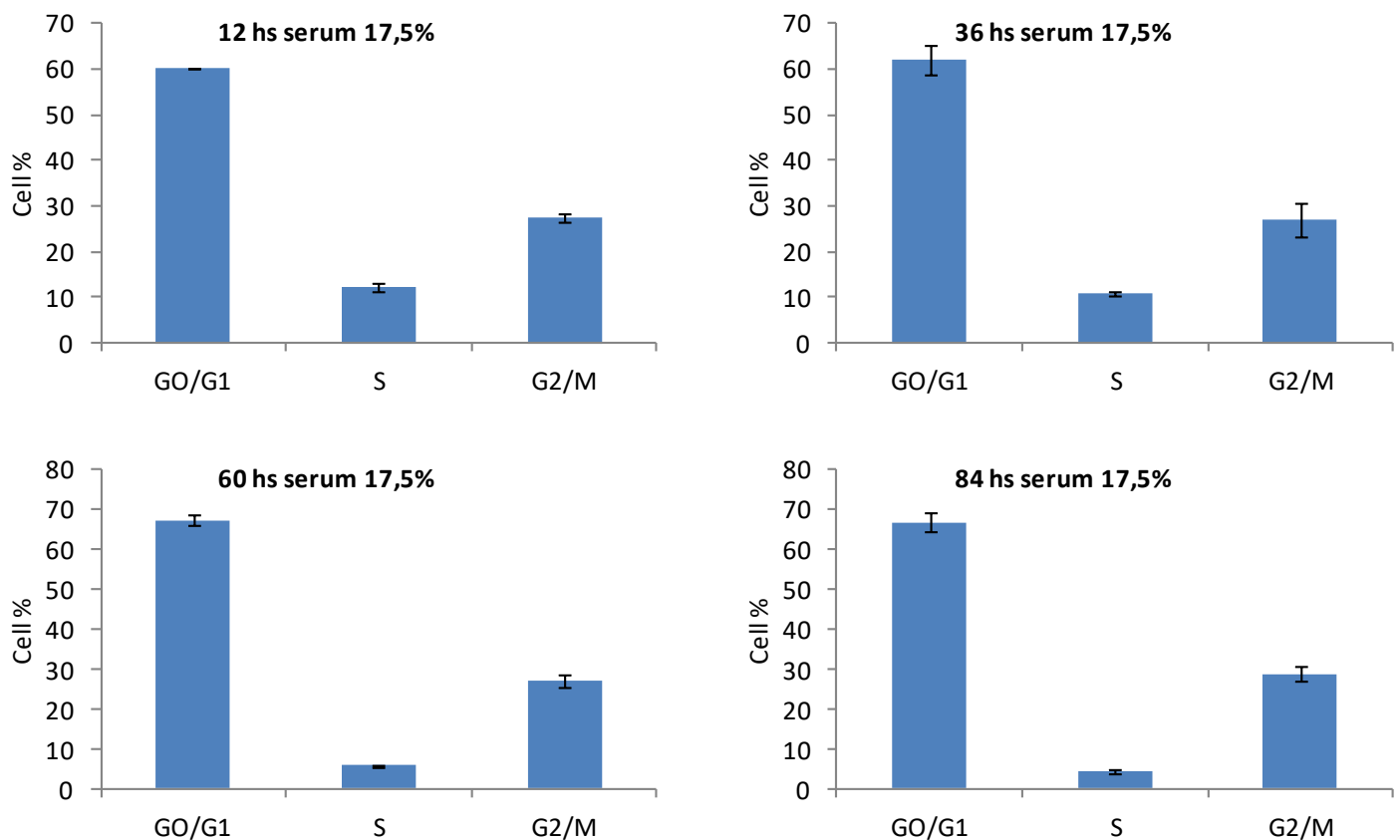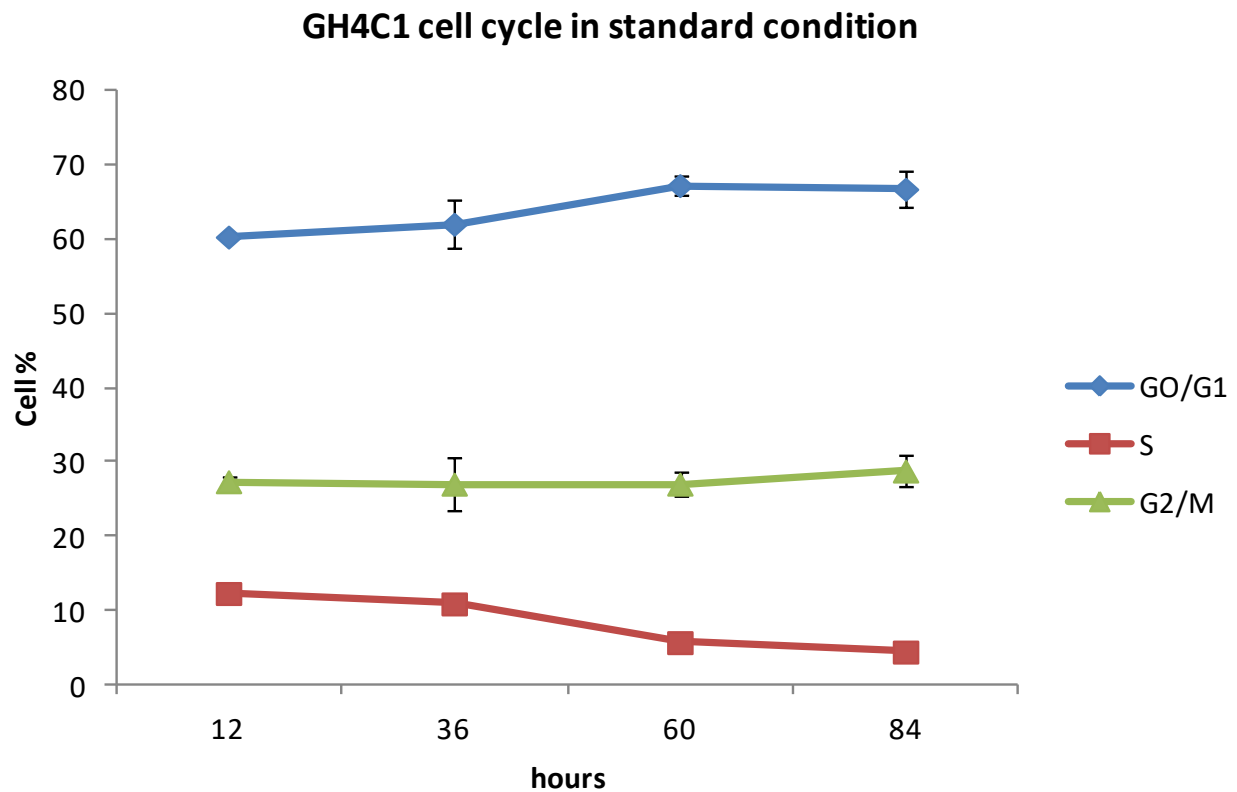
B)

FIG. 17: A) GH4C1 cells cycle in standard condition (without 12n/doublets); B) distribution of each cell cycle phase in the time interval chosen. Each point represent the mean ± SD of three experiments.

Figure 18 shows the results of the logarithmic amplification of the DNA fluorescence histograms shown above. A 7-10% of hypertriploid, 12n cells including possible cell doublets were detected.
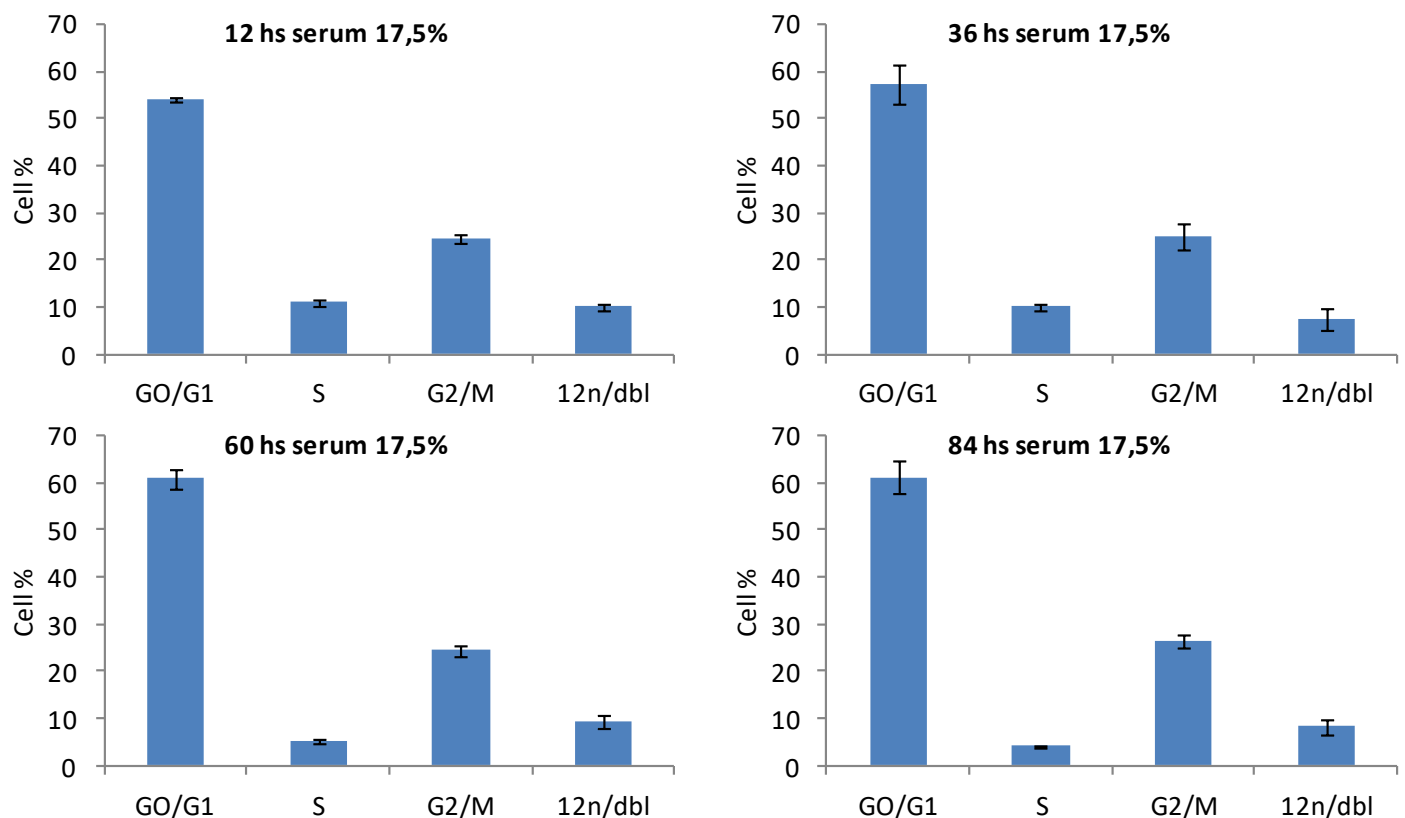
FIG. 18: GH4C1 cells cycle in standard condition (12n/doublets). Each point represents the mean ± SD of three experiments

Cell cycle in serum-depleted medium

Figure 19 shows the distribution of GH4C1 cells in the different phases of the cell cycle (logarithmic expansion included), using a serum-depleted cell culture medium (serum 5,8%). This approach allowed for maintenance of a cell distribution comparable to that of the medium with a standard amount of serum (17,5%) but resulted without any hypertriploid set. Due to the absence of these confounding hypertriploid sets, the use of this culture protocol was

considered ideal for cytometric analysis of asynchronously growing, GH4C1 cells under treatment with pFT22 and IGF1.
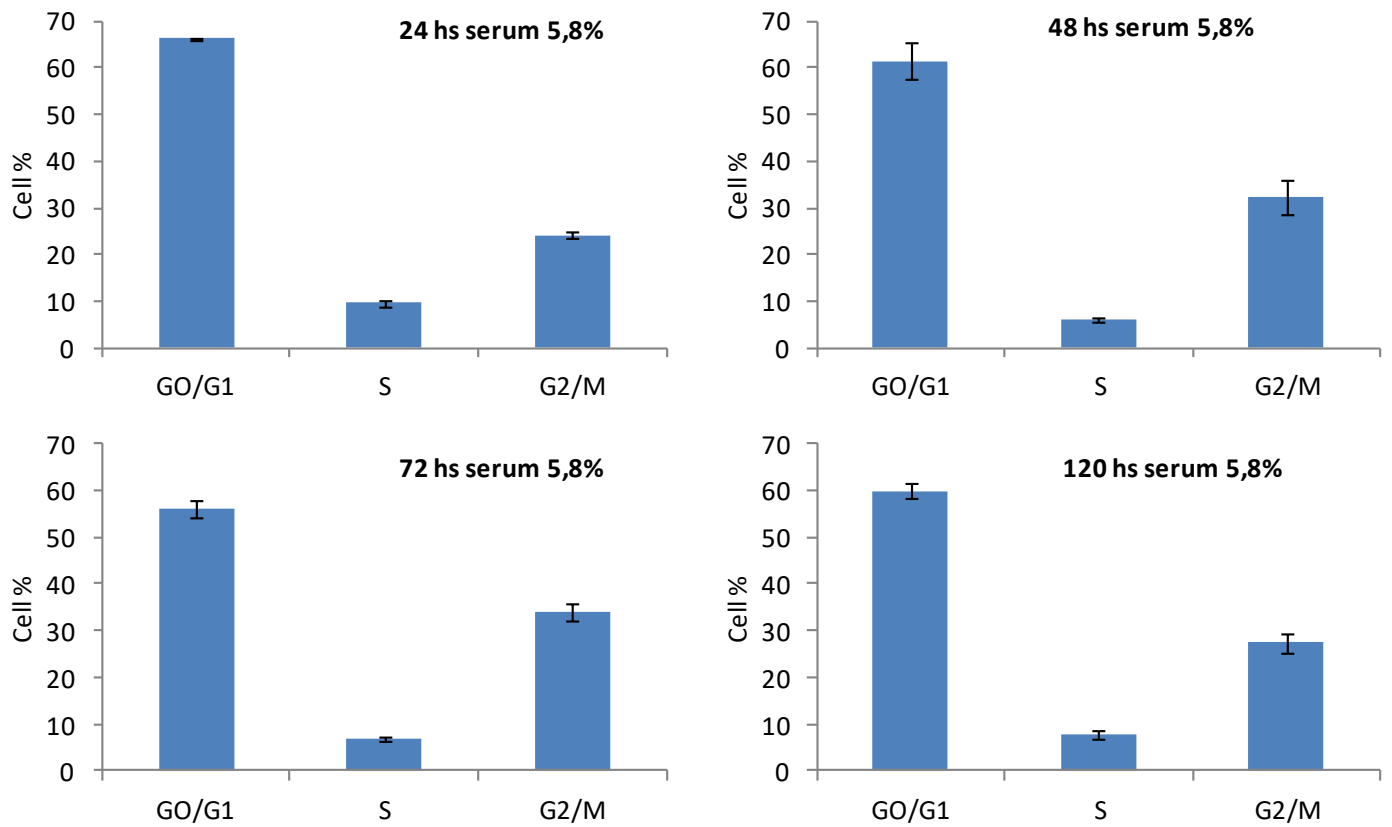

FIG. 19: cell cycle of GH4C1 cells in HAM's F10 5,8% serum up to 120 hs. Each point represents the mean ± SD of three experiments

Flow cytometric analysis of the growth effect of IGF-1 and pFT22

a. IGF-1 effect on the Swiss 3T3 cell line

Figure 20 shows the effect of a single dose of 100 nM IGF-1 on the S-phase (*i.e.* BrdU incorporation) of serum-deprived, mouse fibroblasts Swiss 3T3 cells. Cells were initially synchronized with serum deprivation for 24hs prior of the administration of the peptide. The cytometric measurement was carried out 12 hs later. An increase of more than one third of cells with respect to the control was detected.
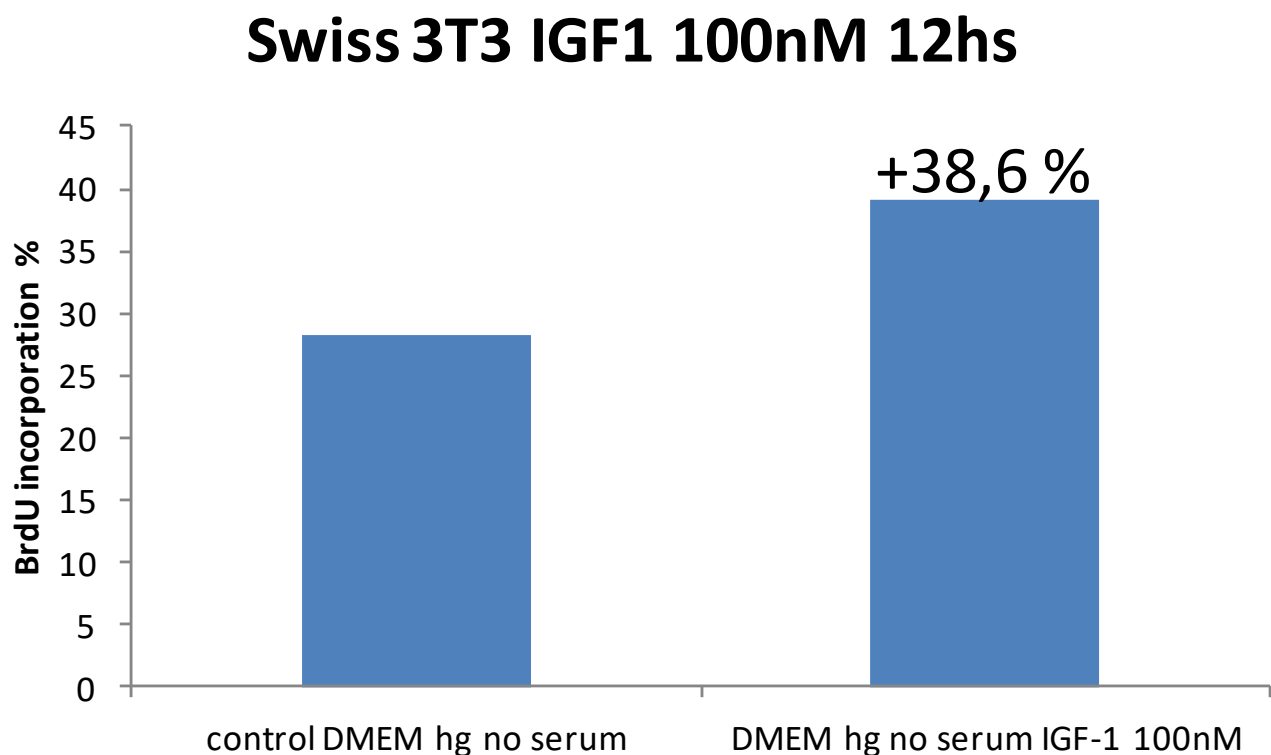
Swiss 3T3 IGF1 100nM 12hs

FIG. 20: percentage of BrdU incorporation (S phase). Data from a single experiment.

b. IGF-1 effect on the Hep G2 cell line

Figure 21 shows the effect of a single dose of 10 nM IGF-1 on the S-phase of serum-deprived, human hepatocarcinoma Hep G2 cells. Cells were initially synchronized with serum deprivation for 24hs prior to the administration of the peptide. The cytometric measurement was carried out 48 hs later. A statistically significant increase of around one fourth of cells with respect to the control was detected.
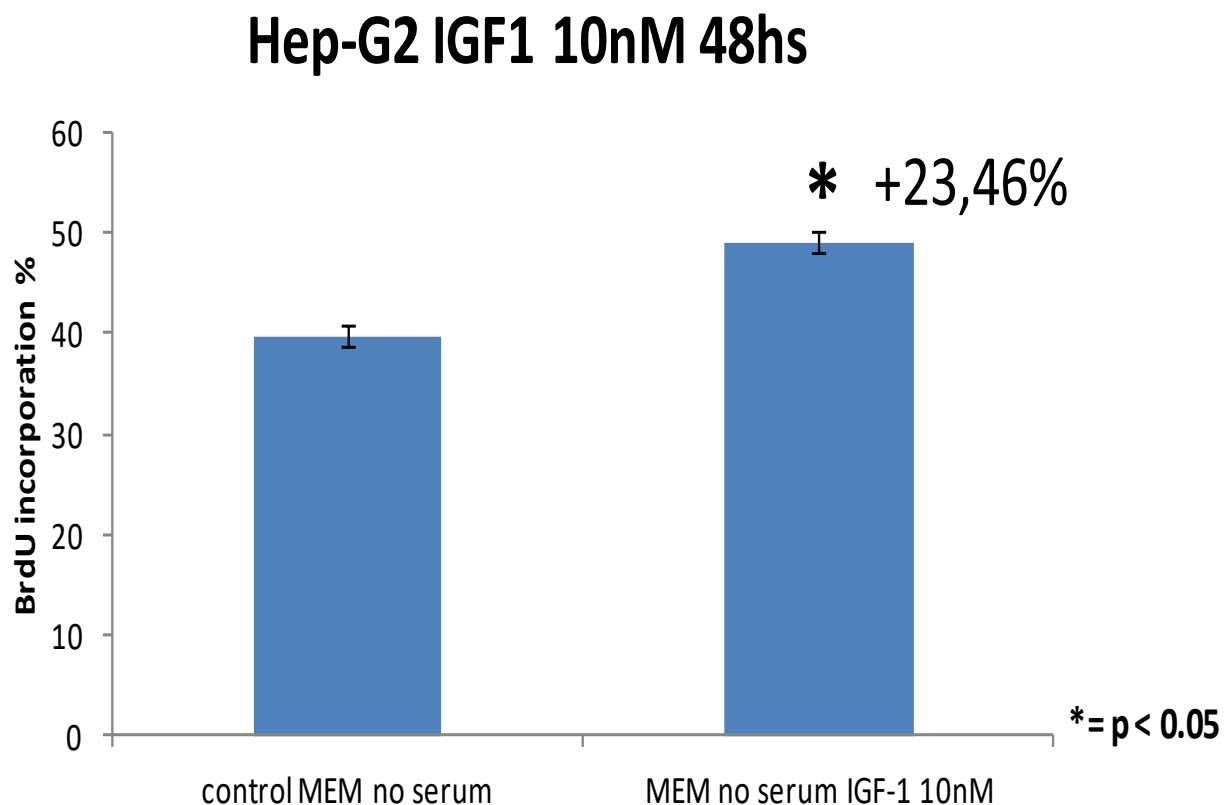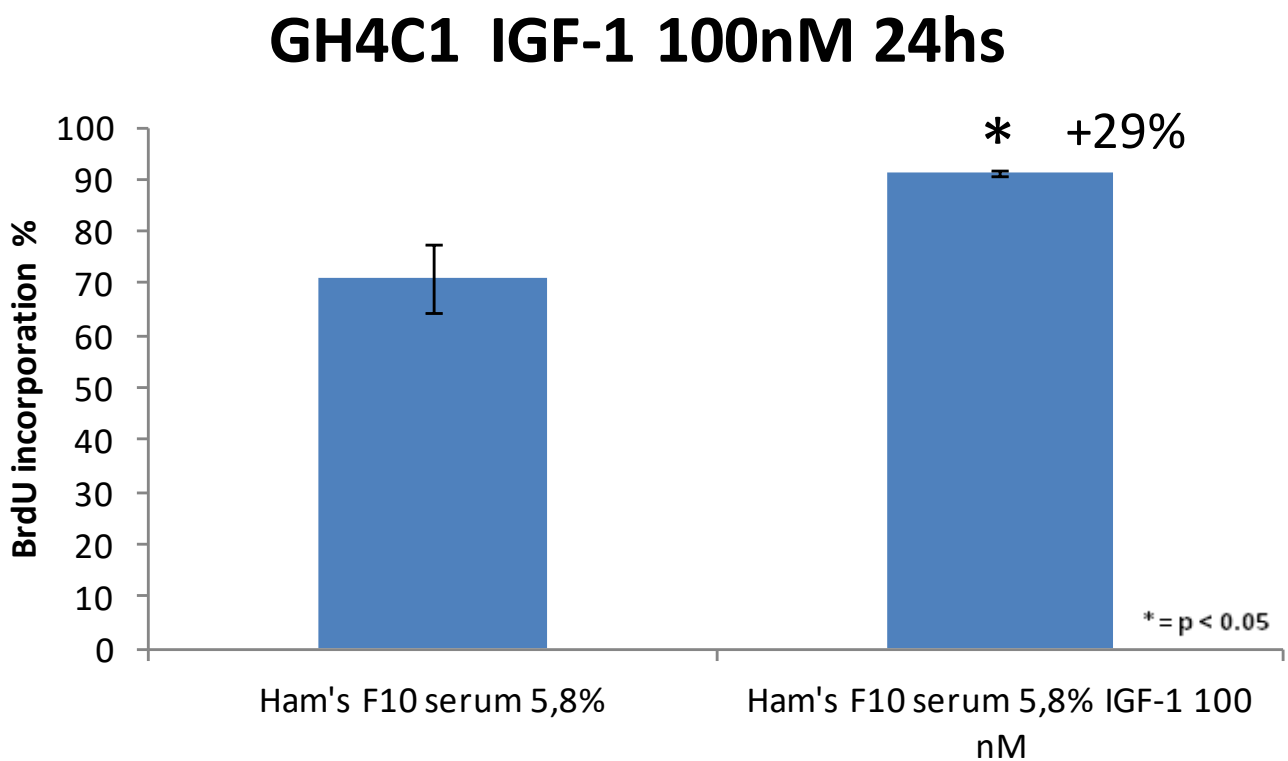
Hep-G2 IGF1 10nM 48hs

FIG. 21: percentage of BrdU incorporation (S phase) Each point represents the mean $\pm$ SD of three experiments

c. IGF-1 and pFT22 effect on the GH4C1 cell line

Figure 22 shows the effect of a single dose of 100 nM IGF-1 on the S-phase of GH4C1 cells, grown for 24 hs with 5,8% serum prior to the administration of the peptide. The cytometric measurements were carried out 24 and 48 hs after peptide administration. A) a statistically significant increase of around one third of cells with respect to the control was detected at 24 hs; B) no statistically significant increase in cells with respect to the control was detected at 48 hs.

GH4C1 IGF-1 100nM 24hs

A)

GH4C1 IGF-1 100nM 48hs
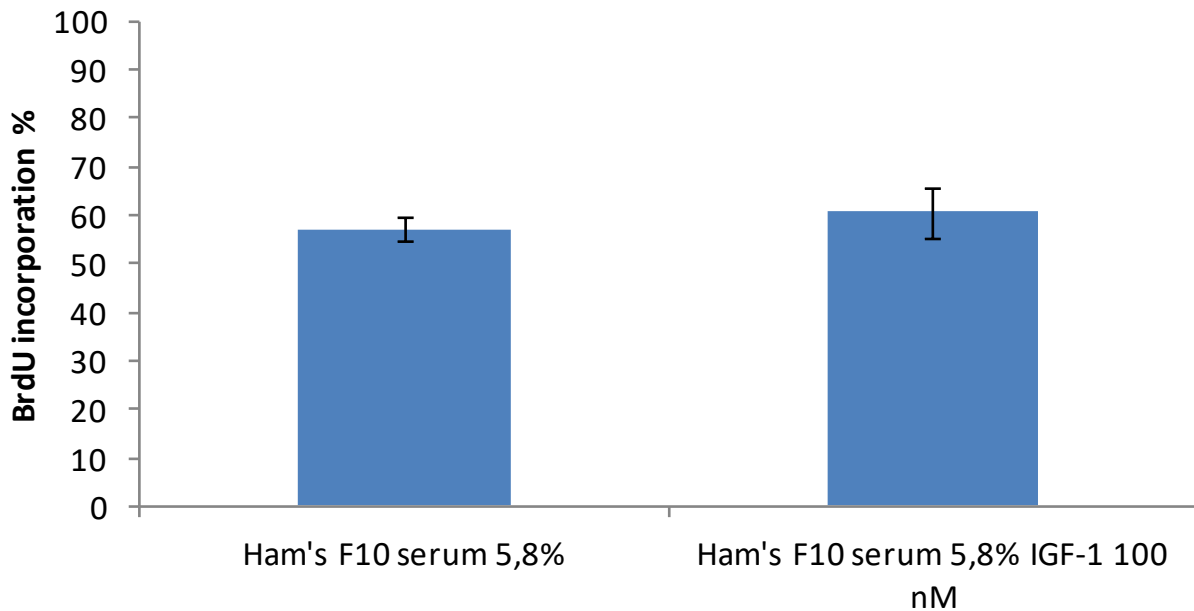
B)

FIG. 22 A and B: percentage of BrdU incorporation (S phase). Each point represents the mean $\pm$ SD of three experiments

Figure 23 shows the effect of a single dose of 100 nM IGF-1 on the S-phase of GH4C1 cells, grown for 24 hs with 5,8% serum prior to the administration of the peptide. The cytometric measurements were carried out 12, 24 and 48hs after peptide administration. A statistically significant increase of cells with respect to the control was detected at all time points, with the maximal increase at 12 hs, accounting for around four fifths of the control, and minor increases at 24 and 48 hs, each accounting for around one third of the control.

A)

B)

GH4C1 pFT22 100nM 48hs
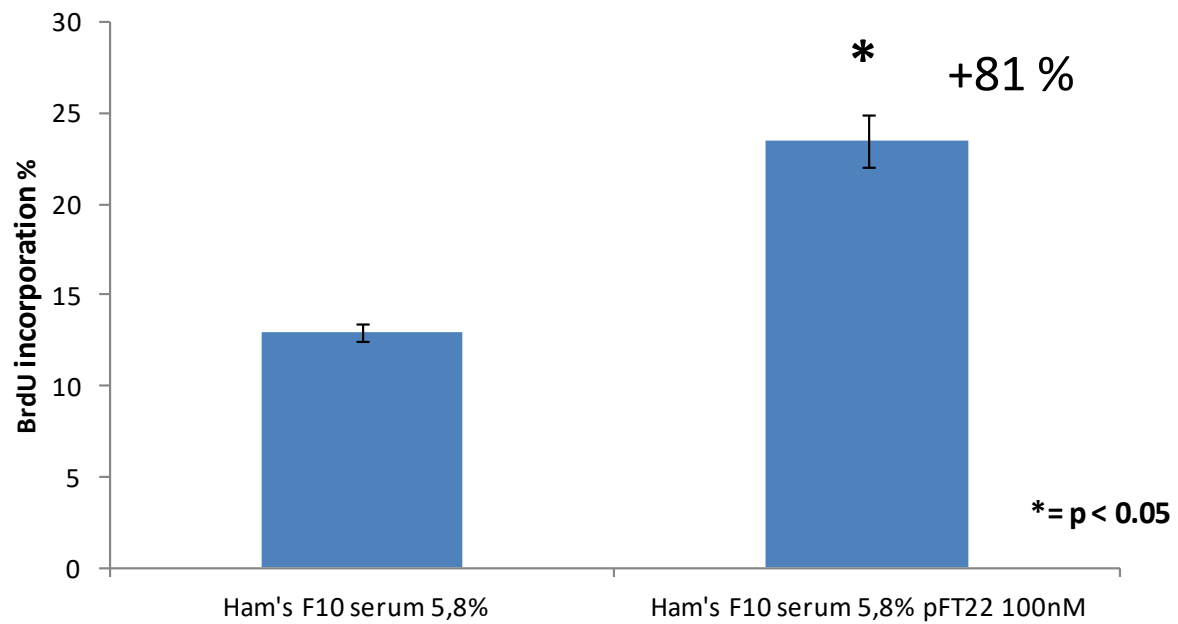
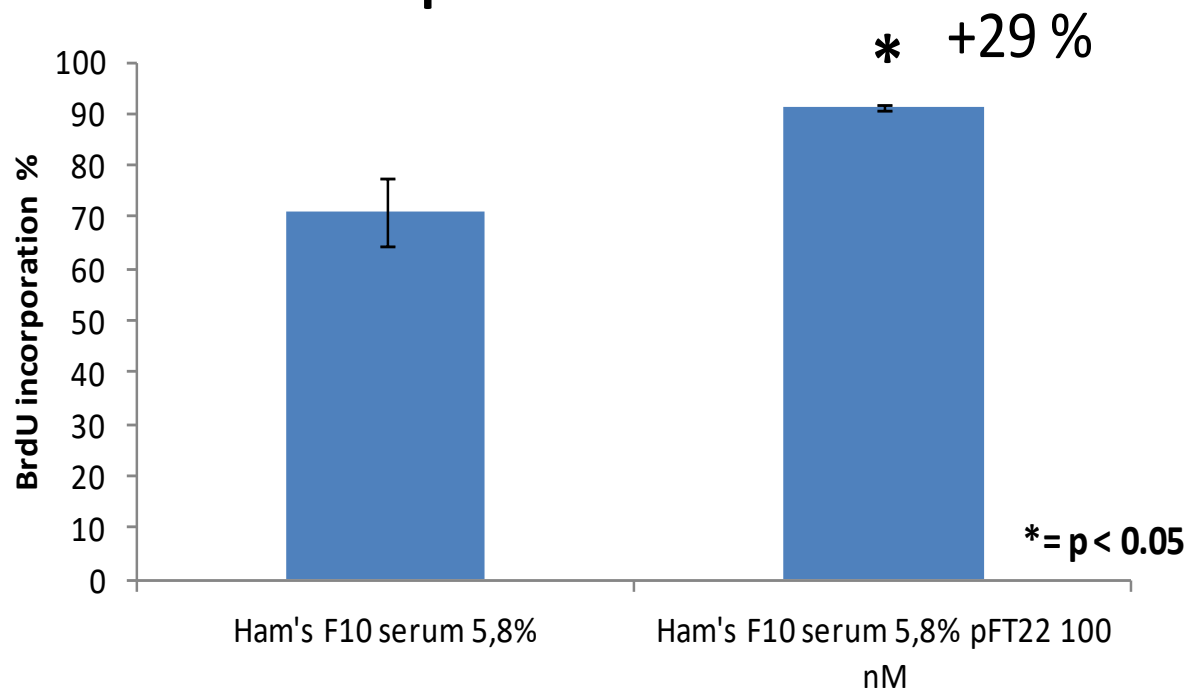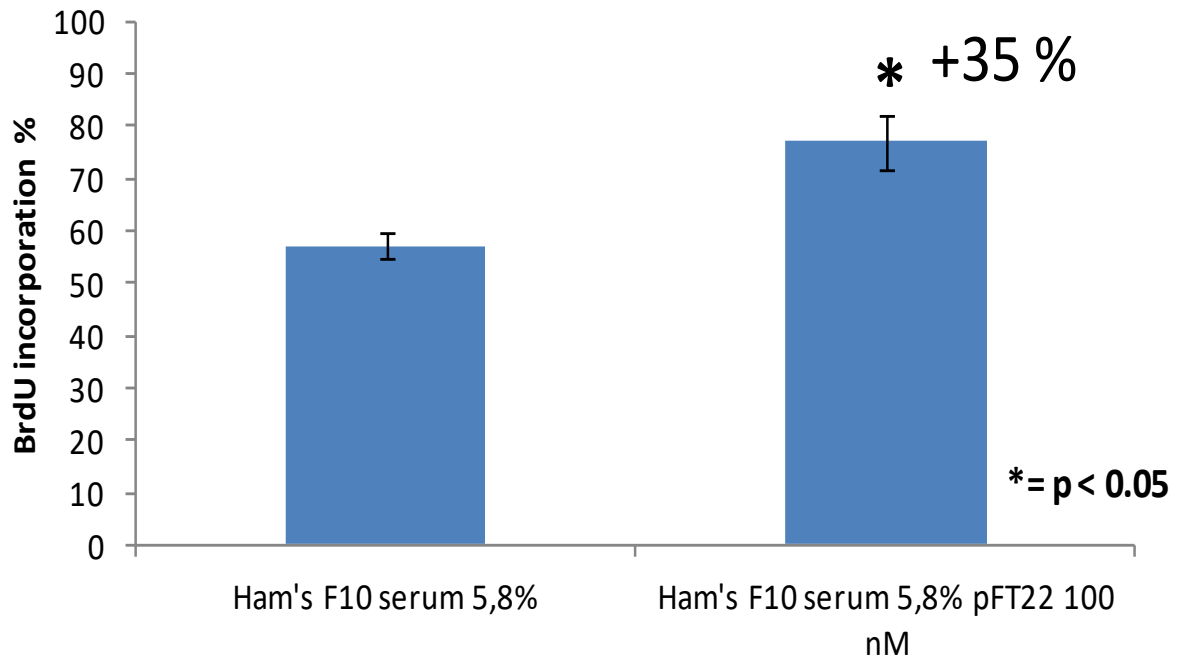FIG. 23: percentage of BrdU incorporation (S phase). Each point represents the mean $\pm$ SD of three experiments in each time interval A) 12hs; B) 24hs; C) 48hs

Figure 24 shows the cumulative effect of repeated doses of either 100 nM pFT22 or IGF-1 on the S-phase of GH4C1 cells, grown for 24 hs with 5,8% serum prior to the administration of the peptide. Each peptide was administered every 48 hs. The cytometric measurements were carried every 24 hs up to 96 hs (4 days). Both peptides were able to stimulate growth of pituitary cells within the first 48 hs, resulting pFT22 more powerful than IGF1 due to an effect lasting longer. However, in the remaining 48 hs both peptides failed to stimulate growth of GH4C1.
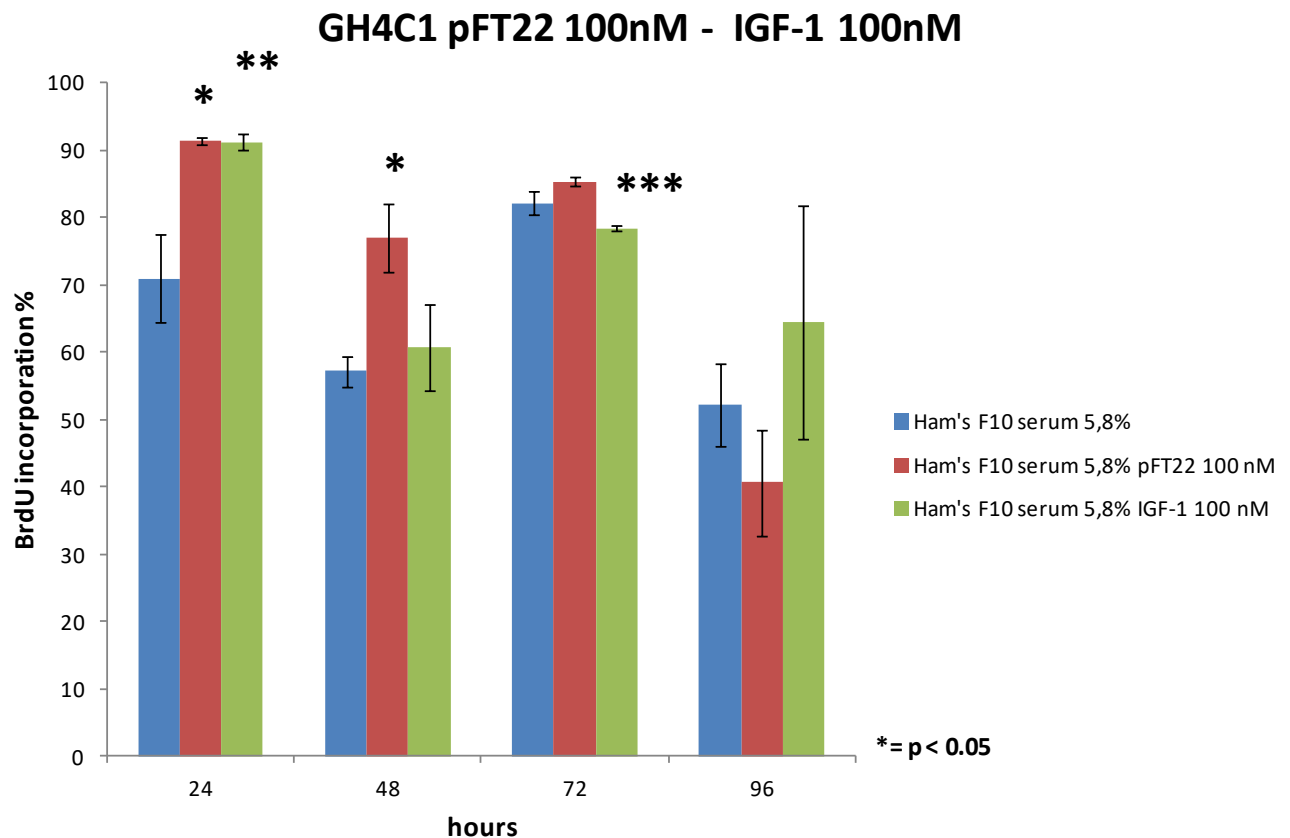
FIG. 24: percentage of BrdU incorporation (S phase) of treatments with pFT22 100nM and IGF-1 100nM up to 96hs. Each point represents the mean ± SD of three experiments

Effect of pFT22 on male rat, anterior pituitary cells in primary monolayer culture

Figure 25 shows the results of BrdU incorporation in nuclei of male rat, anterior pituitary cells in primary monolayer culture for 7 days,. Cells were incubated either in standard medium or in serum-deprived medium, and BrdU detected by immunocytochemistry. Cells continued to replicate for the entire period of study, irrespective of the presence or absence of serum in the culture medium, suggesting conservation of a substantial growth potential.
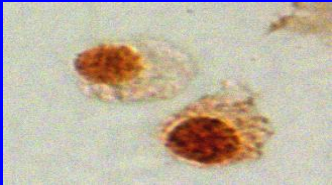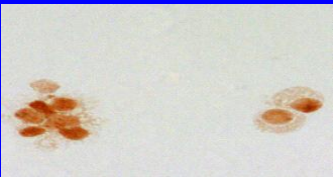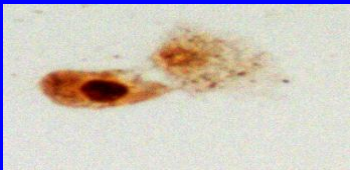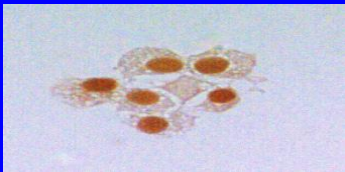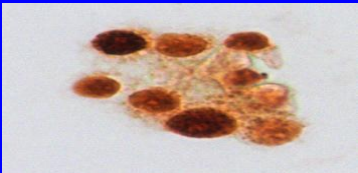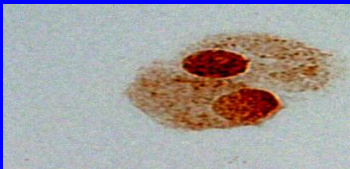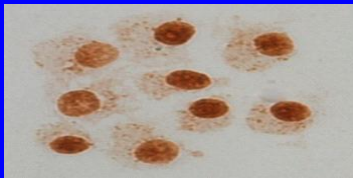
Times of incubation (hrs) / medium	Minimal medium without serum	Standard medium with serum
48 hrs		-
96 hrs		
120 hrs		-
144 hrs	-	
168 hrs		

FIG. 25: BrdU- immunoreactive [IR] cells with nuclear DAB staining. In the left column cells cultured with minimal medium without serum, in the right column cells cultured with standard medium with serum, at different time points.

Figure 26 shows the result of BrdU incorporation in nuclei of asynchronously growing, male rat anterior pituitary cells in primary monolayer culture, as detected by light microscopic immunocytochemistry and morphometry. Cells were treated with a single dose of 100 nM pFT22 or vehicle, and BrdU labeling analyzed 18 hs later. Bars are the mean of more than 100 counted optical fields. A highly statistically significant increase in growing cells with respect to the control was readily apparent.
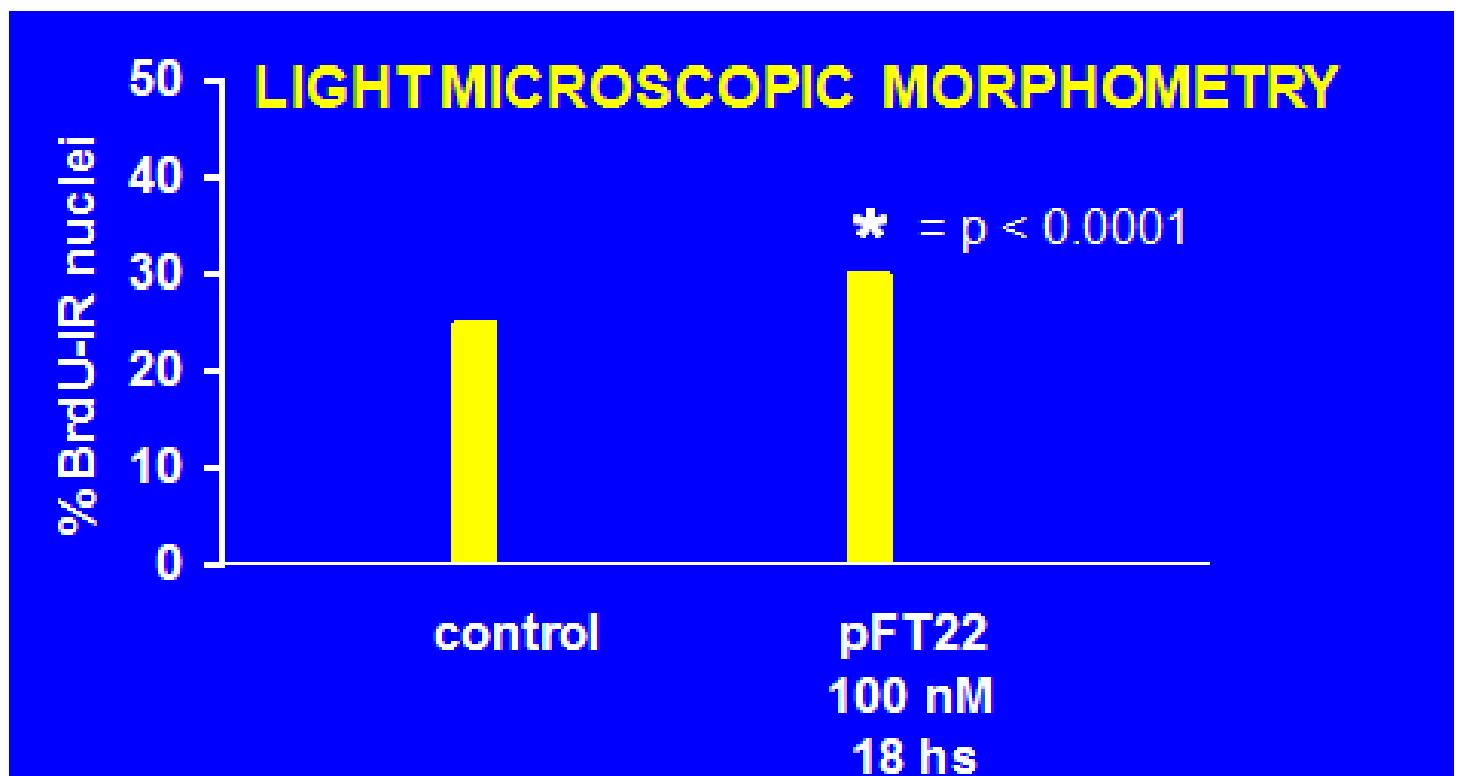
FIG. 26: percentage of BrdU-IR (immunoreactive) nuclei of control and treated pituitary cells 18 hs later the administration of pFT22. Bars are the mean of more than 100 counted optical fields. * = p < 0.0001

Figure 27 shows the staining pattern of male rat, anterior pituitary cells growing in monolayer culture. Both in pFT22 treated and untreated animals, BrdU immunolabeling revealed that intranuclear staining patterns were consistent with cells in all fractions of the S-phase, including initial (early S-phase), intermediate (middle S-phase) and final (late S-phase) steps of DNA synthesis, as well as with cells in mitotic division (G2-M phase).

early S   middle S   late S   G2 - M
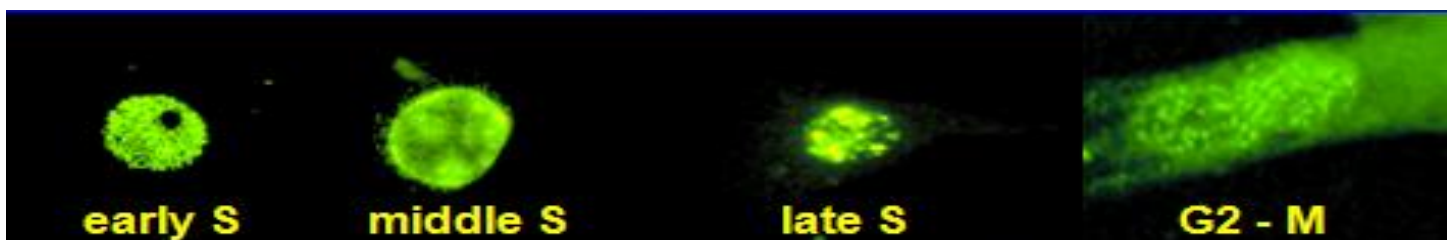
FIG. 27: intranuclear staining patterns of BrdU revealed by immunofluorescence.

Figure 28 shows the results of the flow cytometric analysis of 4 different primary monolayer cultures from the male rat, anterior pituitary. Cells were treated with a single dose of 100 nM pFT22, and measurements were done up to 36 hs following peptide administration. A highly statistically significant increase in cells entering the early S-phase with respect to controls was detected in all cell cultures, indicating that pFT22 stimulated anterior pituitary cells to enter the G1/S transition of the cell cycle.
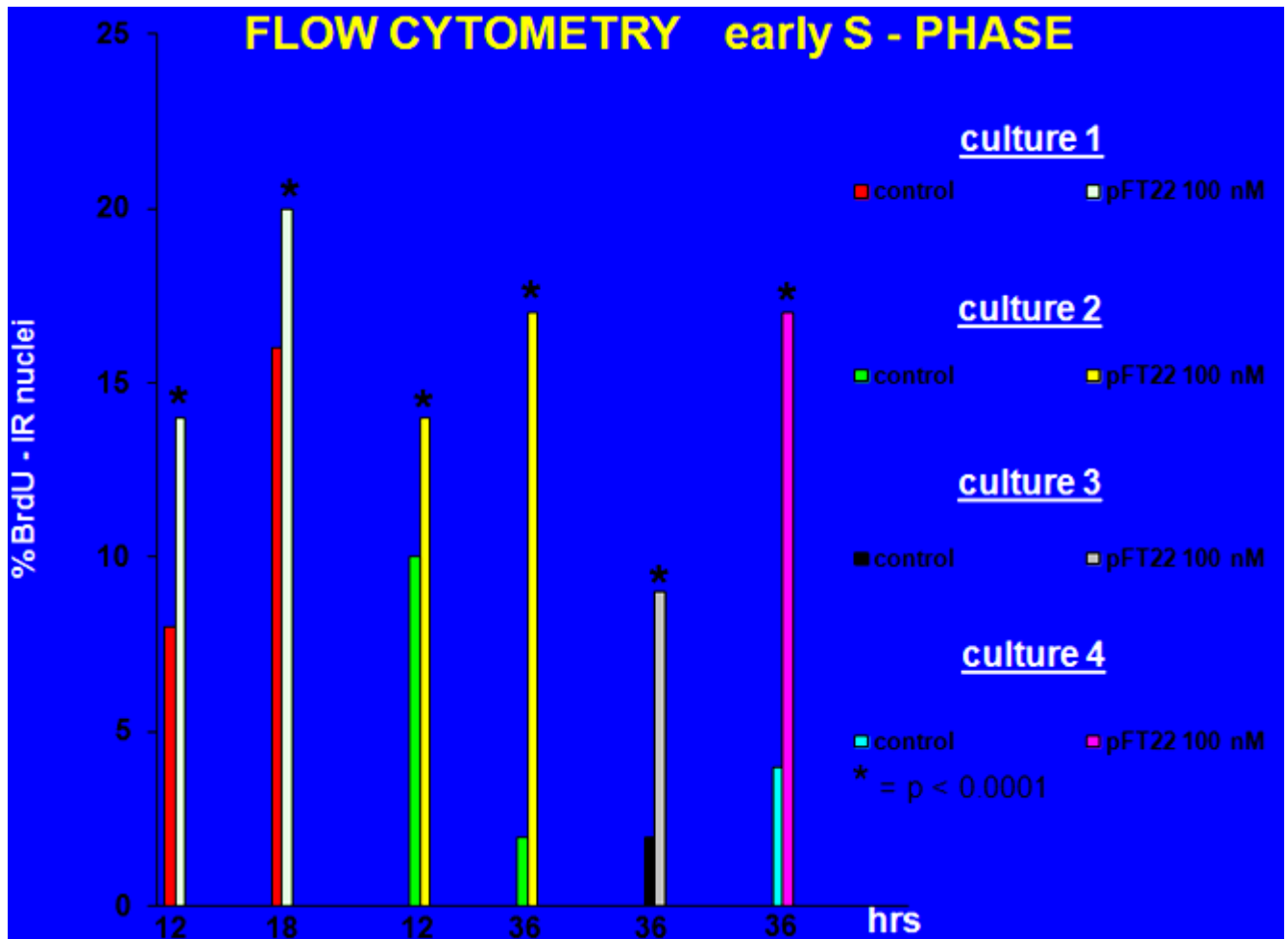
FIG. 28: Percentage of BrdU incorporation (early-S phase). Each point represents the mean $\pm$ SD of three experiments for each monolayer analyzed.

Finally, figure 29 shows the results of the flow cytometric analysis of 3 different primary monolayer cultures from the male rat, anterior pituitary. Cells were treated with a single dose of 100 nM pFT22, and measurements were done up to 48 hs following peptide administration. A statistically significant increase in cells of the S-phase with respect to controls was detected in all cell cultures, indicating that pFT22 stimulated anterior pituitary cells actively replicate their DNA, up to 48 hs.
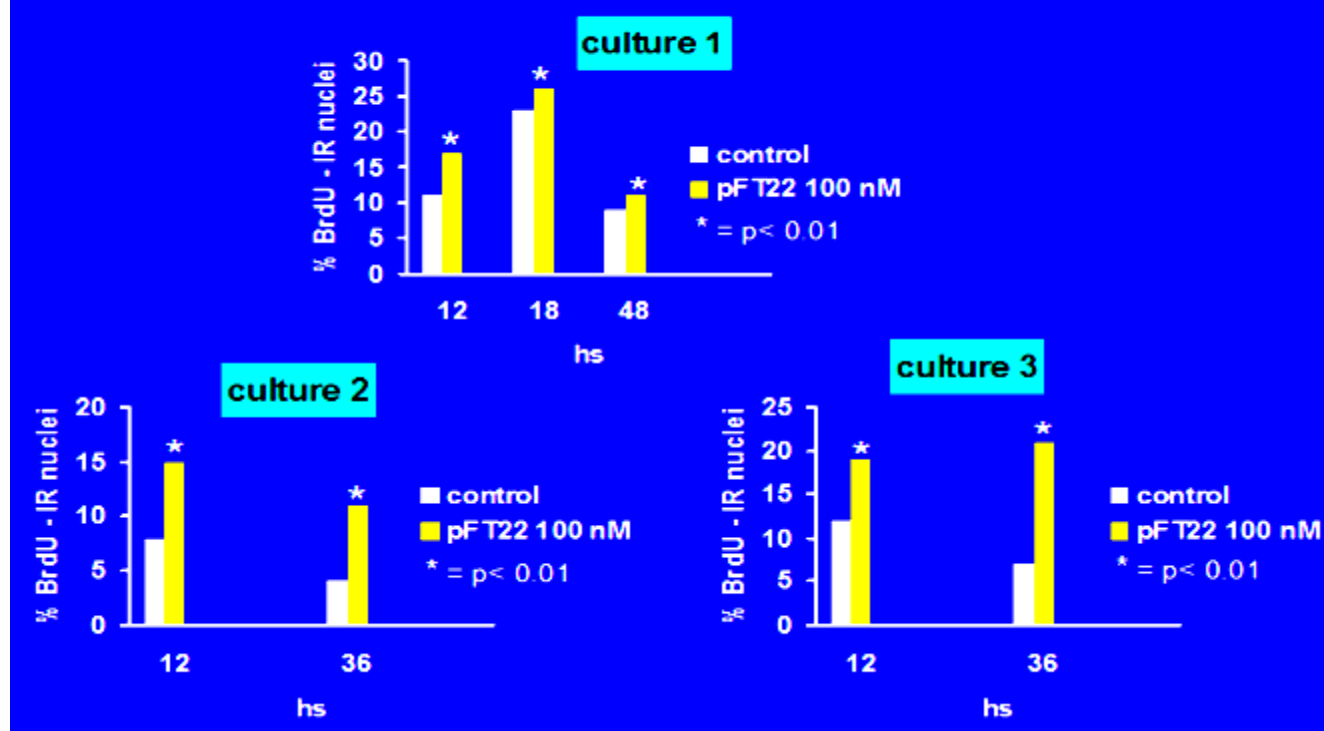
FIG. 29: Percentage of BrdU incorporation (S- phase). Each point represents the mean $\pm$ SD of three experiments for each monolayer analyzed.

Synchronization studies

a. Synchronization using serum starvation

Figure 30A shows the evolution of the percentage of GH4C1 cells in the various phases of the cell cycle following serum starvation, up to 72 hours. This distribution clarify that the large majority of serum-deprived cells are in the G0-G1 phase, indicating that serum starvation favours synchronization of almost two thirds of the GH4C1 cell population. In contrast, figure 30B shows the evolution of the percentages of the <3n and >6n cell rates, *i.e.* the hypotriploid and hypertriploid GH4C1 cells, possibly representing apoptotic cells and either cell doublets or cells growing as agglomerates, respectively. Finally, the Table summarizes the proportion of cells in the various cell cycle phases as a function of the total of cells cleaned by the hypotriploid and hypertriploid sets. This, to get more standardized and reproducible calculations of the cell population ploidy to be applied to all synchronization experiments, although hypertriploid sets could equally be considered viable cell groups due to the typical growth of GH4C1 in chains of floating cells. However, based on the starting assumptions it was clear that synchronization resulted more effective at 24h and 36h, yielding around 74% of the cells in the G0/G1phase.

Confirmation of this assumption is provided by figure 30C. It depicts the logarithmic amplification of the DNA fluorescence histogram of cells at 72 hs

after starvation. In these conditions a particularly marked polyploidy was observed, including 15% of 12n cells and 12% of 24n cells strongly reducing the G0-G1 pool, that accounted only for less than 40% of cells.

NO SERUM

A)

NO SERUM

B)
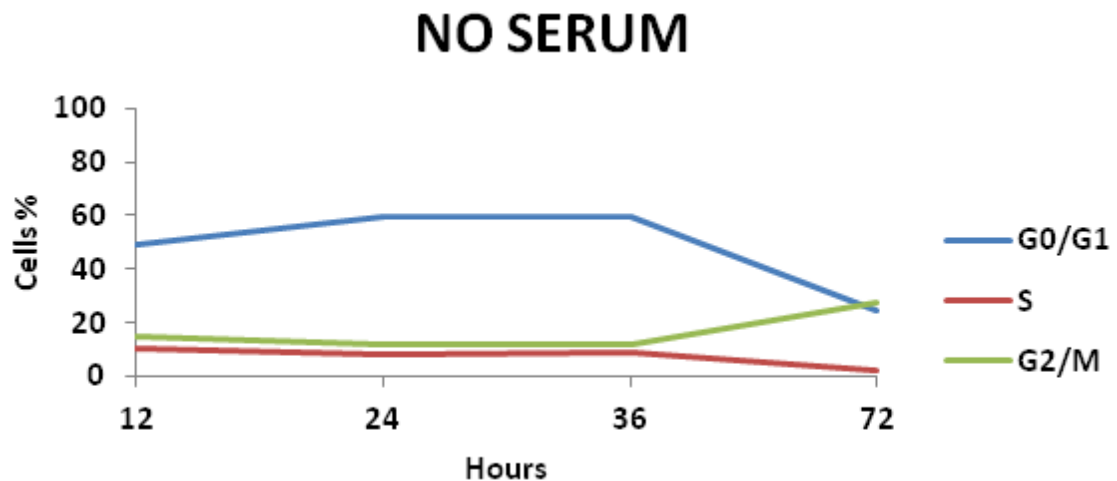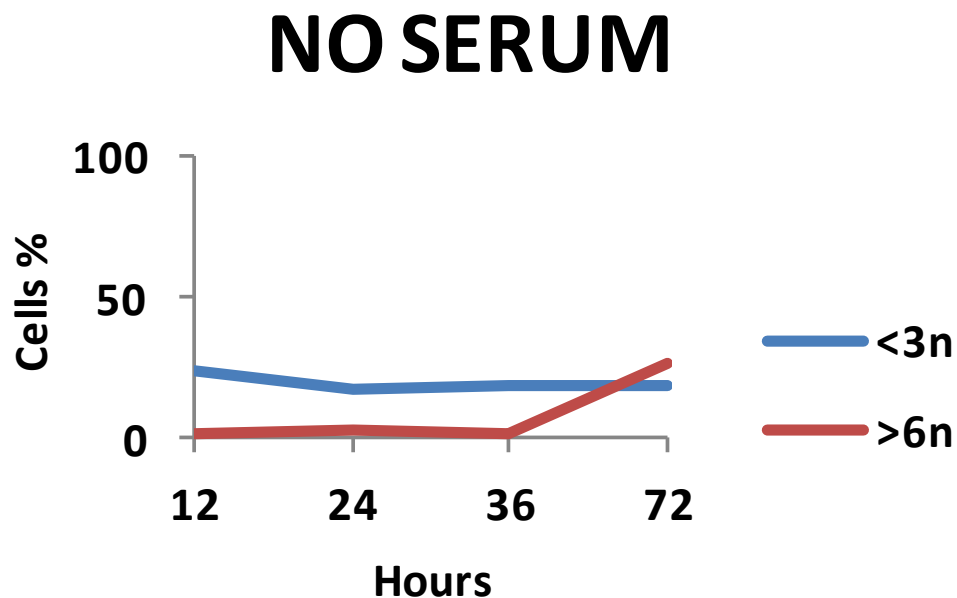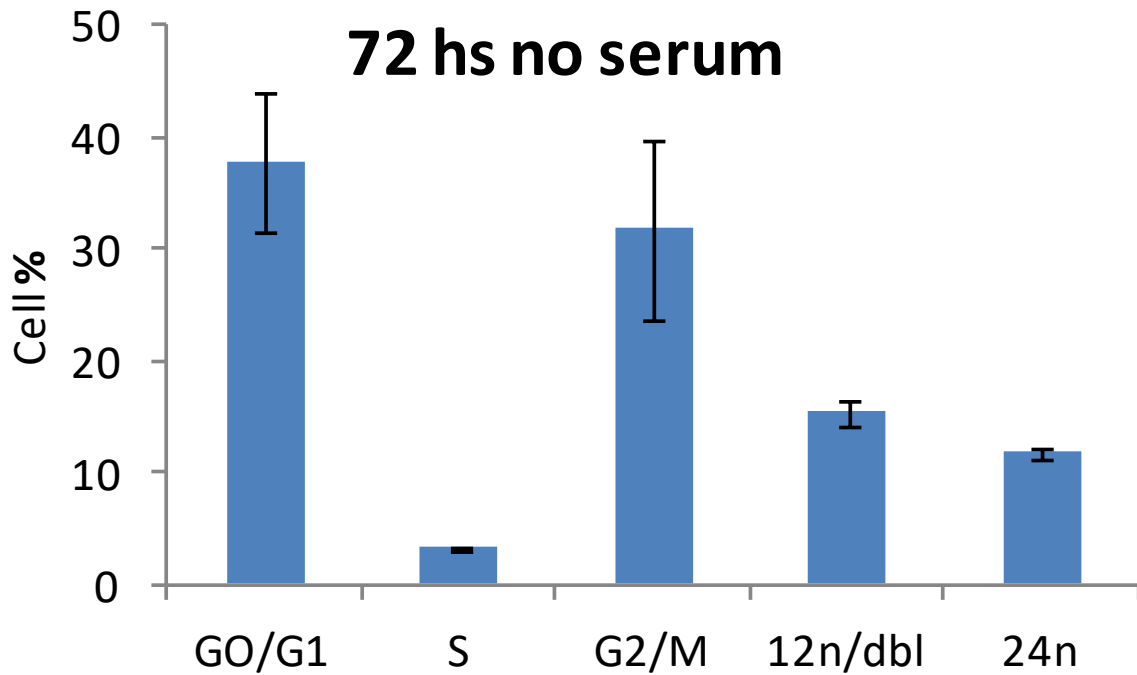
72 hs no serum

C)

NO SERUM	12hs	24hs	36hs	72hs
G0/G1 + S + G2/M	**74,8%**	**80,0%**	**80,0%**	**54,0%**
G0/G1	65,0%	74,0%	74,2%	45,1%
S	12,8%	10,6%	11,1%	4,0%
G2/M	20,2%	15,3%	14,6%	50,8%

D)

FIG. 30: GH4C1 synchronization using serum starvation up to 72hs. A) evolution in the percentage of cells in the various phases of the cycle (G0/G1-S-G2/M phases including the percentages <3n and >6n rates; B) <3n and >6n rates; C) GH4C1 cells cycle after 72hs of serum starvation (12n/doublets) Each point represent the mean $\pm$ SD of two experiments for each monolayer analyzed; D) table of the percentages of total cells in G0/G1-S-G2/M phases of cell cycle excluding the <3n and >6n rates.

b. Synchronization using serum starvation plus hydroxyurea

Figure 31A and B and the relative table shows the results obtained after treatment of serum-deprived GH4C1 with 2mM hydroxyurea, up to 72 hs. While the percentage of cells in G0-G1 slightly decreased, that of cells in G2-M correspondingly increased at the end of the 72 hs of treatment. Remarkably, a progressive increase in the hypotriploid cells was observed, suggesting increase in apoptosis.

A)
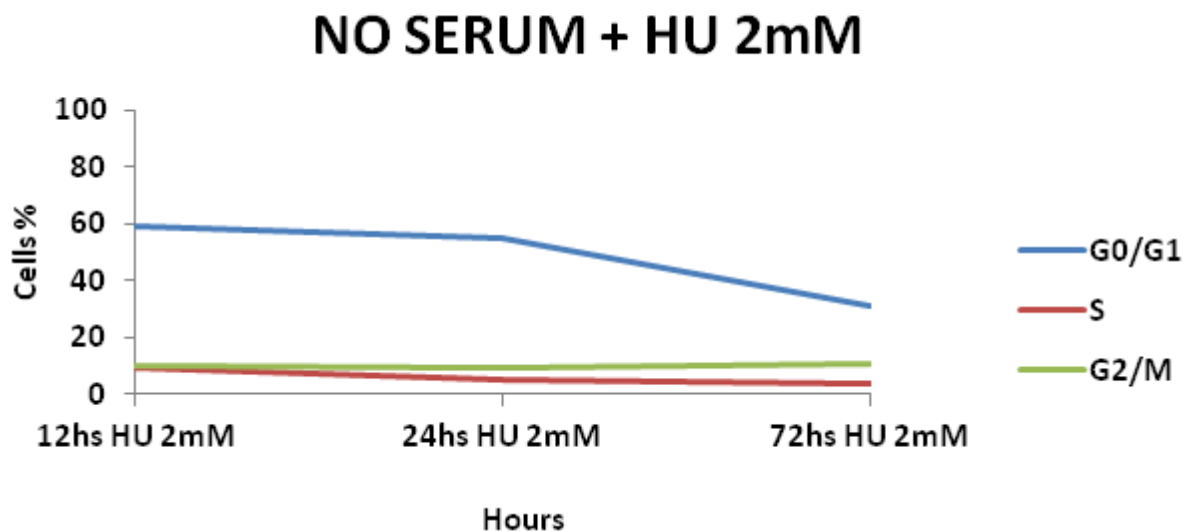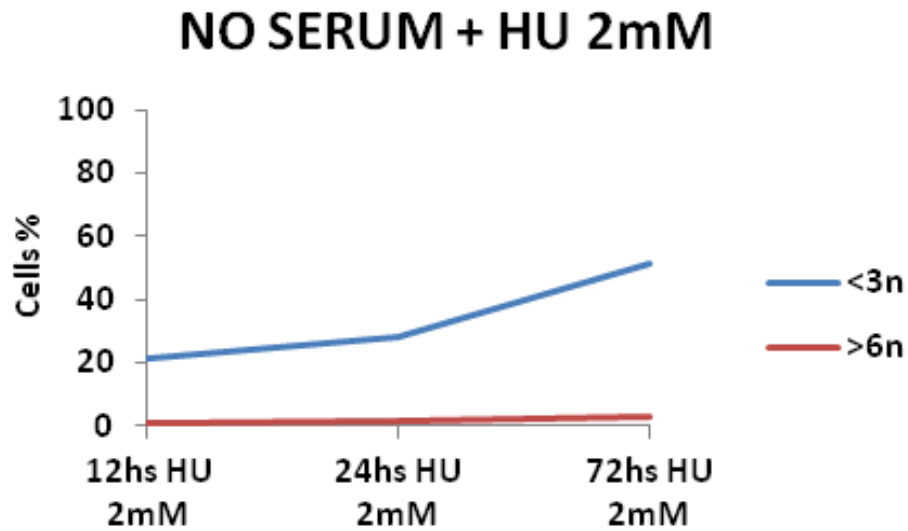
NO SERUM + HU 2mM

B)

NO SERUM + HU 2mM	12hs	24hs	72hs
G0/G1 + S + G2/M	78,0%	70,0%	42,0%
G0/G1	75,3%	78,8%	68,6%
S	12,1%	7,7%	8,1%
G2/M	12,6%	13,4%	23,4%

C)

FIG. 31: GH4C1 synchronization using serum starvation and 2mM hydroxyurea up to 72hs. A) evolution in the percentage of cells in the various phases of the cycle (G0/G1-S-G2/M phases including the percentage <3n and >6n rates; B) <3n and >6n rates; C) table of the percentages of total cells in G0/G1-S-G2/M phases of cell cycle excluding the <3n and >6n rates

Figure 32A and B and the relative table shows the results obtained after treatment of serum-deprived GH4C1 with 4mM hydroxyurea, up to 72 hs. The behavior of cells in the different phases of the cell cycle was quite similar to that observed with 2mM hydroxyurea.

NO SERUM + HU 4mM

A)
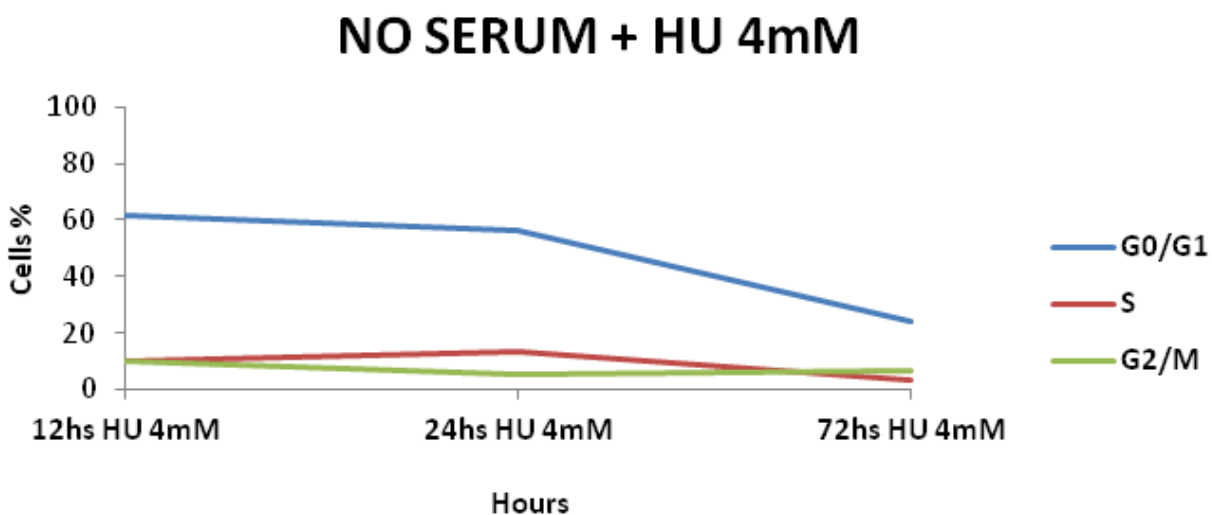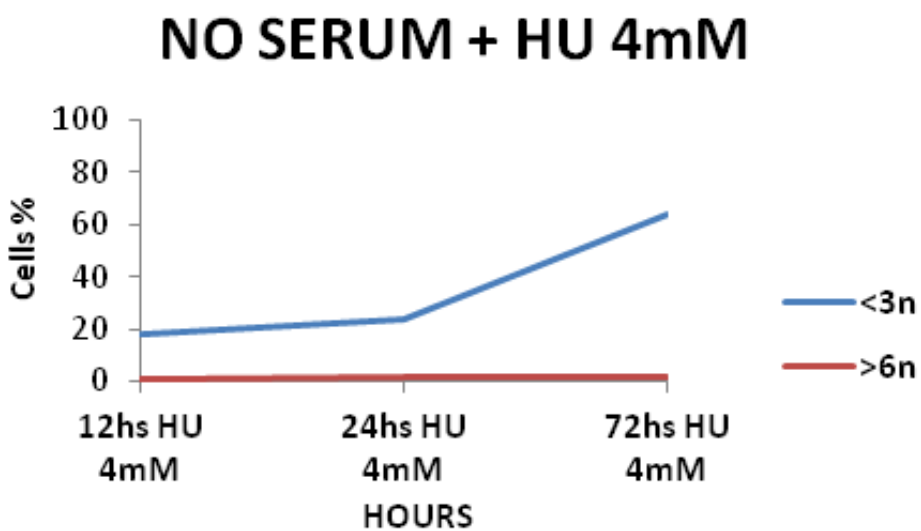
NO SERUM + HU 4mM

B)

NO SERUM + HU 4mM	12hs	24hs	72hs
G0/G1 + S + G2/M	81,6%	74,9%	34,6%
G0/G1	75,2%	75,3%	70,2%
S	12,6%	17,6%	9,5%
G2/M	12,1%	7,1%	20,2%

C)

FIG. 32: GH4C1 synchronization using serum starvation and 4mM hydroxyurea up to 72hs. A) evolution in the percentage of cells in the various phases of the cycle (G0/G1-S-G2/M phases including the percentage <3n and >6n rates; B) <3n and >6n rates; C) table of the percentages of total cells in G0/G1-S-G2/M phases of cell cycle excluding the <3n and >6n rates

Figure 33 and the relative table shows the results obtained after treatment of serum-deprived GH4C1 with either 6mM or 10 mM hydroxyurea, for 24 hs. The behavior of cells in the different phases of the cell cycle was slightly worse than that observed with smaller doses, including a quite substantial percentage of hypotriploid cells (up 25%), suggesting increased apoptosis.

NO SERUM + HU 6mM - 10mM
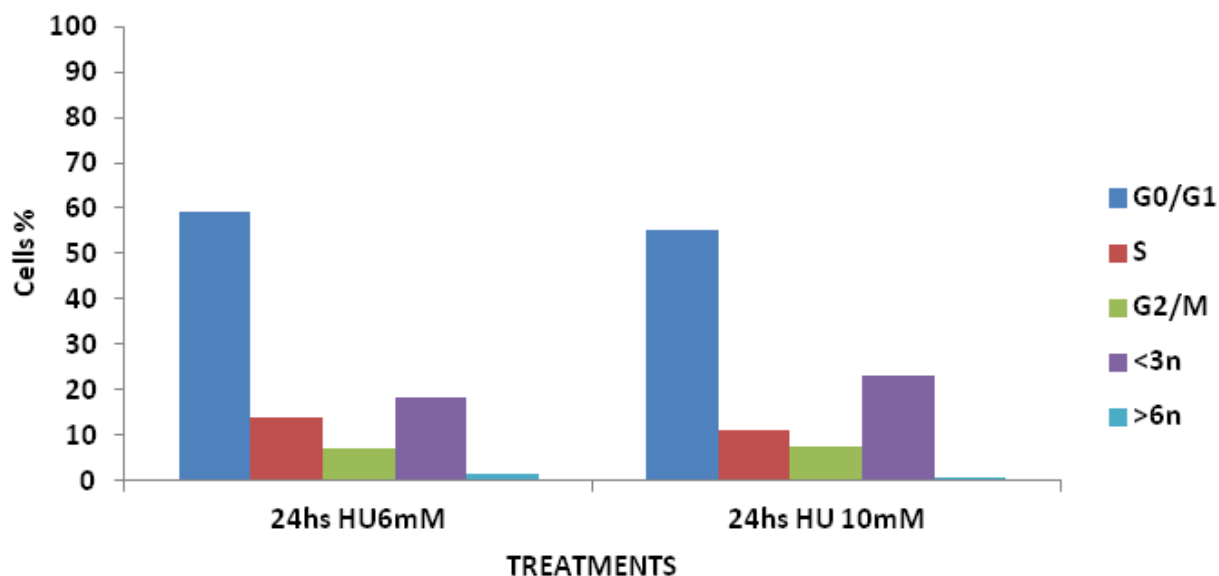
A)

NO SERUM	HU 6mM 24hs	HU 10mM 24hs
G0/G1 + S + G2/M	80,4%	74,1%
G0/G1	73,7%	74,7%
S	17,2%	15,1%
G2/M	8,9%	10,3%

B)

FIG. 33: GH4C1 synchronization using serum starvation and 6mM or 10mM hydroxyurea for 24hs. A) evolution in the percentage of cells in the various phases of the cycle (G0/G1-S-G2/M phases including the percentage <3n and >6n rates; B) table of the percentage of total cells in G0/G1-S-G2/M phases of cell cycle excluding the <3n and >6n rates

Finally, figure 34 and the relative table show the results obtained after treatment of serum-deprived GH4C1 for 24 hs, followed by administration of either 2mM or 4 mM hydroxyurea for 12 hs. No substantial improvement in cell synchronization was detected with respect to the other treatments. In addition, a very substantial percentage of cells (up 25%) resulted hypotriploid, suggesting increased apoptosis likely due to toxic effects of hydroxyurea.
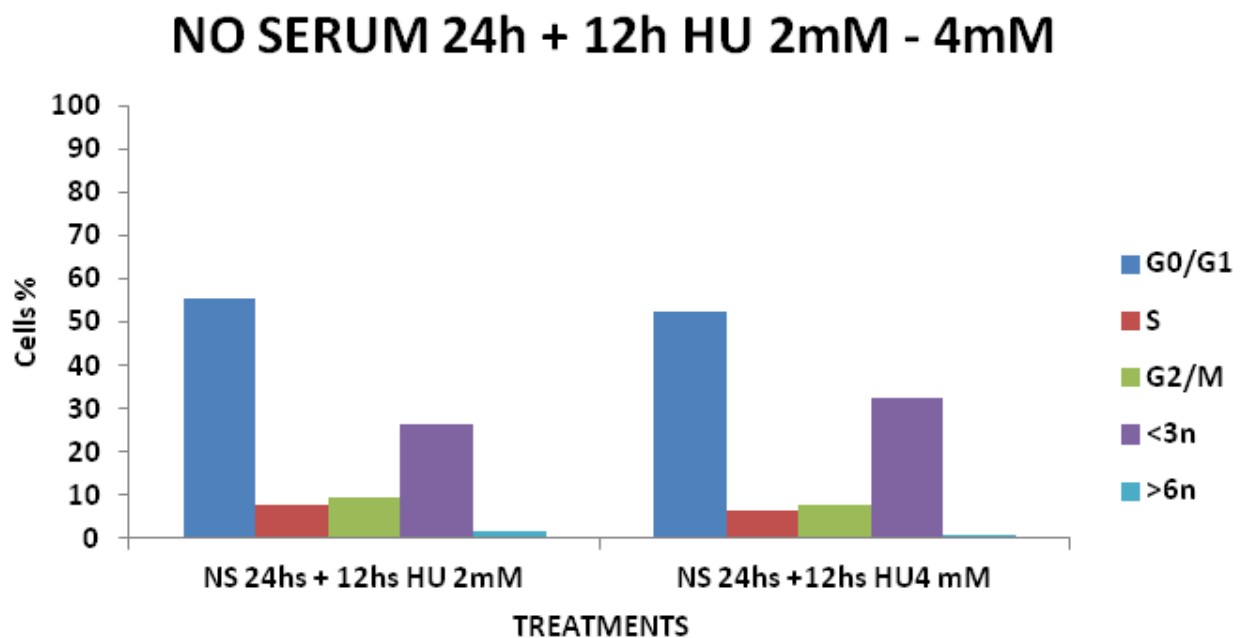
A)

NO SERUM 24hs	+12hs HU 2mM	G0/G1 + S + G2/M
G0/G1 + S + G2/M	72,6%	67,0%
G0/G1	76,3%	78,5%
S	10,6%	9,7%
G2/M	13,8%	11,8%

B)

FIG. 34: GH4C1 synchronization using serum starvation for 24h4s and 2mM or 4mM hydroxyurea in serum starvation for 12hs. A) evolution in the percentage of cells in the various phases of the cycle (G0/G1-S-G2/M phases including the percentage <3n and >6n rates B) table of the percentages of total cells in G0/G1-S-G2/M phases of cell cycle excluding the <3n and >6n rates

Figure 35 summarizes all synchronization treatment protocols tested, showing the real absolute percentages of cells in the different cell cycle phases, including hypotriploid and hypertriploid cells. By comparing all these protocols with a n_xm contingency table, it was determined that the most efficient and statistically significant treatment for synchronization of GH4C1 cells was that using 4mM hydroxyurea for only 12 hs in serum-deprived cells (enlightened in red in the table).

	% G0/G1	% S	% G2/M	% < 3n	% >6n
NS 12h	49,3%	10,4%	15,1%	23,4%	1,9%
NS 12h HU 2mM	59,0%	9,5%	9,9%	21,2%	0,9%
NS 12h HU 4mM	61,4%	10,3%	9,9%	17,9%	0,9%
NS 24h	59,4%	8,6%	12,3%	17,2%	2,3%
NS 24h HU 2mM	55,2%	5,4%	9,4%	28,3%	1,4%
NS 24h HU 4mM	56,4%	13,2%	5,3%	23,6%	1,7%
NS 24h HU6mM	59,3%	13,9%	7,2%	18,4%	1,4%
NS 24h HU 10mM	55,3%	11,2%	7,6%	23,2%	0,9%
NS 36h	59,4%	8,9%	11,7%	18,7%	1,7%
NS 24h + 12h HU 2mM	55,4%	7,7%	9,5%	26,3%	1,5%
NS 24h +12h HU4 mM	52,6%	6,5%	7,9%	32,3%	1,0%
NS 72h	24,5%	2,2%	27,6%	18,6%	27,2%
NS 72h HU 2mM	31,4%	3,7%	10,7%	51,2%	3,3%
NS 72h HU 4mM	24,3%	3,3%	7,0%	63,8%	1,9%

FIG. 35: contingence table; χ2= 368843, 52 freedom degree, P=0,000; NS = no serum; HU = hydroxyurea.

Evaluation of reversibility of the cell cycle block after synchronization with serum starvation and hydroxyurea 4mM

Figure 36 shows the behavior of GH4C1 cells synchronized with the best protocol previously identified (serum starvation + 4mM hydroxyurea for 12 hs) once that they were re-feeded for 24 hs with standard culture medium but still serum-deprived. It was clear that part of the cells blocked in the G0-G1 phase by the treatment with hydroxyurea were able to re-enter the cell cycle. This was supported by the statistically significant increase of cells in the S-phase and reduction of cells in the G2-M phase, as compared with control

cultures kept for the entire 36 hs of the experiment in standard medium with serum.

HU block reversibility after 24hs
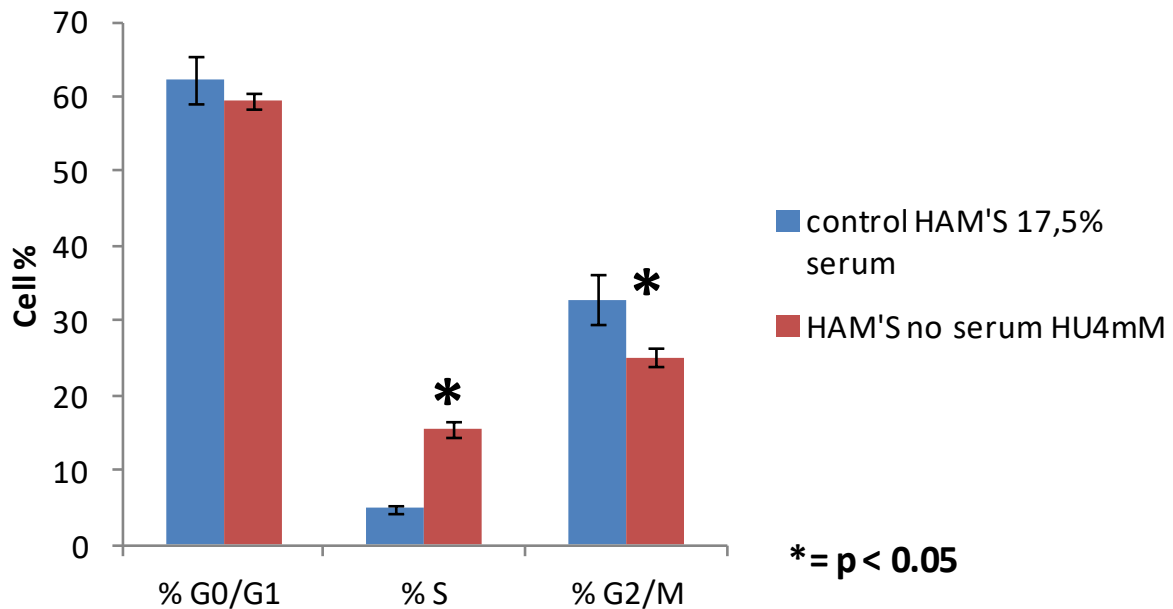
FIG. 36: HU block reversibility after 24hs HU removal and medium replacement; control: GH4C1 cells grown in standard condition. Each point represents the mean $\pm$ SD of three experiments.

Figure 37 shows the logarithmic amplification of the previously reported distribution of GH4C1 cells following removal of the hydroxyurea treatment, and the re-enter of a cell fraction into the cell cycle. Similar to synchronized cultures, these de-synchronized cultures still exhibited a consistent fraction of hypertriploid cells, up to 48 hs.

12 hs 4mM HU no serum + 24 hs no serum

12 hs 4mM HU no serum + 48 hs no serum
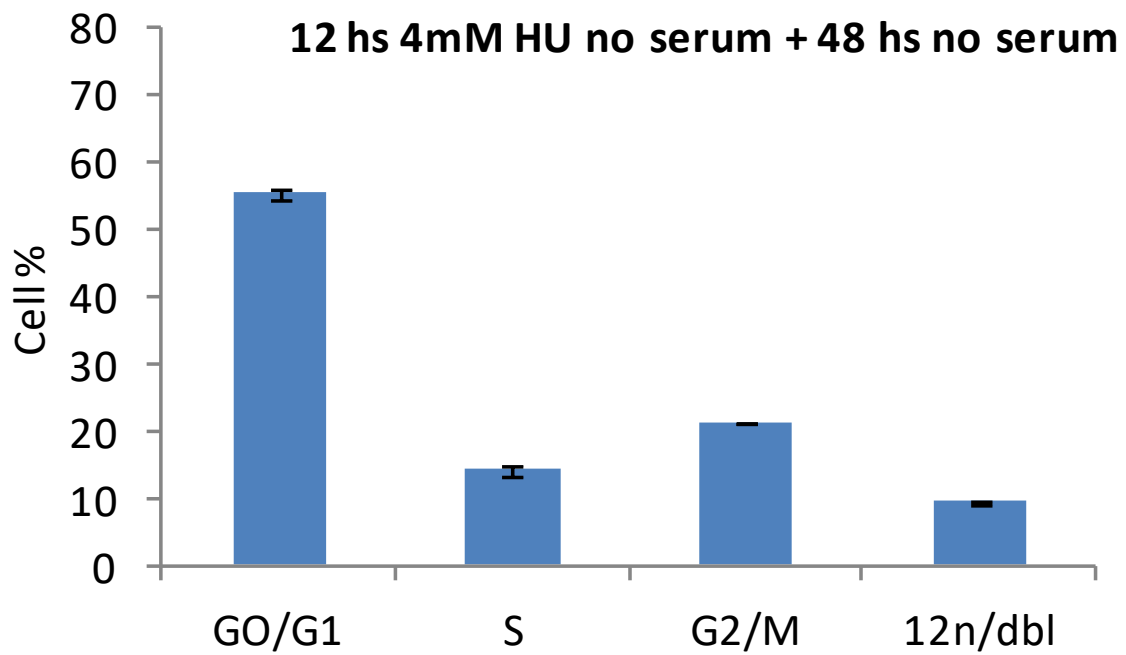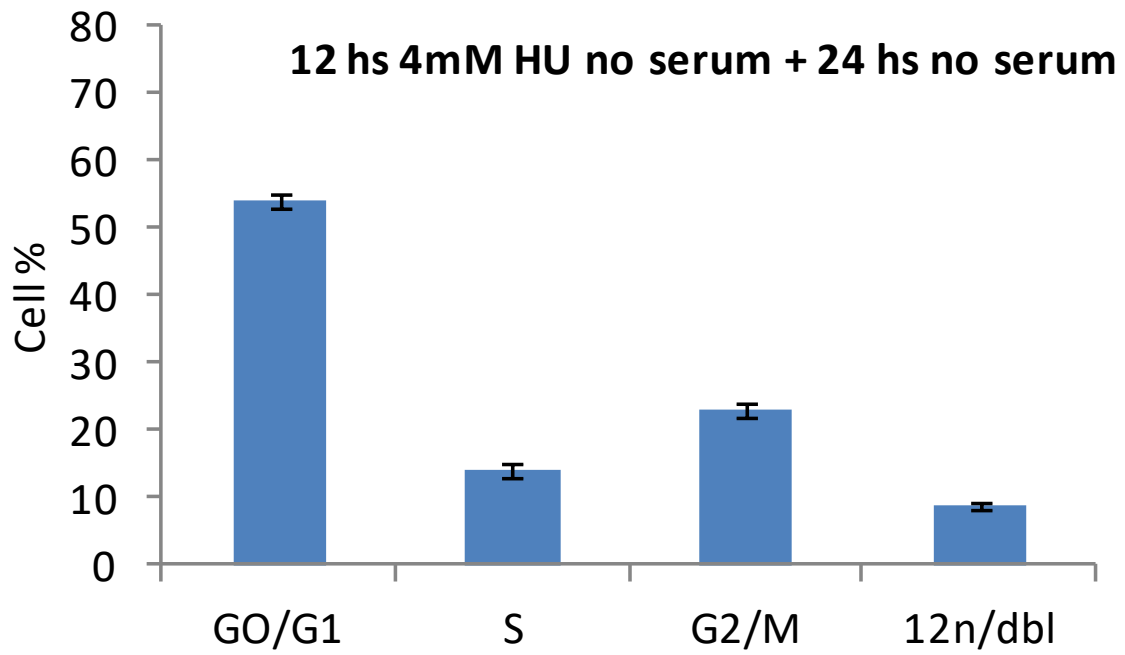
FIG. 37: GH4C1 cells cycle at 24 and 48hs following HU removal. Each point represents the mean $\pm$ SD of three experiments.

DISCUSSION

1. *Evidence for a role of nonTRH cryptic peptides, and TRH itself as regulators of growth and differentiation of anterior pituitary cells*

A potential physiological role for the nonTRH, cryptic fragments derived from the processing of the TRH prohormone, proTRH in the rat hypothalamic tuberoinfundibular system and, possibly anterior pituitary cells is still largely unknown. However, all these neuropeptides have the molecular features to be released in both the hypothalamic-pituitary portal system and/or the anterior pituitary interstitum, to act as either neuroendocrine, paracrine, or autocrine hormones.

Indeed, in rodent models nonTRH sequences from the C-terminal fragment of proTRH have been found to act either as regulators of anterior pituitary secretion (9, 10, 12, 37, 38, 42, 43) or as neuromodulators of the neural circuitries involved in the reaction to drug addiction (44, 45).

In contrast, very few data are available on a possible role of the nonTRH peptides derived from the N-terminal fragment of proTRH. Currently, the only effect hypothesized concerns preproTRH$_{53-74}$ or pFT22 that has been involved as a pain modulator in the rodent central nervous system (48-54). However, pFT22 can be co-secreted with mature TRH and the other N-terminal fragment, preproTRH$_{25-50}$ or pYE from the hypothalamic ME *in*

vitro, primarily in conditions of reduced levels of circulating thyroid hormones (22) thus suggesting a possible functional role in the anterior pituitary. Whether this neuroendocrine regulation concerns the secretion of anterior pituitary hormones or the control of growth and/or differentiation of anterior pituitary cells remains, at present, still unsolved.

In addition, pFT22 has been found in rat anterior pituitary somatotrophs (26), where proTRH and its N-terminal peptides can be processed and secreted *in vitro* in response to thyroid hormones and glucocorticoids (31). This has suggested a very specific tissue-dependent regulation of proTRH in the anterior pituitary (28), likely expressing the capacity of proTRH-derived molecules to act as intrapituitary, autocrine and/or paracrine factors (77). Whether this autocrine / paracrine regulation is aimed at regulating the secretion of specific anterior pituitary cell types or their growth and/or differentiation remains a mystery. However, it is relevant that proTRH processing and release of TRH occur in human anterior pituitary adenomas, primarily of the somatomammotroph lineage (GH- and PRL-secreting adenomas). This has suggested that TRH itself and nonTRH peptides might play a role in regulating growth and differentiation of pituitary cells including the adenomatous ones (28, 29).

To shed light on all these aspects, it should be considered that TRH may be synthesized by thyrotrophs, somatotrophs and gonadotrophs both in the early

postnatal period and adult life (24, 26, 78, 79). In particular, adult male rat gonadotrophs may *in vitro* release mature TRH after administration of the decapeptide gonadotropin-releasing hormone (GnRH) (24). This is consistent with the observation that GnRH is as effective as TRH in inducing thyrotroph differentiation in rat fetal, pituitary cell cultures (80). Since GnRH may be synthesized by gonadotrophs both in rats and humans (81, 82), it is possible to presume that it might be part of an autocrine/paracrine system for pituitary release of TRH in the course of mammalian thyrotroph differentiation. Indeed, a network of common differentiating signals is shared by thyrotrophs and gonadotrophs, as in the case of the nuclear transcription factor GATA isoform 2 (GATA2). GATA transcription factors comprise a family of six nuclear zinc finger, tissue-specific gene activators (GATA 1-6) that may be found in many developing tissues (83). Within the fetal pituitary, GATA2 is expressed in a ventral-dorsal gradient and, according to Dasen et al. (84) this gradient is responsible for gonadotrophs and thyrotrophs differentiation. In particular, the high levels of GATA2 in the ventral region would induce the gonadotroph phenotype. In contrast, in the dorsal area GATA2 would interact with the Pituitary-1 (Pit1) transcription factor to elicit thyrotroph differentiation (85). It is therefore intriguing that thyrotroph sensitivity to differentiating effect of TRH starts in prenatal life. In particular, 1 nM TRH is capable of inducing thyrotroph differentiation in rat pituitary fetal cultures just after 1 day of incubation (86). This is in keeping with the evidence that rat thyrotrophs

proliferate maximally in the early postnatal period (87), when TRH levels in the hypothalamus are low, then to largely differentiate when TRH secretion rises later during development (88). The fact that mice with knockout of the TRH gene have at birth normal thyrotroph number but reduced thyrotroph function (89), and that a marked reduction in the number of TSH-cells occurs in these mutants during postnatal life (90) supports the concept that TRH is not a primary factor for thyrotroph growth during fetal development but may become important later, as a differentiating agent for thyrotroph maturation.

A similar consideration may be valuable also in man. Anencephalic fetuses may have a normal number of pituitary thyrotrophs at birth (91 - 94), suggesting that in humans growth of TSH-cells during fetal life might be, at least partially, independent of the TRH influence (95). Results of some experiments raise the possibility that TRH exerts time- and dose-dependent, differentiating effects also in adult life. *In vivo* administration of 200 µg TRH twice daily for 7-14 days increases the number of adult male, rat TSH-cells. In contrast, a longer treatment (34 days) does not amplify thyrotroph amount, that remains at basal levels (96). In addition, intraperitoneal administration of 25 µg TRH to thyroidectomized, adult male rats produces an initial pituitary proliferation spurt at 12 h, followed by a growth decline at 24 h (97). Thus, it is possible that these growth arrests represent differentiation phases of adult thyrotroph cells.

A similar reasoning might be invoked to interpret the growth-inhibitory action of TRH in the rat tumoral, lactotroph GH3 and somatotroph GH4 cell lines. Chronic treatment with 1 nM TRH increases GH3 cellular growth, whereas doses of TRH ranging from 2 to 100 nM inhibits it in both GH3 and GH4 cells (98, 99). Similarly, synthesis and release of TRH by human prolactin (PRL)-secreting, growth-hormone (GH)-secreting and non-secreting pituitary adenomas (28, 100), and detection of TRH-R mRNA in the same tumoral types and in TSH adenomas (101), raise the possibility that TRH acts through an autocrine/paracrine mechanism to promote differentiation during pituitary tumorigenesis.

In summary, a physiologic role of TRH is either to stimulate proliferation or induce differentiation of pituitary thyrotrophs (and possibly other cell types) in relation to the concentration of the tripeptide in the pituitary, stage of fetal development and age of postnatal life. An additional role might be played by TRH as a differentiating signal during pituitary tumoral growth.

Whether similar conclusions could be applied also to the nonTRH cryptic peptides and, in particular to those of the N-terminal fragment remains to be elucidated. An initial answer would like to be provided by this PhD thesis, focusing the investigation on the potential growth effect of pFT22 on anterior pituitary cells.

2 . *Evolutionary and structural features of pFT22*

A first step in this study has been to understand the potential evolutionary role of pFT22, and some of its structural features possibly relevant for a role as a growth factor.

Using a well established bioinformatic approach, it has been possible to understand that pFT22 is a peptide highly conserved in the rodent proTRH molecule. In particular, both amino-acid (AA) similarities and possible common ancestor homology have been proved in the rodent group. This suggests that the peptide must play a very peculiar and selective activity in the tuberoinfundibular and anterior pituitary of these mammals. Since regulation of the mammalian pituitary growth and form requires very specific factors (102), it would be tempting to speculate that pFT22 might be involved in such a regulation. In addition, around one third of the AA sequence of pFT22 can be recognized in the human N-terminal fragment of proTRH, where no dibasic cleavage proteolysis is expected to occur (103). This raises the possibility that some very ancient role of the pFT22 sequence is conserved in humans as a part of a longer peptide corresponding to the entire human N-terminal fragment of proTRH. As a result, the whole N-terminal fragment might retain a still unknown functional activity for anterior pituitary cells in man, possibly a growth factor activity.

These functional considerations are supported by the studies here conducted on the 3D structure of pFT22 in aqueous solution. Using circular

dichroism, it has been possible to show that once pFT22 is dissolved in a standard aqueous environment it stays in a conformational state with a very high statistical potential, *i.e.* it can assume a number of different 3D structures as a function of the chemical-physical properties of the medium and interacting biological membranes. This condition is called random coil, and can be figured out as a peptide tangle continuously changing its conformational state in dependence on temperature, pH, and surrounding molecules (104). In the present experiments, we used a quite acidic solvent (distilled water) that has been shown to induce random coil also in a tripeptide like TRH (105), whose 3D structure can be stabilized by increase in the solvent pH (between 7 and 9) or bonding of carbon chains to its AA (106). Therefore, we conclude that the pFT22 molecule has the potential to become conformationally stable. In particular, this stabilization is expected once it would interact with phospholipids of the pituitary cell membranes, that are rich in carbon chains and it would find a neutral environmental pH. Such a condition would be a pre-requisite for its binding to a specific membrane receptor, currently unknown. Studies are in progress to verify all these assumptions.

3. *Role of pFT22 as a powerful growth factor for anterior pituitary cells, and in particular for somatomammotrophs*

To study the role of pFT22 as a possible growth factor for anterior pituitary cells, we choose two different cell systems including the rat adenoma cell line GH4C1, able to co-secrete both GH and PRL in basal conditions and primary monolayer cultures of male rat anterior pituitary.

GH4C1 cells are rat adenomatous cells of the somatomammotroph lineage widely used as a suitable model for studying *in vitro* hormone-receptor interactions in the anterior pituitary gland, primarily those involved in the regulation of somatotrophs. In fact, these cells have been shown to maintain a number of receptors for hypothalamic neurohormones, and pituitary hormones and to respond with secretion of GH and PRL to a number of stimulants (33, 34, 35, 64 - 68).

However, Gh4C1 cells have also been shown to modify their growth rate in response to a number of peripheral hormones (estradiol, T3) and growth factors including TRH itself, EGF, bFGF, insulin, PDGF (35, 64, 65, 67 - 72) , and IGF1.

In addition to its regulatory action on GH and PRL biosynthesis and secretion in anterior pituitary cells and cell lines (72, 107 - 112), IGF1 has been shown to increase cell replication both in normal anterior pituitary cells, primarily lactotrophs (113 - 116) and in PRL-secreting GH3 adenomatous cell lines (117, 118). Since GH4C1 cells are a clonal expansion of GH3 cells, a

similar growth promoting effect of IGF1 is expected. Therefore, IGF1 has been chosen as a reference growth factor to be compared with the possible growth activity of pFT22 in GH4C1 cell lines.

Indeed, the present studies based on analysis of the total DNA content in basal conditions, and after stimulation with either IGF1 and pFT22 have shown that pFT22 exerts a growth-promoting effect on GH4C1 cells to an extent comparable to that of IGF1. This phenomenon is observable in a dose range of 10-100 nM, that is consistent with that of many growth factors acting in the anterior pituitary gland (35, 64, 65, 67 – 72, 113 - 118).

This stimulatory effect of both IGF-1 and pFT22 on the growth of GH4C1 cells was confirmed using flow cytometric analysis, that revealed a trophic action of pFT22 even more powerful and long lasting (up to 48 hs) than that of IGF1. The reliability of these results and of the cytometric analysis in flow was supported by the use of other cell lines, well known to respond to IGF-1 including the mouse fibroblasts Swiss 3T3, and the human hepatocarcinoma cell line HEpG2 that exhibited a statistically significant increase in cell growth to the stimulatory action of IGF1 (119 - 122).

Confirmation of a possible physiological role of pFT22 as a growth factor for normal anterior pituitary cells was proved in primary monolayer cultures of male rat, anterior pituitary. These cells responded to pFT22 with a highly statistically significant increase in the number of cells entering the DNA replication step (S-phase). Although we did not analyze the pituitary cellular

subtypes responsive to pFT22, however it is likely at least part of them be somatomammotrophs (26, 30, 31). This possibility is supported by the evidence that primary pituitary cells were seeded to a concentration identical to that used in the GH4C1 experiments, they responded to the same amounts of pFT22 (100 nM), and the growth effect that they displayed followed a time response consistent with that found in GH4C1 cells (within 48 hs after peptide administration). All these data confirm preliminary studies developed by our group in the past (56, 57), showing that primary cultures of rat anterior pituitary were responsive to a single doses of pFT22 in a time range similar to that used in the present experiments.

Interestingly, primary pituitary monolayer cultures were prepared maintaining the transitional zone of the rat anterior pituitary, that contains adult pituitary stem cells (74). Here we show that our basal cell cultures were able to replicate for 7 days also in the absence of serum, suggesting presence of cells with increased growth potential like adult pituitary stem cells (74). Therefore, we cannot exclude that part of the cells responding to pFT22 are undifferentiated pituitary stem cells (74, 123). This possibility would play a very relevant role in the most recent technological approaches focused on reconstruction of a bioartificial anterior pituitary as a therapeutic tool to definitely treat panhypopituitarism like that occurring as a consequence of congenital transcription factor mutations in children, and traumatic brain injury

in adults (124). Studies are in progress to evaluate the involvement of adult rat, pituitary stem cells in the growth stimulatory action of pFT22.

Finally, in the attempt to ameliorate the response of GH4C1 cells to the growth effects of pFT22 and IGF1, we initiated a series of experiments aimed at finding culture protocols able to synchronize at best this cell line. Synchronization, in fact, would represent an ideal condition to investigate in detail the intracellular signaling systems involved in the response of pFT22, as well as to isolate a specific pFT22 receptor, still unknown. Although these studies are in progress, however the current results have indicated that hydroxyurea might be a useful molecule to reach this aim. This molecule, in fact, has been shown to inhibit the ribonucleotide reductase in a number of mesenchymal cell lines, with the effect of reversibly blocking a large proportion of culture cells in the quiescent pool, G0-G1 (125 - 130)

CONCLUSIONS

The primary aim of this PhD thesis was to prove that the nonTRH, cryptic sequence of the N-terminal fragment of proTRH, preproTRH$_{53-74}$ (pFT22) can act as a growth factor for mammalian anterior pituitary cells. The results presented support this assumption, showing that pFT22 exerts a powerful *in vitro* growth effect on both normal anterior pituitary cells of the male rat, and on rat adenomatous cells of the somatomammotroph lineage. This effect

results even higher than that of a well known growth factor for anterior pituitary cells like IGF1. We suggest that pFT22 is involved in the regulation of cell growth in the anterior pituitary and, if proved to interact with adult pituitary stem cells might become a suitable molecular tool to regulate their replication also in bioartificial systems for tissue engineering. Studies are in progress to define the molecular structure of the peptide during its interaction with the plasma membrane in physiological conditions, the existence of a specific membrane receptor, and the intracellular signaling systems activated during its growth promoting effects.

ACKNOWLEDGEMENTS

I would thank Prof. Lucio Cocco (Cell Signalling Laboratory, Dept. of Biomedical and Neuromotor Sciences, University of Bologna School of Medicine, Bologna, Italy) for providing Swiss 3T3 cells.

Finally, I am very grateful to all my colleagues in the Human Anatomy Section: Davide Dallatana, Elena Bassi, Marco Alfieri, Elia Consolini, Daniela Galli, Cecilia Carubbi, Silvia Martini, Giulia Pozzi, Elena Masselli, Cristina Micheloni for their continuous help and kindness during the tenure of my PhD course.

Last but not least I really wish to thank my parents who has supported me during all these years.

REFERENCES

1. **Morrell JI, Rosenthal MF, McCabe JT, Harrington CA, Chikaraishi DM, Pfaff DW.** Tyrosine hydroxylase mRNA in the neurons of the tuberoinfundibular region and zona incerta examined after gonadal steroid hormone treatment. Mol Endocrinol. Sep;3(9):1426-33. 1989

2. **Lechan RM, Wu P, Jackson IM, Wolf H, Cooperman S, Mandel G, Goodman RH**: Thyrotropin-releasing hormone precursor: characterization in rat brain. Science 231:159–161, 1986

3. **Lechan RM, Wu P, Jackson IMD**: Immunolocalization of the thyrotropin- releasing hormone prohormone in the rat central nervous system. *Endocrinology* 119:1210–1216, 1986

4. **Fekete C, LechanRM**: Negative feedback regulation of hypophysiotropic thyrotropin-releasing hormone (TRH) synthesizing neurons: role of neuronal afferents and type 2 deiodinase. Front Neuroendocrinol 28:97–114, 2007

5. **Xin X, Varlamov O, Day R, Dong W, Bridgett MM, Leiter EH, Fricker LD**: Cloning and sequencing analysis of cDNA encoding rat carboxypeptidase D. *DNA Cell Biol*16:897–909, 1997

6. **Fricker LD, Berman YL, Leiter EH, Devi LA**: Carboxypeptidase E activity is deficient in mice with the fat mutation. Effect on peptide processing. *J Biol Chem*271:30619–30624, 1996

7. **Schaner P, Todd RB, Seidah NG, Nillni EA**: Processing of prothyrotropin releasing hormone by the family of prohormone convertases. *J Biol Chem* 272:19958–19968, 1997

8. **Nillni EA, Sevarino KA, Jackson IMD**: Identification of the thyrotropin-releasing hormone prohormone and its post-translational processing in a transfected AtT20 tumoral cell line. *Endocrinology* 132:1260–1270, 1993

9. **Eduardo A. Nillni, and Kevin A. Sevarino**: The Biology of pro-Thyrotropin-Releasing Hormone-Derived Peptides Endocr. Rev. 20: 599-648, 1999

10.   **Nillni EA, Koenig JI, Aird F, Seidah NG, Bartnick A**: PreproTRH178–199 and two novel peptides derived from its processing are regulated during suckling. In: Program of the 81st Annual Meeting of The Endocrine Society, San Diego, CA, (Abstract p1–319), p 202, 1999

11.   **Cruz IP, Nillni EA**: Intracellular sites of prothyrotropin-releasing hormone processing. *J Biol Chem* 271:22736–22745, 1996

12.   **Nillni EA, Sevarino KA, Jackson IMD** Processing of proTRH to its intermediate products occurs before the packing into secretory granules of transfected AtT20 cells.*Endocrinology* 132:1271–1277, 1993

13.   **Xu H, Shields D**: Prohormone processing in the trans-Golgi network: endoproteolytic cleavage of prosomatostatin and formation of nascent secretory vesicles in permeabilized cells. *J Cell Biol* 122:1169–1184, 1993

14.   **Tooze SA, Chanat E, Tooze J, Huttner WB** Secretory granule formation. In: Loh YP (ed) Mechanisms of Intracellular Trafficking and Processing of Proproteins. CRC Press, Inc., Boca Raton, FL, pp 158–177, 1993

15.   **Seidah NG, Chretien M** : Proprotein and prohormone convertases of the subtilisin family recent developments and future perspectives. *Trends Endocrinol Metab* **3**:133–140, 1992

16.   **Bradbury, A. F., Finnie, M. D. A, and Smyth, D. *G*.** Nature 298,686-688, 1982

17.   **Kizer, J. S., Busby, W. H., Cottle, C., and Youngblood, W. W.** Proc. Natl. Acad. Sci. *U. S.* A. 81, 3228-3232, 1984

18.   **Eipper, B. A., and Mains, R. E**. Annu. Reu. Physiol. *50,* 333-344, 1988

19.   **Eipper B, May V, Cullen EI, Sato SM, Murthy ASN, Mains RE** : Cotranslational and posttranslational processing in the production of bioactive peptides. In: Meltzer HY (ed) Psychopharmacology: The Third Generation of Progress. Raven Press, New York, pp 385–400, 1987

20.   **Burgess TL, Kelly RB** : Constitutive and regulated secretion of proteins. *Annu Rev Cell Biol* 3:243–293, 1987

21.   **Lechan RM, Segerson TP**. Pro-TRH gene expression and precursor peptides in rat brain. Observations by hybridization analysis and immunocytochemistry. Ann N Y Acad Sci.553:29-59. 1989

22.   **Bruhn TO, Taplin JH, Jackson IMD** Hypothyroidism reduces content and increases *in vitro* release of pro-TRH peptides from the median eminence.*Neuroendocrinology* **53**:511–515, 1991

23.   **May V, Wilber JF, U'Prichard DC, Childs GV.** Persistence of immunoreactive TRH and GnRH in long-term primary anterior pituitary cultures.Peptides. May-Jun;8(3):543-58. 1987

24.   **Peters A, Heuer H, Schomburg L, De Greef WJ, Visser TJ, Bauer K.** Thyrotropin-releasing hormone gene expression by anterior pituitary cells in long-term cultures is influenced by the culture conditions and cell-to-cell interactions. Endocrinology. Jul;138(7):2807-12. PubMed PMID: 9202221. 1997

25.   **Rondeel JMM, Klootwijk W, Linkels E, van Haasteren GAC, de Greef WJ, Visser TJ**. Regulation of thyrotropin-releasing hormone in the posterior pituitary. Neuroendocrinology 61:421–429. 1995

26.   **Bruhn TO, Rondeel JM, Bolduc TG, Jackson IM.** Thyrotropin-releasing hormone (TRH) gene expression in the anterior pituitary. I. Presence of pro-TRH messenger ribonucleic acid and pro-TRH-derived peptide in a subpopulation of somatotrophs. Endocrinology. Feb;134(2):815-20. 1994

27.   **Bruhn TO, Bolduc TG, Maclean DB, Jackson IM.** Protrh peptides are synthesized and secreted by anterior pituitary cells in long-term culture. Endocrinology. Jul;129(1):556-8. 1991

28. **Le Dafniet M, Lefebre P, Barret A, Mechain C, Feinstein MC, Brandi AM, Peillon F.** Normal and adenomatous human pituitaries secrete thyrotropin-releasing hormone in vitro: modulation by dopamine, haloperidol and somatostatin. J Clin Endocrinol Metab 71:480–486. 1990

29. **Pagesy P, Croissandeau G, Le Dafniet M, Peillon F, Li JY**. Detection of thyrotropin-releasing hormone (TRH) mRNA by the reverse transcriptionpolymerase chain reaction in the human normal and tumoral anterior pituitary. Biochem Biophys Res Commun 182:182–187. 1992

30. **Bruhn TO, Bolduc TG, Rondeel JM, Jackson IM.** Thyrotropin-releasing hormone gene expression in the anterior pituitary. II. Stimulation by glucocorticoids. Endocrinology. Feb;134(2):821-5. 1994

31. **Bruhn TO, Rondeel JM, Bolduc TG, Jackson IM.** Thyrotropin-releasing hormone gene expression in the anterior pituitary. III. Stimulation by thyroid hormone: potentiation by glucocorticoids. Endocrinology. Feb;134(2):826-30. 1994

32.   **Luo L(1), Jackson IM.** Thyrotropin-releasing hormone and c-fos/c-jun genes are colocalized in rat anterior pituitary cells: stimulation of transcription by glucocorticoids. Endocrinology. Jun;136(6):2705-10. 1995

33.   **Albert PR, Tashjian AH Jr.** Relationship of thyrotropin-releasing hormone-induced spike and plateau phases in cytosolic free Ca2+ concentrations to hormone secretion. Selective blockade using ionomycin and nifedipine. J Biol Chem. Dec 5;259(24):15350-63. 1984

34.   **Aizawa T, Hinkle PM.** Thyrotropin-releasing hormone rapidly stimulates a biphasic secretion of prolactin and growth hormone in GH4C1 rat pituitary tumor cells. Endocrinology. Jan;116(1):73-82. 1985

35.   **A Schonbrunn, A Tashjian.** Epidermal growth factor and thyrotropin-releasing hormone act similarly on a clonal pituitary cell strain. Modulation of hormone production and inhibition of cell proliferation. The Journal of cell biology, 1980

36.   **Valentijn K, Bunel DT, Liao N, Pelletier G, Vaudry H**: Release of pro-thyrotropin-releasing hormone connecting peptides PS4 and PS5 from perifused rat hypothalamic slices. *Neuroscience* **44**:223–233, 1991

37.   **Roussel J-P, Hollande F, Bulant M, Astier H**: A prepro-TRH connecting peptide (prepro-TRH$_{160-169}$) potentiates TRH-induced TSH release from rat perfused pituitaries by stimulating dihydropyridine- and omega-conotoxin-sensitive Ca^{2+} channels.*Neuroendocrinology* **54**:559–565, 1991

38.   **F E Carr, A H Reid, and M W Wessendorf**: A cryptic peptide from the preprothyrotropin-releasing hormone precursor stimulates thyrotropin gene expression. Endocrinology, 1993

39.   **Allaerts W, Carmeliet P, Denef C**: New perspectives in the function of pituitary folliculo-stellate cells. Mol Cell Endocrinol 71:73-81, 1990

40.   **Vankelecom H, Andries M, Billiau A, Denef C**: Evidence that folliculo-stellate cells mediate the inhibitory effect of interferon- y on hormone secretion in rat anterior pituitary cell cultures. Endocrinology 130:3537-3546, 1992

41.   **Morand I, Fonlupt P, Guerrier A, Trouillas J, Calle A, Remy C, Rousset B, Munari-Silem Y**: Cell-to-cell communication in the anterior pituitary: Evidence for gap junction-mediated exchanges between endocrine cells and folliculostellate cells. Endocrinology 137:3356-3367, 1986

42.   **Redei E, Hilderbrand H, Aird F**: Corticotropin release inhibiting factor is encoded within preproTRH. *Endocrinology* **136**:1813–1816, 1995

43.   **McGivern RF, Rittenhouse P, Aird F, Van de Kar LD, Redei E**: Inhibition of stress-induced neuroendocrine and behavioral responses in the rat by prepro-thyrotropin-releasing hormone 178–199. *J Neurosci* **17**:4886–4894, 1997

44.   **Legradi G, Rand WM, Hitz S, Nillni EA, Jackson IMD, Lechan RM**: Opiate withdrawal increases proTRH gene expression in the ventrolateral column of the midbrain periaqueductal gray. *Brain Res* **729**:10–19, 1996

45.   **Gahn LG, Sevarino KA**: Preprothyrotropin-releasing hormone mRNA in the rat central gray is strongly and persistently induced during morphine withdrawal. *Neuropeptides* **30**:207–212, 1996

46.   **Nillni EA, Legradi G, Lechan RM**, Opiate withdrawal (OW) regulates proTRH post-translational processing in the ventrolateral column of the midbrain periaqueductal gray (PAG). Program of the 81st Annual Meeting of The Endocrine Society, San Diego, CA, (Abstract P1–323), p 203, 1999

47.   **Lechan RM, Wu P, Jackson IMD**: Immunocytochemical distribution in rat brain of putative peptides derived from thyrotropin-releasing hormone prohormone. *Endocrinology* **121**:1879–1891, 1987

48.   **Van den Bergh P, Wu P, Jackson IM, Lechan RM**: Neurons containing a N-terminal sequence of the TRH-prohormone (preproTRH53–74) are present in a unique location of the midbrain periaqueductal gray of the rat. *Brain Res* **461**:53–63, 1988

49.   **Lovick TA**: Depaulis A, Bandler R (eds) The Midbrain Periaqueductal Gray Matter: Functional, Anatomical and Neurochemical Organization. Plenum Press, New York, pp 101–120, 1991

50.   **Fardin V, Oliveras JL, Besson JM**: A reinvestigation of the analgesic effects induced by stimulation of the periaqueductal grey matter in the rat. I. The production of behavioral side effects together with analgesia. *Brain Res* **306**:105–123, 1984

51.   **Lewis VA, Gebhart GF**: Evaluation of the periaqueductal central gray (PAG) as a morphine-specific locus of action and examination of morphine-induced and stimulation-produced analgesia at coincident PAG loci. *Brain Res* **124**:283–303, 1977

52.   **Bandler R, Shipley MT**: Columnar organization in the midbrain periaqueductal gray: modules for emotional expression. *Trends Neurosci* **17**:379–388, 1994

53.   **Tortorici V, Vasquez E, Vanegas H**: Naloxone partial reversal of the antinociception produced by dipyrone microinjected in the periaqueductal gray of rats. Possible involvement of medullary off- and on-cells. *Brain Res* **725**:106–110, 1996

54.   **Rosen JB, Weiss SR, Post RM** Contingent tolerance to carbamazepine: alterations in TRH mRNA and TRH receptor binding in limbic structures. *Brain Res* **651**:252–260, 1994

55.   **Lechan RM, Toni R**: Thyrotropin-releasing hormone neuronal systems in the central nervous system. In: Nemeroff CB (ed) Neuroendocrinology. CRC Press, Boca Raton, FL, pp 279–329, 1992

56.   **Toni R, Vitale M, Mosca S, Zamai L, Martelli AM, Cocco L**: PreproTRH$_{53-74}$ stimulates primary cultures of rat anterior pituitary to enter early-S phase. 21st Annual Meeting of the Society for Neuroscience, New Orleans LA,: 388.11 (abstract),1991

57.   **Malaguti A, Mosca S, Della Casa C, Vitale M, Martelli AM, Toni R**: PreproTRH$_{53-74}$: evidence for a role as a growth factor in primary cultures of male rat anterior pituitary. It J Anat Embryol; 107: 268 (abstract), 2002

58.   **Sevarino KA, Wu P, Jackson IM, Roos BA, Mandel G, Goodman RH**: Biosynthesis of thyrotropin-releasing hormone by a rat medullary thyroid carcinoma cell line.*J Biol Chem* **263**:620–623, 1988

59.   **Wu P, Jackson IMD**: Identification, characterization, and localization of thyrotropin-releasing hormone precursor peptides in perinatal rat pancreas. *Ann NY Acad Sci* **553**:489–491, 1989

60. **Wu P, Jackson IMD**: Identification, characterization, and localization of thyrotropin-releasing hormone precursor peptides in perinatal rat pancreas. *Regul Pept* **22**:347–360, 1988

61. **Tashjian AH Jr., et al.** Establishment of clonal strains of rat pituitary tumor cells that secrete growth hormone. Endocrinology 82: 342-352, 1968

62. **A.H. Tashjian, Jr., P. M. Hinkl¢, and P. S. Dannies**, in "Endocrinology" (R. O. Scow, ed.), p. 648. Excerpta Med. Found., Amsterdam, 1973

63. **Tashjian AH Jr.** Clonal strains of hormone-producing pituitary cells. Methods Enzymol. 58: 527-535, 1979

64. **Kiino DR, Dannies PS:** Insulin and 17 ,B-estradiol increase the intracellular prolactin content of GH4Cl cells. Endocrinology 109:1264-1269, 1981

65.   **Filipcík P, Strbák V, Brtko J.** Thyroid hormone receptor occupancy and biological effects of 3,5,3,-L-triiodothyronine (T3) in GH4C1 rat pituitary tumour cells. Physiol Res. 47(1):41-6; 1998

66.   **Kirkland WL, Sorrentino JM, Sirbasku DA.** Control of cell growth. III. Direct mitogenic effect of thyroid hormones on an estrogen-dependent rat pituitary tumor cell line. J Natl Cancer Inst. Jun;56(6):1159-64. 1976

67.   **Kirkland WL, Sorrentino JM, Sirbasku DA.** Control of cell growth. III. Direct mitogenic effect of thyroid hormones on an estrogen-dependent rat pituitary tumor cell line. J Natl Cancer Inst. Jun;56(6):1159-64. 1976

68.   **Gilchrist CA, Park JH, MacDonald RG, Shull JD.** Estradiol and triiodothyronine increase production of insulin-like growth factor-I (IGF-I) and insulin-like growth factor binding protein-3 (IGFBP-3) by GH4C1 rat pituitary tumor cells. Mol Cell Endocrinol. Oct 30;114(1-2):147-56. 1995

69.   **Kiino DR, Dannies PS.** Hormonal regulation of prolactin storage in a clonal strain of rat pituitary tumor cells. Yale J Biol Med. Sep-Dec;55(5-6):409-20. 1982

70.   **Riss TL1, Stewart BH, Sirbasku DA**. Rat pituitary tumor cells in serum-free culture. I. Selection of thyroid hormone-responsive and autonomous cells. In Vitro Cell Dev Biol. 25(2):127-35; 1989

71.   **Neufeld G, Gospodarowicz D.** Basic and acidic fibroblast growth factors interact with the same cell surface receptors. J Biol Chem. Apr 25;261(12):5631-7. 1986

72.   **Fagin S, Brown A, Melmed S:** Regulation of pituitary insulin-like growth factor I messenger ribonucleic acid levels in rats harbouring somatomammotrophic tumors: implications for growth hormone autoregulation. Endocrinology 122:2204–2210, 1988

73.   **Kanduc D(1).** Homology, similarity, and identity in peptide epitope immunodefinition. J Pept Sci. 2012 Aug;18(8):487-94. doi: 10.1002/psc.2419. Epub Jun 14 2012

74.   **Chen J, Hersmus N, Van Duppen V, Caesens P, Denef C, Vankelecom H**: The adult pituitary contains a cell population displaying stem/progenitor cell and early embryonic characteristics. Endocrinology 146:3985–3998, 2005

75.   **Seki, A., Coppinger, J. A., Jang, C. Y., Yates, J. R. and Fang, G..** Bora and the kinase Aurora a cooperatively activate the kinase Plk1 and control mitotic entry. *Science* 320(5883): 1655-1658. 2008

76.   **Zhu, H., Coppinger, J. A., Jang, C. Y., Yates, J. R., 3rd and Fang, G..** FAM29A promotes microtubule amplification via recruitment of the NEDD1-gamma-tubulin complex to the mitotic spindle. *J Cell Biol* 183(5): 835-848. 2008

77.   **Denef C, Baes M, Schramme C.** Paracrine interactions in the anterior pituitary: role in the regulation of prolactin and growth hormone secretion. In: Ganong WF, Martini L, eds. Frontiers in neuroendocrinology. New York: Raven Press;;115:48. 1986

78.   **Childs GV, Cole DE, Kubek M, Tobin RB, Wilber JF.** Endogenous thyrotropin-releasing hormone in the anterior pituitary: sites of activity as identified immunocytochemical staining. J Histochem Cytochem, 26: 901-8. 1978

79.   **Childs GV, Yan HY, Tobin RB, Wilber JF, Kubek M.** Effects of thyroidectomy, propylthiouracil, and thyroxine on pituitary content and immunocytochemical staining of TSH and TRH. J Histochem Cytochem, 29: 357-63. 1981

80.   **Heritier AG, DuBois PM.** Re-evaluation of gonadotropinreleasing hormone (GnRH) action on pituitary cell differentiation with special regard to its effect on LH and TSH cell types. J Neuroendocrinol, 6: 33-7. 1994

81.   **Pagesy P, Li JY, Berthet M, Peillon F.** Evidence of gonadotropin releasing hormone mRNA in the rat anterior pituitary. Mol Endocrinol, 6: 523-8. 1992

82.   **Miller GM, Alexander JM, Klibanski A.** Gonadotropin-releasing hormone messenger mRNA expression in gonadotroph tumors and normal human pituitary. J Clin Endocrinol Metab, 82: 1974-82. 1996

83.   **Simon MC.** Gotta have GATA. Nat Genet, 11: 9-11. 1995

84.   **Dasen JS, O'Connell SM, Flynn SE, et al.** Reciprocal interactions of Pit-1 and GATA-2 mediate signaling gradient-induced determination of pituitary cell types. Cell, 97: 587-98. 1999

85.   **Gordon DF, Lewis SR, Haugen BR, et al.** Pit-1 and GATA-2 interact and functionally cooperate to activate the thyrotropin beta-subunit promoter. J Biol Chem, 272: 24339-47. 1997

86.   **Heritier AG, DuBois PM.** Influence of thyroliberin on the rat pituitary cell type differentiation: an in vitro study. Endocrinology, 132: 634-9. 1993

87.   **Taniguchi Y, Yasutakaka S, Kominami R, Shinohara H.** Mitoses of thyrotrophs contribute to the proliferation of the rat pituitary gland during the early postnatal period. Anat Embryol, 206: 67-72. 2002

88.   **Dussault JH, Labrie F.** Development of the hypothalamic pituitary-thyroid axis in the neonatal rat. Endocrinology; 97: 1321-4. 1975

89.   **Yamada M, Saga Y Shibusawa N, et al.** Tertiary hypothyroidism and hyperglycemia in mice with targeted disruption of the thyrotropin-releasing hormone gene. Proc Natl Acad Sci, 94: 10862-7. 1997

90.   **Shibusawa N, Yamada M, Hirato J, et al.** Requirement of thyrotropin-releasing hormone for the postnatal functions of pituitary thyrotrophs: ontogeny study of congenital tertiary hypothyroidism in mice. Mol Endocrinol, 14: 137-46. 2000

91.   **Herlant M.** Etude endocrinologique d'un cas d'anencephalie. Ann Endocrinol (Paris), 14: 899. 1953

92.   **Grasso S, Filetti S, Mazzone D, Pezzino V, Vigo R, Vigneri R.** Thyroid pituitary function in eight anencephalic infants. Acta Endocrinol (Copenh), 93: 396-401. 1980

93.   **Pezzino V, Distefano G, Belfiore A, Filetti S, Mazzone D, Grasso S.** Role of thyrotropin-releasing hormone in the development of pituitary-thyroid axis in four anencephalic infants. Acta Endocrinol (Copenh), 101: 538-41. 1982

94.   **Pilavdzic D, Kovacs K, Asa SL.** Pituitary morphology in anencephalic human fetuses. Neuroendocrinology;65, 164-72. 1997

95.   **Beck-Peccoz P, Cortelazzi D, Persani L, et al.** Maturation of pituitary-thyroid function in the anencephalic fetus. Acta Med Austriaca, 19: 72-6. 1992

96.   **Stratmann IE, Ezrin C, Kovacs K, Sellers EA.** Effect of TRH (thyrotropin-releasing hormone) on the fine structure and replication of TSH and prolactin cells in the rat. Z Zellforsch Mikrosk Anat, 145: 23-37. 1973

97.   **Kunert-Radek J, Pawlikowski M.** The effect of thyrotropin releasing hormone on cell proliferation in the anterior pituitary gland of thyroidectomized rats. Neuroendocrinology, 17: 92-5. 1975

98.   **Yajima Y, Saito T.** Effects of TRH on cell proliferation of rat pituitary cells (GH3). In vitro, 18: 1009-16. 1982

99.   **Ramsdeel JS.** Thyrotropin-releasing hormone inhibits GH4 pituitary cell proliferation by blocking entry into S phase. Endocrinology, 126: 472-9. 1990

100.   **Le Dafniet M, Blumberg-Tick J, Gozlan H, Barret A, Joubert D, Peillon F.** Altered balance between thyrotropin-releasing hormone and dopamine in prolactinomas and other pituitary tumors compared to normal pituitaries. J Clin Endocrinol Metab, 69: 267-71. 1989

101.   **Kim K, Arai K, Sanno N, Teramoto A, Shibasaki T.** The expression of thyrotropin-releasing hormone receptor 1 messenger ribonucleic acid in human pituitary adenomas. Clin Endocrinol (Oxf), 54: 309-16. 2001

102.   **Scully KM, Rosenfeld MG.** Pituitary development: regulatory codes in mammalian organogenesis. Science. Mar 22;295(5563):2231-5. 2002

103.   **Yamada M(1), Radovick S, Wondisford FE, Nakayama Y, Weintraub BD, Wilber JF.** Cloning and structure of human genomic DNA and hypothalamic cDNA encoding human prepro thyrotropin-releasing hormone. Mol Endocrinol. Apr;4(4):551-6. 1990

104.   **Mura M, Wang J, Zhou Y, Pinna M, Zvelindovsky AV, Dennison SR, Phoenix DA.** The effect of amidation on the behaviour of antimicrobial peptides. Eur Biophys J. Apr;45(3):195-207. 2016

105.   **Wolfgang Voelter, Karl Zech, Peter Göbel, Oskar Oster, Antonio Attanasio.** Circulardichroismusuntersuchungen des Thyreotropin-Releasinghormons (TRH) Circular Dichroism Investigations of TRH. Chemisches Institut der Universität Tübingen Z. Naturforsch. 30 b, 142-143 1975

106.   **Nutt RF, Holly FW, Homnick C, Hirschmann R, Veber DF, Arison BH.** Synthesis of thyrotropin-releasing hormone analogues with selective central nervous system effects. J Med Chem. Jun;24(6):692-8. 1981

107.   **Yamashita S & Melmed S:** Insulin-like growth factor I action on rat anterior pituitary cells: suppression of growth hormone secretion and messenger ribonucleic acid levels. Endocrinology 118 176–182. 1986

108.   **Fagin JA, Pixley S, Slanina S, Ong J & Melmed S:** Insulin-like growth factor I gene expression in GH3 rat pituitary cells: messenger ribonucleic acid content, immunocytochemistry and secretion. Endocrinology 120 2037–2043. 1987

109.   **Abe H, Molitch ME, Van Wyk JJ, Underwood LE:** Human growth hormone and somatomedin C suppress the spontaneous release of growth hormone in unanesthetized rats. Endocrinology 113:1319–1324. 1983

110.   **Ceda GP, Davis RG, Rosenfeld RG, Hoffman AR:** The growth hormone (GH)-releasing hormone (GHRH)-GH-somatomed in axis: evidence for rapid inhibition of GHRH-elicited GH release by insulin-like growth factors I and II. Endocrinology 120:1658–1662. 1987

111.   **Namba S, Morita S, Melmed S:** Insulin-like growth factor I action on growth hormone secretion and messenger ribonucleic acid levels: interactions with somatostatin. Endocrinology 124:1794–1799. 1989

112.   **Castillo AI, Aranda A.:** Differential regulation of pituitary-specific gene expression by insulin-like growth factor 1 in rat pituitary GH4C1 and GH3 cells. Endocrinology. Dec;138(12):5442-51. 1997

113.   **Fernández M, Sánchez-Franco F, Palacios N, Sánchez I, Villuendas G & Cacicedo L:** Involvement of vasoactive intestinal peptide on insulin-like growth factor I-induced proliferation of rat pituitary lactotropes in primary culture: evidence for an autocrine and/or paracrine regulatory system. Neuroendocrinology 77 341–352. 2003

114.   **Oomizu S, Takeuchi S & Takahashi S**: Stimulatory effect of insulin-like growth factor-I on proliferation of mouse pituitary cells in serum-free culture. *Journal of Endocrinology* **157** 53–62, 1998

115.   **Fernandez M, Sanchez-Franco F, Palacios N, Sanchez I & Cacicedo L**: IGF-I and vasoactive intestinal peptide (VIP) regulate cAMP-response element-binding protein (CREB)-dependent transcription via the mitogen-activated protein kinase (MAPK) pathway in pituitary cells: requirement of Rap1. *Journal of Molecular Endocrinology* 34 699–712, 2005

116. **Gutiérrez S, Petiti JP, De Paul AL, Mukdsi JH, Aoki A, Torres AI, Orgnero EM**. Antagonic effects of oestradiol in interaction with IGF-1 on proliferation of lactotroph cells in vitro. Histochem Cell Biol. 2005 Sep;124(3-4):291-301. Epub Oct 28. 2005

117. **Newton CJ, Buric R, Trapp T, Brockmeier S, Pagotto U, Stalla GK.** The unliganded estrogen receptor (ER) transduces growth factor signals. J Steroid Biochem Mol Biol. Apr;48(5-6):481-6. 1994

118. **Hayashi I**: Growth of GH3, a rat pituitary cell line, in serum free, hormone-supplemented medium. In Methods for Serum-Free Culture of Cells of the Endocrine System, pp 1–13. Eds DW Barnes, DA Sirbasku & GH Sato. New York: Alan R Liss, Inc. 1984

119. **Huynh H, Chow PK, Ooi LL, Soo KC.** A possible role for insulin-like growth factor-binding protein-3 autocrine/paracrine loops in controlling hepatocellular carcinoma cell proliferation. Cell Growth Differ. Mar;13(3):115-22. 2002

120.   **Martelli AM, Tabellini G, Bortul R, Manzoli L, Bareggi R, Baldini G, Grill V, Zweyer M, Narducci P, Cocco L.** Enhanced nuclear diacylglycerol kinase activity in response to a mitogenic stimulation of quiescent Swiss 3T3 cells with insulin-like growth factor I. Cancer Res. Feb 15;60(4):815-21. 2000

121.   **Zini N, Martelli AM, Neri LM, Bavelloni A, Sabatelli P, Santi S, Maraldi NM.** Immunocytochemical evaluation of protein kinase C translocation to the inner nuclear matrix in 3T3 mouse fibroblasts after IGF-I treatment. Histochem Cell Biol. Jun;103(6):447-57. 1995

122.   **Takuwa N, Takuwa Y, Yanagisawa M, Yamashita K, Masaki T.** A novel vasoactive peptide endothelin stimulates mitogenesis through inositol lipid turnover in Swiss 3T3 fibroblasts. J Biol Chem. May 15;264(14):7856-61. 1989

123.   **Karine Rizzoti:** Adult pituitary progenitors/stem cells: from in vitro characterization to *in vivo* function Division of Stem Cell Biology and Developmental Genetics, MRC National Institute for Medical Research, The Ridgeway, Mill Hill, London NW7 1AA, UK, European Journal of Neuroscience, Vol. 32, pp. 2053–2062, 2010

124.   **R. Toni, E. Bassi, N. Zini, A. Zamparelli, F. Barbaro, D. Dallatana, S. Mosca, G. Lippi, G. Spaletta, E. Bassoli, L. Denti, A. Gatto, A. Parrilli, M. Fini, R. Giardino, M. Sandri, S. Sprio, A. Tampieri.** Bioartificial endocrine organs: at the cutting edge of translational research in endocrinology. Bio-inspired Regenerative Medicine: Materials, Processes and Clinical Applications, Pan Stanford Publishing. 2016

125.   **Adams RL, Lindsay JG.** Hydroxyurea reversal of inhibition and use as a cellsynchronizing agent. J Biol Chem. Mar 25;242(6):1314-7, 1967

126.   **Tobey RA1, Oishi N, Crissman HA.** Cell cycle synchronization: reversible induction of G2 synchrony in cultured rodent and human diploid fibroblasts. Proc Natl Acad Sci U S A. Jul;87(13):5104-8, 1990

127.   **Tobey RA.** Production and characterization of mammalian cells reversibly arrested in G1 by growth in isoleucine-deficient medium. Methods Cell Biol;6:67-112, 1973

128.   **Fox MH, Read RA, Bedford JS.** Comparison of synchronized Chinese hamster ovary cells obtained by mitotic shake-off, hydroxyurea, aphidicolin, or methotrexate. Cytometry. May;8(3):315-20, 1987

129.   **Pagano M1, Pepperkok R, Verde F, Ansorge W, Draetta G.EMBO J.** Cyclin A is required at two points in the human cell cycle. Mar;11(3):961-71, 1992

130.   **Banfalvi G.** Overview of cell synchronization. Methods Mol Biol.;761:1-23. 2011